博士論文

Stabilization and Synchronization for Hierarchical Dynamical Networks

（階層化動的ネットワークの安定化と同期化）

グエン　ディン　ファ
Nguyen Dinh Hoa

A Thesis Submitted in Partial Fulfillment of the Requirements
for the Degree of Doctor of Philosophy
Department of Information Physics and Computing
Graduate School of Information Science and Technology
The University of Tokyo
Academic Year 2014

Thesis Title	Stabilization and Synchronization for Hierarchical Dynamical Networks
By	Nguyen Dinh Hoa
Field of Study	Information Physics and Computing
Thesis Advisor	Professor Shinji Hara, Ph.D.

ABSTRACT

In this thesis, we propose several approaches for the stabilization and synchronization of hierarchical dynamical networks which are presented in the following three main parts.

The first part introduces our viewpoints and formulations of hierarchical dynamical networks. We first investigate multi-agent dynamical systems from the viewpoint of hierarchical dynamical networks where each agent is cast as a subsystem in the hierarchical network. For homogeneous hierarchical multi-agent networks, the subsystems are identical. On the other hand, for heterogeneous hierarchical networks, the interconnection structures in subsystems are different and the numbers of agents in subsystems are distinct. Next, we study the entraiment in nonlinear multi-agent networks, in particular oscillator networks described by Goodwin-type models. In this case, each agent is a nonlinear oscillator and the oscillator network is excited by a periodic exogenous signal.

The second part is devoted to propose a new and systematic method to design hierarchical feedback controllers for both homogeneous and heterogeneous linear hierarchical dynamical networks such that the prescribed hierarchical structures of the networks are preserved. The key idea is to employ the LQR approach where the weighting matrices are selected with proper hierarchical structures. This gives us an LQR controller with a specific hierarchical structure. As a result, the closed-loop system has the desired hierarchical structure. When not all states of subsystems are measurable, we propose local observers to reduce the output feedback design to the state feedback case which is already resolved. In a further step, we elaborate more on the selection of weighting matrices so that the proposed LQR controller is able to selectively shift the undesirable poles of the subsystems without affecting to other poles.

The last part in the thesis presents a framework to analyze the entrainment in nonlinear oscillator networks forced by external periodic signals. Utilizing harmonic balance method, the conditions for entrainment are proposed. Next, the monotone properties of the entrainment are figured out. The network of 3rd-order Goodwin oscillators which has been used to describe circadian rhythms is employed in this research to illustrate the theoretical results. Interestingly, some obtained results agrees with the experiment observations. Thus, they would be helpful to get more insights and to further studying circadian oscillations. Moreover, the networks of higher-order Goodwin-type oscillators are considered where the obtained results for networks of 3rd-order Goodwin oscillators can be similarly achieved.

ACKNOWLEDGEMENT

During my three years at University of Tokyo for pursuing a PhD degree, I have experienced a lot about the Japanese culture and lifestyle. This will be one of the most unforgettable time period in my life. And to obtain the research outcomes for writing this thesis is really a great effort which would not be completed without many supports from other people around me.

First and foremost, I would like to send the most sincere thanks to my supervisor, Prof. Shinji Hara, for his supervision and supports. With his remarkable patience and brilliant, I have a freedom in choosing my research topics and get the advices to gradually focus on the right way to obtain the meaningful results. He also understand and advocate me for other problems in the ordinary life, especially in the second half of my PhD period when I got married and then had a baby. This thesis would not be finished without his continuous facilitation for all the time.

Next, I would like to gratefully thank Assoc. Prof. Koji Tsumura for his comments and suggestions through the weekly seminars in our laboratory as well as in my defense committee. They are really useful for me to improve the research. I would also like to gratefully thank the other committee members, Prof. Hoshino, Prof. Nara and Prof. Fujimoto, for their valuable comments to revise my thesis. I greatly appreciate their conscientious reading and attention of my thesis defense in spite of their tight schedules.

My special thanks to Dr. Kojima and the students in the laboratory, especially former students Dr. Ohki, Dr. Hori, Mr. Yoshioka, who talked and discussed with me about various problems in our researches and our daily lifes. Those discussions are effective not only to them but also to me for a better understanding about different subjects. In addition, thanks to their helps when I had troubles in my Japanese language, things could go smoothly afterward.

Many thanks should be sent to AUN/SEED-NET, JICA for their financial support during three years of my PhD and other related problems.

Finally, I would like to send the deep thanks to my wife and my parents for all their understandings and supports through years. With their encouragements and sympathies, I have time to concentrate on my research with comfort. By this chance, I would also like to thank my little daughter who has made my life more meaningful since she was born.

Contents

List of Tables

Page

List of Figures

Page

Notations and Acronyms

Notations

$\mathbb{R}$	The set of real numbers
$\mathbb{R}^n$	The set of real vectors with dimension n
$\mathbb{R}^{n\times m}$	The set of real matrices with dimension $n \times m$
$\mathbb{C}$	The set of complex numbers
$\mathbb{C}^n$	The set of complex vectors with dimension n
$\mathbb{C}^{n\times m}$	The set of complex matrices with dimension $n \times m$
$\mathbb{C}_-$	The open left-haft complex plane
diag	Diagonal or block-diagonal matrices
Re()	The real part
Im()	The imaginary part
$\otimes$	Kronecker product
$\odot$	Khatri-Rao product
$A \succeq 0$	A is a positive semidefinite matrix
$A \succ 0$	A is a positive definite matrix
$\sigma(A)$	The eigenvalue set of A
A^T	The transpose matrix of A
A^*	The transpose conjugate matrix of A
$\dot{x}$	The time derivative of x
i	The complex unit, $i^2 = -1$

Acronyms

LTI	Linear Time Invariant
ODE	Ordinary Differential Equation
SISO	Single Input Single Ouput
LQR	Linear Quadratic Regulator
SCN	Suprachiasmatic Nucleus

CHAPTER 1

INTRODUCTION

1.1 Motivation

1.1.1 Hierarchical dynamical networks

Recently, there is a great number of researches that have been conducted in networked systems arise from many different fields such as biology, power systems, economics, social science. One essential feature of networked systems is that they used to possess hierarchical structures leading to the large-scale feature and complex behaviors of the systems. Examples of hierarchical networks can be ubiquitously found such as world wide web, internet, power grids, social networks [2–4], gene networks [5, 6], quorum-sensing networks [7]. In control community, much effort has been made for modeling and control of hiearchical, networked systems. It is then realized that the interconnections between the network elements play an important role in the behaviors of the network, for instance consensus, formation or synchronization [8, 9]. Specifically, eigenvalues and eigenvectors of the matrix representing the interconnections in the network are essential factors for determining the network behaviors. Therefore, many studies have been focusing on the analysis and synthesis of the interconnection matrix in the network and its eigenvalues and eigenvectors. However, this problem is not easy for large-dimension networks because of the limitations on computational cost, the decentralized communication constraint of the network, etc. Fortunately, when the network has a hierarchical structure, the problem may be reduced to designing the interconnection matrices in the individual layers and the interconnections between them with smaller sizes, hence the design may be simplified. Moreover, the hierarchical structure enables us to achieve a global target in the network by designing the local communication topologies in the lower layers which gives a powerful technique to analyze and synthesize the networks in a distributed fashion. Therefore, designing networked systems in a hierarchical manner would be efficient for the real systems.

It is observed from the practical hierarchical networks that the interconnection structures inside the subsystems in the network are usually dense whereas the communication topologies between the subsystems are sparse [2, 4]. In other words, the communications between the subsystems are represented by low rank matrices. Bearing this in mind, [10–12] generalized the existing result in [13] and focused on the information flow between subsystems in the hierarchical networks and proposed a concept of low rank interconnection. This framework was shown to have several advantages in comparison with previous works such as a faster consensus speed and an explicit eigenvalue distribution of the interconnection matrix

in the whole network composing of the eigenvalue distributions of the subsystems. Nevertheless, only some special topologies were considered in [10–12]. Then continuing this research line, [14] and [15] presented a new class of low rank inter-group connection namely eigen-connection to design hierarchical networks with homogeneous and heterogeneous groups such that only some specific eigenvalues of local interconnection matrices are selectively shifted. The eigen-connection framework utilizes the left or right eigenvectors associated with unexpected eigenvalues of local interconnection matrices to construct the input or output matrices for the low rank communication between subsystems. Moreover, the eigenvalue set of the interconnection matrix in the whole network is almost explicitly determined.

Although the framework in [14] and [15] provides an efficient way to analyze hierarchical dynamical networks with the eigen-connection structure, how to synthesize such hierarchical dynamical networks in a systematic manner is still lacking. As discussed earlier, the synthesis of hierarchical dynamical networks would be essential and efficient for practical applications due to the advantages of the hierarchical structures. Therefore, a systematic design method for hierarchical dynamical networks is really a crucial issue. This motivates us to develop in this thesis a systematic approach for synthesis of hierarchical linear dynamical networks.

Given a multi-agent systems in which the agents are initially independent, then each agent tries to collaborate with the others to achieve some local and global objectives for the whole network by sending out a unique, aggregated signal to communicate with others and receiving from them their aggregated signals to adjust its behavior. From the theoretical point of view, this set up of multi-agent systems can be viewed as a two-layer hierarchical network where each agent is considered as a subsystem in the lower layer and the collaboration among agents is treated as the interconnection among subsystems in the upper layer. Accordingly, a question raises up here that:

How can we design hierarchical dynamical networks to achieve prescribed hierarchical structures?

Besides, the hierarchical dynamical networks should be designed to attain some global objectives of which a standard goal is the stabilization for the whole network.

In literature, there are several researches using LQR approach to design decentralized or distributed controllers for multi-agent networked systems such as in [16–19]. A recent work [20] tried to use the LQR method to design hierarchical dynamical systems but the system matrices of the subsystems and the interconnection among subsystems are required to belong to some special structures such as operator algebras or semi-groups. In this thesis, we employ the Linear Quadratic Regulator (LQR) method to design a hierarchical decentralized optimal feedback controller for a given hierarchical dynamical network such that it has a prescribed hierarchical structure, however our formulation of multi-agent dynamical networks do not assume special structures as in [16–20]. Therefore, the question now becomes ***under what LQR setting, the obtained optimal controller gives the multi-agent dynamical network a desirable prescribed hierarchical structure?***

On the other hand, for stabilizing a system, several pole placement techniques could be utilized which would place some or all the poles of the closed-loop system at expected positions. There have been some works in the literature, e.g. [21–24]utilizing the LQR method to selectively shift the system poles. However, that methods are only applicable for a single LTI system and is not usable in multi-agent dynamical networks. This motivates us to further develop our proposed hierarchical state feedback LQR optimal controller to selectively shift the undesired eigenvalues of the agents without moving other eigenvalues. An advantage of this study is that for MIMO subsystems with a small number of undesirable eigenvalues, this controller results in low-rank interconnection among agents which is useful for cooperation among agents to atten some global objectives such as rapid consensus of agents [10–12].

1.1.2 Oscillator networks

Oscillator networks is one type of multi-agent dynamical networks that can be found in many real systems such as electrical and electronic circuits, biological systems. In biology, oscillator networks are indispensable parts that play major roles at many levels. Let us consider the vertebrates as an example. In an early state of development, the segmentation clocks are essential factors for the somitegenesis. Then the neural oscillations in the brain control the recognition, memory and behaviors of the vertebrates, for instance the central pattern generators regulate their movements. Moreover, the oscillations in blood circulation, hormonal release, appetite, etc manage different processes happened in the body and any malfunction of them can lead to significant effects. Thus, analysis of biological oscillator networks is an emergent issue not only for the biologists but also the engineering scientists to reveal their dynamical behaviors and then utilize them for the synthesis of oscillator networks in engineering applications.

Circadian oscillations is a very typical example of biological oscillations that occur in most living creatures [25–30]. Because of the existence of an endogenous oscillator networks inside a living creature with the period near the length of a day, i.e., 24 hours, its behaviors are adjusted in a repetitive manner. Furthermore, the endogenous oscillator networks are entrainable meaning that they can be regulated by external periodic timing cues named zeitgebers, for instance the daily Light-Dark cycle. This is necessary to derive exact 24-hour oscillations in that circadian oscillator networks. Therefore, the questions on the entrainment of circadian networks by the zeitgebers are essential. From the viewpoint of control theory, the circadian networks can be formulated as nonlinear oscillator networks(e.g. third-order Goodwin oscillator networks [31]) excited by exogenous periodic inputs representing zeitgebers. Hence, by analyzing the entrainment in that driven nonlinear oscillator networks, we may get useful insights to the biological mechanisms of circadian rhythms and the obtained results may be helpful for medical applications of light for treating the diseases related to circadian rhythms, e.g., sleep disorder [29]. Unfortunately, there have not been completed results on the entrainment of nonlinear oscillator networks.

Motivated by those facts, we investigate in this thesis Goodwin-type nonlinear oscillator networks which is a generalization of the third-order Goodwin oscillator networks used to model the circadian networks [31]. Then our goal is to propose a control framework for systematically analyzing the entrainment in that nonlinear oscillator networks excited by external periodic signals. More specifically, we attempt to figure out the following two features of the entrainment. The first feature is the conditions for the entrainment, i.e., the conditions for the interconnection matrix in the network as well as the external input such that the entrainment occurs. The second feature is the relation between frequency, amplitudes and phases of entrained network oscillations and those of exogenous inputs. In some cases, we may obtain the explicit approximations for those relations, but in other situations, we only have the implicit estimations reflected through the monotonicity of them.

1.2 Overview

1.2.1 Multi-agent dynamical networks

Motivated by the behaviors of animals and humans observed in nature such as groups of birds, schools of fishes, colonies of ants, crowds, etc, scientists have been trying to develop models and algorithms explaining those phenomena and then to apply them to other situations in the real world such as in engineering, biology, transportation. The terminologies multi-agent systems and multi-agent networks hence appear to describes those systems and phenomena where each agent corresponds to an individual in the group and the agents interact with the others resulting in a multi-agent system or multi-agent network. So far, a huge number of researches have been conducted to study multi-agent systems, especially in the field of control systems [8,32,33]. Some initial works [34], [35] has inspired many later researches on various problems such as the flocking, consensus, formation, alignment problems [8, 9, 36–39].

One of most active application area which has been considering is multi-vehicle networks where each vehicle is cast as an agent and the vehicles communicate with others to achieve global targets such as a same velocity (consensus) or a prescribed shape between the positions of vehicles (formation). The researches on this area come from an emergence in the development of unmanned aerial vehices (UAVs), unmanned ground vehicles (UGVs), autonomous underwater vehicles (AUVs). In such problems, the agents were usually modeled as integrators or double integrators and the states of agents represent the positions or velocities of vehicles. Many control laws then have been proposed to design the communication topologies between agents such that the global goals are achieved [9,33]. Later on, Hara et al. introduced a quite a general class of multi-agent networks namely LTI systems with generalized frequency variable [40]. This framework enables us to investigate multi-agent networks with more general dynamics rather than integrators or double-integrators and associated problems such as stability, robust stability [41, 42].

Another important research area for multi-agent dynamical systems is in biology. With

their diversity from micro to macro scales, biological systems provide a very rich source of practical multi-agent dynamical systems for the control research. Let us take gene regulatory networks (GRNs) as an example due to their important roles in the development of living creatures. Each gene in a GRN can be considered as an agent and the interactions between genes lead to the behavior of the GRN. Cyclic GRNs then have been extensively studied [43–45] revealing that the oscillations of proteins could be analytically analyzed, and hence giving us biological insights into the biological process, for example the roles of specific biological parameters.

Power systems recently becomes an active research area for multi-agent dynamical systems due to the increasing demands for the renewable energy resources and their integration into the grid and the cooperation between the power sources and the households to save energy, sustain the stability, autonomously and optimally operate the whole power network. One direction that recently has been investigated intensively is to cast the power systems as phase oscillator networks [46–49]. Particularly, Kuramoto model is used to study the synchronization in power networks which shows the role of interactions between power sources to the stability and synchronization of the whole network.

A network of identical linear agents basically can be described in Figure 1.1 where $h(s)$ denotes the transfer function of agents and A represents the interconnection between agents. It then can be observed that the eigenvalues and eigenvectors of the interconnection matrix A play very important roles in the behaviors of the multi-agent network. For example, if $h(s) = 1/s$, A is a Laplacian matrix having a simple eigenvalue 0 and the associated eigenvector with all elements equal to 1 then the multi-agent network will reach consensus [8,9]. Therefore, to control linear multi-agent networks, we need to analyze and synthesize the eigen-structure of the interconnection matrix A. Nevertheless, it is not easy if the dimension of A is large. Luckily, if A has a hierarchical structure, i.e., the multi-agent network contains smaller sub-networks then the eigen-structure of A may be determined based on thoses of the interconnection matrices in the sub-networks. Thus, it will be beneficial if we can design hierarchical multi-agent networks where the eigen-structure of the whole network can be derived from the eigen-structures of the levels in the network.

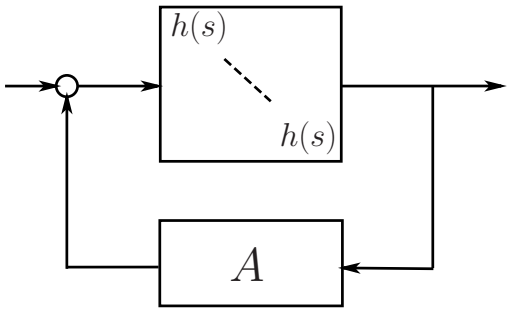

Figure 1.1: Block diagram of a multi-agent network.

1.2.2 Oscillator networks

Oscillation and synchronization are research topics with long history. They were observed for clock pendulums by Huyghens since the 17th century [50] and now can be ubiquitously seen around the world such as simultaneous flash of fireflies, orchestra of crickets, peacemaker cells in the heart, neural oscillations in the brain, electronic circuits, etc [50, 51]. Oscillation and synchronization are then not only phenomena but also essential mechanisms in many physical systems especially when many oscillators are coupled [50,52], for instance in circadian systems [28,29,53–55]. Hence, understanding the behaviors in networks of coupled oscillators is a emergent demand. Actually, in a network of coupled oscillators, each oscillator can be considered as an agent and the whole network can be cast as a multi-agent network. Therefore, oscillator networks are indeed a special type of multi-agent networks and hence our concern in this type of networks is related to the previous part.

To study the oscillations and synchronization, several approaches have been proposed including phase response curve [56,57], Kuramoto model [58]. The phase response curve was initially introduced by Winfree [56] to investigate some biological oscillations and then was successfully applied to neural oscillations [57]. This method is useful for relaxation oscillators but may not give analytical insights for non-relaxation oscillators. Then Kuramoto modified the works of Winfree and presented a model of phase oscillators which is now called after his name [58]. An advantage of Kuramoto model is that we have an analytical expression for the interconnection strength between oscillators such that they synchronize. Subsequently, other authors also explored oscillator networks under the effect of exogenous periodic signals using Kuramoto model, for example [59]. However, Kuramoto model is quite simple in the sense that it only uses the phases and frequencies of oscillators and therefore one may not see the physical meaning through those two variables. Thus, in this thesis we consider the models of oscillators represented by ODEs which describe the physical processes with physical parameters. Then by studying the networks of that oscillators, we may obtain physical insights to the synchronization and entrainment in the networks. Particularly, we will pay attention to the networks of circadian oscillations represented by Goodwin model [60,61] and show that our obtained results agree with existing experimental results and hence may be useful for further studying circadian rhythms.

1.3 Scopes of the thesis

The researches in this thesis are aimed at the following issues.

1. To propose an efficient and systematic method to design hierarchical decentralized optimal feedback controllers for hierarchical linear dynamical networks to achieve a prescribed hierarchical structure *by choosing appropriate LQR performance index including both global and local objectives.*

2. To develop a framework for systematically analyzing the entrainment in nonlinear oscillator networks.

Accordingly, there are two novelties in this thesis as stated below.

1. A new and systematic method to design *hierarchical state feedback optimal* LQR controllers for hierarchical linear dynamical networks in which:

   - The prescribed hierarchical structure of the network is achieved.
   - The global optimality of the designed controllers are obtained.
   - The controllers selectively shift the undesirable eigenvalues of the subsystems in the network.

   The output feedback controllers are also designed by introducing local observers for the subsystems. Furthermore, the proposed method is applicable for both homogeneous and heterogeneous hierarchical networks.

2. A framework for analyzing the entrainment in nonlinear oscillator networks excited by external periodic inputs with:

   - The conditions for the entrainment.
   - The relations between frequency, phases and amplitudes of induced network oscillations and those of external inputs.

1.4 Organization

The next contents in this thesis is organized as follows.

Chapter 2 introduces our viewpoints of muti-agent dynamical systems as hierarchical dynamical networks from which the contributions of this thesis are built. We first present an overview of the stabilization and synchronization in muti-agent dynamical systems. Next, our formulation of hierarchical dynamical systems is introduced. Accordingly, we describe the problems considered in this thesis and then our approaches to solve them.

Chapter 3 is devoted to design hierarchical, optimal LQR controllers for hierarchical, homogeneous linear dynamical systems. It is shown that by using both local and global performance indexes, the prescribed hierarchical structure of the network is achieved with a proper choices of weighting matrices. In addition, the global control objective is reflected in the global performance index. On the other hand, it is shown that the weighting matrices can be further selected such that only undesirable eigenvalues of the network are selectively shifted while the other eigenvalues are not affected.

Chapter 4 deals with a more general problem of designing hierarchical, optimal LQR controllers for hierarchical heterogeneous linear dynamical systems. A systematic approach is proposed utilizing similar ideas as in Chapter 3 to design hierarchical optimal LQR controllers.

Even though the subsystems contain different numbers of agents and hence have different local communication structures, the proposed controller is able to regulate them individually while maintaining a global target by incorporating the communication structure in the upper layer into a global performance index. Furthermore, the proposed method is then employed to solve a consensus problem in an application of vehicle platoons where the velocities of vehicles are controlled to be the same and their distances are controlled at desired values.

In Chapter 5, we propose a framework for analyzing the entrainment by external periodic signals in Goodwin-type nonlinear oscillator networks. The conditions for entrainment are proposed showing that the network structure should satisfy a specific condition and the frequency and amplitude of the external signal should be in certain ranges so that the entrainment can occur. Afterward, the monotonicity on the relations between the profiles of the exogenous input and network oscillations are figured out.

Chapter 6 investigates a more specific class of nonlinear oscillator networks than Chapter 5 namely third-order Goodwin oscillator networks. Though the order of oscillators in this chapter is lower than in Chapter 5, we show that the obtained results still capture essential features. Interestingly, utilizing the theoretical framework for a biological model of circadian networks give us some results that support the realistic experiments on circadian rhythms. Since the theoretical results relate to some biological parameters, they may give more insights and may be helpful for further studying of circadian oscillations.

Chapter 7 summarizes the works in the thesis and introduce some possible research topics for further investigations.

CHAPTER 2

STABILIZATION AND SYNCHRONIZATION FOR MULTI-AGENT DYNAMICAL NETWORKS

2.1 Literature Review

2.1.1 Hierarchical linear dynamical systems

Hierarchical dynamical systems, a type of networked systems universally appear in the real world, such as world wide web, internet, power grids, social networks [2–4], gene networks [5, 6], quorum-sensing networks [7]. Since the hierarchical structure provides an ability to achieve a global target in the network by designing the local communication topologies in the lower layers, the dimension of the network design problem can be significantly reduced to the design of local subsystems. Furthermore, the network can be designed in a decentralized fashion which is usually required in many practical systems.

Due to the advantages of the hierarchical networks, they have been extensively investigated [10–15, 62, 63]. By constructing the network based on a hierarchical graph, [62] showed that the formation of vehicles are stable if the graphs representing the communication structures in the layers are suitably selected. In addition, the eigenvalues of Laplacian matrix corresponding to the hierarchical graph are the eigenvalues of Laplacian matrices of subgraphs. The authors in [13] developed a hierarchical network for increasing the rate of consensus between vehicles but the structure in each layer is quite special that the vehicles communicates in a cyclic manner. Since the eigenvalues of circulant matrices were known, the eigenvalues of the system matrix in the whole network could be obtained. In a more recent paper [63], the authors introduced a concept of patterned linear systems where the identical agents in each subsystem were connected in a pattern, then the subsystems might be connected in another pattern and hence the total system had a hierarchy. However, the patterns considered in [63] are elementary and the information of all agents in each subsystem were transmitted to other subsystems. It should be noted that the hierarchical networks in the real world usually have dense interactions inside the sub-networks and sparse communication between them [4]. Therefore, the proposed frameworks in [13, 63, 64] seem to fail in possessing this characteristic.

This motivates the authors in [10–12] to generalize the hierarchical cyclic pursuit scheme and emphasize the effect of communications between subsystems in the network. More specifically, in the works [10–12], only aggregated information of the agents in a subsystem is utilized to communicate with other subsystems which led to a concept of low rank interconnection. This low rank property of intergroup connections was then shown to result in a faster conver-

gence speed than in [13]. Another nice feature is that the eigenvalues of the system matrix in the whole network could be explicitly determined from the eigenvalues of the matrices describing the local communication structures as seen in previous works. Hence, the approach of generalized hierarchical networks with low rank inter-group connections may give us an effective tool to design hierarchical network with expected eigenvalue distribution. However, this is not always true in fact. Then continuing this line of research, [14] and [15] presented a new class of low rank inter-group connection namely eigen-connection to design hierarchical networks with homogeneous and heterogeneous groups such that only some specific eigenvalues of the local interconnection matrices are selectively affected. To do so, the eigen-connection structure employed the eigenvectors of local interconnection matrices associated with unexpected eigenvalues and as a result, those eigenvalues were moved while the other eigenvalues remained unchanged. This new connection structure completely explained the obtained results in [10–12, 62]. Furthermore, it could be used not only for stabilizing the hierarchical network as in [14] but also for achieving other global goals such as consensus as in [15, 65].

Nevertheless, for practical systems, we cannot always choose the input or output matrices from the eigen-connection as in [14, 15, 65]. Moreover, even in case we can choose the input or output matrices, there were no systematic ways to design the output matrix as the input matrix was selected and vice versa. Figure 2.1 shows the a comparison of some existing results on hierarchical dynamical networks where the red-shaded area shows the limitations of the researches.

<table>
<tr><th>Researches</th><th>Inter-layer</th><th>I/O of subsystems</th><th>Inf. exchange</th><th>Agents</th><th>Topology</th><th>Network</th></tr>
<tr><td>[10]</td><td>dense</td><td>free to choose</td><td>Low rank</td><td rowspan="3">integrator</td><td>cyclic</td><td rowspan="6">homogeneous</td></tr>
<tr><td>[62]</td><td rowspan="8">sparse</td><td>could be given</td><td rowspan="2">High rank</td><td>special</td></tr>
<tr><td>[13, 63, 64]</td><td rowspan="5">free to choose</td><td rowspan="3">cyclic</td></tr>
<tr><td>[11]</td><td rowspan="5">Low rank</td></tr>
<tr><td>[12]</td><td rowspan="2">general</td></tr>
<tr><td>[14]</td><td rowspan="3">any</td></tr>
<tr><td>[15, 65]</td><td>heterogeneous</td></tr>
<tr><td>This thesis</td><td>could be given</td><td>integrator</td><td>both</td></tr>
</table>

Figure 2.1: Researches on hierarchical dynamical networks.

As seen above, many of the existing results on hierarchical networked control so far were for the analysis, and only a few works have dealt with the systematic synthesis. One of natural ways to develop a systematic procedure for control system design is to set up an LQR optimal control problem.

In [16], the authors attempted to find the optimal control laws for spatially invariant systems in a distributed fashion. Although the work was devoted to infinite dimensional systems, it still contributes valuable ideas on the design of distributed optimal LQR and H_2, H_∞ controllers. Subsequently, several other works [17, 18, 66] tried to figure out the classes of system matrices for the network such that the obtained LQR controller has a distributed or decentralized structure that is similar to the structure of the system matrices and therefore the information structure of the network is preserved. Motee et al. [17] used the notion of operator algebra to characterize the structure constraint for the system such that the optimal LQR controller also has that structure. Some operator algebras introduced in [17] are spatial decaying operators, ciculant matrices, upper and lower triangular matrices. Next, [18] presented a class of matrices namely almost Toeplitz matrices to show that the solution of the algebraic Riccati equation is almost Toeplitz as well. Consequently, in order to design the LQR controller for hierarchical networks, [66] generalized the operator algebras in [17] and introduced more general classes of structured matrices that preserve their structures under the LQR design approach. A simple hierarchical network was considered in [67] where a lower bidiagonal LQR controller was derived for a chain network of agents and then applied to obtain a sub-optimal controller for a platoon of heavy duty vehicles whose system matrix is tridiagonal. On the other hand, the paper [68] investigated identical decoupled systems and proposed a way to design controllers based on the LQR approach such that the identical systems are coupled in a special manner and the whole network is stable. Actually, the introduced feedback controller in [68] had a hierarchical structure with two layers and the considered system can be viewed as a hierarchical network of integrators, but the controller are sub-optimal with respect to the chosen performance index. For the consensus in the network of integrators, [19] designed an optimal Laplacian matrix utilizing two cost functions in the LQR problem where the communications between agents were taken into account in the weighting matrices. Massioni and Verhaegen [69] studied a class of two-layer hierarchical networks that is similar to the one in [14] and proposed an optimization-based approach to design distributed controllers for such type of networks. By transforming the system matrix into a block-diagonal form, i.e., the system could be decomposable, the controller design problem could be decomposed into smaller problems and the controller had the same structure as the system matrix. Note that the purposes of [69] and [14] are different although the hierarchical networks they considered have the same form. [69] aimed at designing a controller for such hierarchical networks while [14] attempted to design the system matrix having such kind of hierarchical structure.

On the other hand, the problem of designing LQR controller to selectively shift un-

expected eigenvalues of a system matrix has been investigated in several works for instance [21–24]. In [21] and [22], the authors presented a way to construct the weighting matrices based on the real and imaginary parts of the eigenvectors associated with unexpected eigenvalues such that only those eigenvalues are shifted while the other eigenvalues are not altered. Furthermore, the controller could be designed to move unexpected eigenvalues to a specified region in the left-haft complex plane. On the other hand, [23] and [24] introduced an iterative approach to change unexpected eigenvalues by choosing the weighting matrices from the eigenvectors associated with unexpected eigenvalues. Consequently, they showed the explicit relations between the unexpected eigenvalues and the ones that they would be moved to, and hence the domains of the new eigenvalues could be pointed out. The approaches in [21–24] can be effective for a single system without structure but how to use them for networked systems, especially hierarchical networked systems is not trivial. In other words, the methods for choosing the weighting matrices in [22–24] cannot readily be utilized for hierarchical networks. Figure 2.2 reviews some researches on LQR design for linear dynamical systems that are related to this direction.

♯ of changed eigenvalues	Single systems	Networked systems
all		[17–19, 66–68]
some selected	[21–24]	**This thesis**

Figure 2.2: Researches on feedback LQR controller design.

This thesis aims to propose a new, systematic method to design hierarchical decentralized optimal controllers for hierarchical dynamical networks based on the LQR approach with the notion of low rank inter-layer interactions examined in [14], [15]. In this new framework, the main focus is how to choose the weighting matrices in the LQR setting to derive a cooperative (state feedback or output feedback) controller which has a prescribed desirable hierarchical structure. As a solution to this problem, we propose a systematic design method by considering a class of performance indexes consisting of both global (or upper layer) and local (or lower layer) objectives with total control input penalty. Subsequently, the desired hierarchical structure of the network can be achieved by choosing suitable weighting matrices in the performance index. An advantage of our LQR-based synthesis method is to take the global/local objectives into account in addition to just stabilizing by decentralized control.

Furthermore, we present an idea of selective pole shift motivated from [21–24] for non-hierarchical systems where the LQR approach was utilized and the unexpected eigenvalues were selectively shifted by suitable choice of the weighting matrices. We then try to link the eigen-connection properties required in [14] with the idea of selective pole shift from the view

point of hierarchical decentralized control synthesis.

2.1.2 Entrainment in nonlinear oscillator networks

In this thesis, we pay attention to the entrainment in circadian networks since it is an interesting and important type of biological oscillations which appears in many species of living organisms such as bacterial [30], the fungus Neurospora [26], Drosophila [25], mammals [27–29]. It is now well known that there are cellular clocks inside the living organisms which can autonomously generate such circadian oscillations. Due to that internal clocks, the living creatures adjust their behaviors and adapt themselves to the changes of the outside environment. One of the most important features of the circadian clocks is that they can be entrained by periodic factors in the environment called zeitgebers [29, 70, 71]. This remarkable property of circadian rhythm therefore becomes a very important research topic to understand its underlying mechanisms. The sources of zeigebers can be natural or artificial for instance the daily light, temperature or food, among which the daily light is a main zeitgeber for the circadian network [29, 70–72]. From the control system viewpoint, we can consider the circadian network as a dynamical system forced by an external periodic input representing the zeitgeber. Without external inputs, that dynamical system itself exhibits an autonomous periodic oscillating pattern. Hence, a natural question raises up that how the oscillations produced by the system in presence of exciting periodic inputs look like. Particularly, it is worth seeing how the amplitudes and phases of induced oscillations in the system relate to those of exciting inputs. Therefore, the goal of this paper is to find out the answers for those problems and we will refer the daily light as the zeitgeber for the circadian system. This research has a significant importance since it is close to the practical applications, for instance the use of bright light or melatonin in clinical treatment of sleep disorders such as delayed/advanced sleep phase, seasonal affective disorder (SAD), shift work, etc.

In mammals, the circadian timing system has a master clock network in suprachiasmatic nucleus (SCN) which coordinates the circadian rhythms and regulates the peripheral circadian clocks [28, 29, 53–55]. The master circadian network is shown to be directly entrained by the daily Light-Dark cycle through the retina to coherently oscillate with period equal to Light-Dark period since circadian oscillators autonomously oscillate but their periods are not exactly 24 hrs [27, 29]. Furthermore, there exists a phase shift between synchronized circadian oscillations and Light-Dark signal [27, 29, 54, 70]. In [70], the phase shift was shown to be increasingly leading toward long periods and lagging toward short periods. There are also evidences from experiments, for example in older rats that to increase the amplitude of circadian oscillations to a desired level requires an increase in amplitude of Light-Dark signal [29]. However, the biological mechanisms under that phenomena have not been yet well understood though there are some researches on circadian rhythms based on dynamical system theory. They mostly focus on the synchrony of circadian oscillations and only a few papers deal with the dependence of amplitude and phase shift of circadian oscillations

to external inputs. The research in [26] focused on how the period of circadian rhythm and the temperature compensation depend on the stability of FRQ-protein. In [71], the relation between amplitudes of the zeitgeber and circadian oscillators was studied but only for the entrainment range. The article [73] studied the synchronization of circadian oscillators described by a modified Goodwin model where the oscillators communicate through a mean-field. The sync rate in a simple phase model which may be used for circadian network was investigated in [74]. Leloup et al. [25] investigated the effect of light's magnitude to the phase shift of circadian oscillations with some models of circadian rhythms in Drosophila and Neurospora, but no analytical relation was obtained.

2.2 Formulation of hierarchical dynamical systems

2.2.1 Homogeneous hierarchical dynamical systems

Consider a homogeneous multi-agent dynamical system having n_2 agents in which the mathematical model of each agent is as follows,

$$\begin{aligned} \dot{x}_i &= A_1 x_i + B_1 u_i, \\ y_i &= C_1 x_i,\ i = 1, \ldots, n_2, \end{aligned} \tag{2.1}$$

with $A_1 \in \mathbb{R}^{n_1 \times n_1}$, $B_1 \in \mathbb{R}^{n_1 \times m}$, $0 < m \leq n_1$, $C_1 \in \mathbb{R}^{p \times n_1}$, where $x_i \in \mathbb{R}^{n_1}$ is the state vector of the ith subsystem, and $u_i \in \mathbb{R}^m$ and $y_i \in \mathbb{R}^p$ are the vectors containing all the inputs and measured outputs of the ith subsystem, respectively. Let us denote

$$u = [u_1^T, \ldots, u_{n_2}^T]^T, y = [y_1^T, \ldots, y_{n_2}^T]^T, x = [x_1^T, \ldots, x_{n_2}^T]^T.$$

Subsequently, the whole network model now can be described by

$$\begin{aligned} \dot{x} &= (I_{n_2} \otimes A_1)x + (I_{n_2} \otimes B_1)u, \\ y &= (I_{n_2} \otimes C_1)x. \end{aligned} \tag{2.2}$$

From the theoretical point of view, such a multi-agent system can be considered as a two-layer hierarchical system, where each agent is cast as a subsystem in the lower layer and those subsystems are interconnected in the upper layer. Accordingly, the interconnection among agents in a multi-agent system can be treated in the associated two-layer hierarchical system. The circumstance of hierarchical systems with more layers can be treated in a similar manner.

Figure 2.3 displays an example showing how a network of linearized Testosterone hormone oscillators can be treated as a hierarchical network under our formulation where each hormone oscillator is an agent.

2.2.2 Heterogeneous hierarchical dynamical systems

Consider a multi-agent system having N agents whose model is represented by

$$\begin{aligned} \dot{x}_i &= A_i x_i + B_i u_i, \\ y_i &= C_i x_i,\ i = 1, \ldots, N, \end{aligned} \tag{2.3}$$

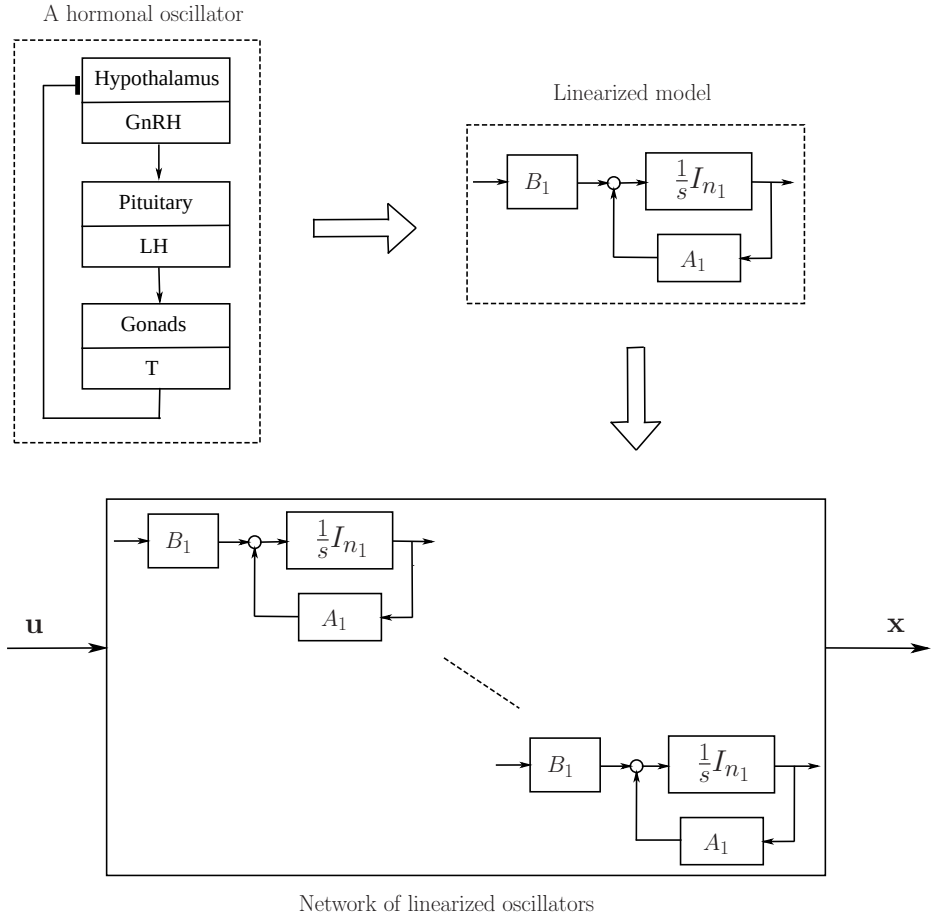

Figure 2.3: Illustration for the formulation of a homogeneous hierarchical network.

where $A_i \in \mathbb{R}^{n_i \times n_i}$, $B_i \in \mathbb{R}^{n_i \times m_i}$, $0 < m_i \leq n_i$, $C_i \in \mathbb{R}^{p_i \times n_i}$, $x_i \in \mathbb{R}^{n_i}$ is the state vector of the ith subsystem, and $u_i \in \mathbb{R}^{m_i}$ and $y_i \in \mathbb{R}^{p_i}$ are the vectors containing all the inputs and measured outputs of the ith subsystem, respectively. Denote

$$u = [u_1^T, \ldots, u_N^T]^T, x = [x_1^T, \ldots, x_N^T]^T, y = \left[y_1^T, \quad \ldots, \quad y_N^T\right]^T,$$

then the whole network model is described by

$$\begin{aligned} \dot{x} &= \text{diag}\{A_i\}_{i=1,\ldots,N} x + \text{diag}\{B_i\}_{i=1,\ldots,N} u, \\ y &= \text{diag}\{C_i\}_{i=1,\ldots,N} x. \end{aligned} \tag{2.4}$$

Similarly to the scenario of homogeneous multi-agent systems, we can view this heterogeneous multi-agent system as a two-layer heterogeneous hierarchical system, where each agent is cast as a subsystem in the lower layer and that subsystems are interconnected in the upper layer. And the situation of hierarchical systems with more layers can be extended straightforwardly.

An example is shown in Figure 2.4 where the network includes N groups of vehicles, each group may have a different number of vehicles and the communicating topology inside the groups are different. This vehicle network can be cast as a third-layer hierarchical network where each vehicle is a subsystem in the bottom layer, the vehicles in each group are

communicated in the middle layer, and the groups of vehicles are interconnected in the top layer.

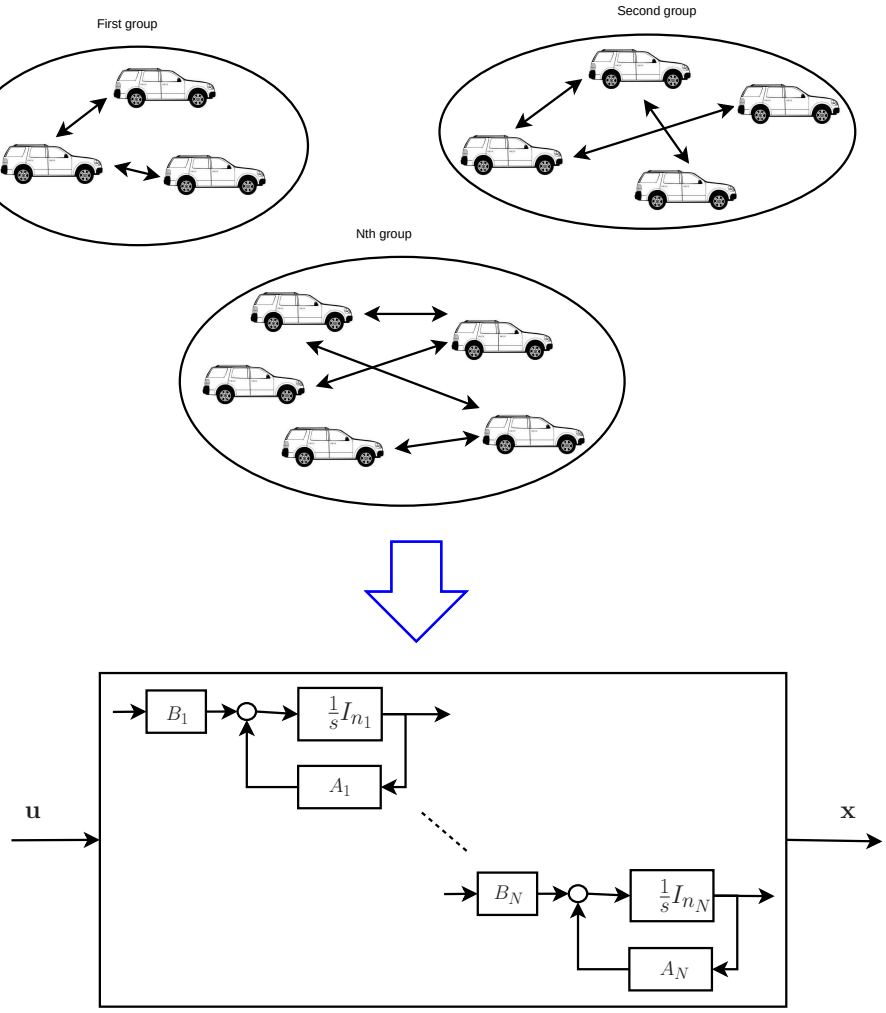

Figure 2.4: Illustration for the formulation of a heterogeneous hierarchical network.

2.2.3 Nonlinear oscillator networks

In this thesis, we consider networks of oscillators represented by qth-order ($q \geq 2$) Goodwin-type model

$$\begin{cases} \dfrac{dX_1}{d\tau} &= k_1 \dfrac{K^p}{K^p + X_q^p} - k_{q+1} X_1, \\ \dfrac{dX_2}{d\tau} &= k_2 X_1 - k_{q+2} X_2, \\ &\vdots \\ \dfrac{dX_q}{d\tau} &= k_q X_{q-1} - k_{2q} X_q. \end{cases} \tag{2.5}$$

This model is a generalization of the classical 3rd-order Goodwin model in [25, 26, 60, 61] to represent a process with nonlinear negative feedback which may be found for instance in

biochemical networks. Then we can rewrite each Goodwin-type oscillator as follows,

$$\begin{cases} z &= h(s)u, \\ u &= f(z), \end{cases} \tag{2.6}$$

where z is used to denote x_q, $h(s) = \dfrac{1}{(s+b_1)(s+b_2)\cdots(s+b_q)}$ and $f(z) = \dfrac{1}{1+z^p}$. Assuming that the oscillator network has n oscillators interacting through an interconnection matrix A then the whole network model under the effect of the same external input $w(t)$ is described as follows,

$$\begin{cases} z &= H(s)u, \\ y &= \mathcal{F}z, \\ u &= Ay + w\mathbf{1}_n, \end{cases} \tag{2.7}$$

where $H(s) = h(s)I_n, \mathcal{F} = fI_n$ and

$$\begin{aligned} u &= \begin{bmatrix} u_1 & u_2 & \dots & u_n \end{bmatrix}^T, \\ y &= \begin{bmatrix} y_1 & y_2 & \dots & y_n \end{bmatrix}^T, \\ z &= \begin{bmatrix} z_1 & z_2 & \dots & z_n \end{bmatrix}^T. \end{aligned}$$

Figure 2.5 shows the block diagram of the network described in (2.7). Then the analysis for this type of nonlinear oscillator networks excited by an external periodic input $w(t)$ includes the following two problems:

1. What are the conditions for the entrainment of network oscillations by the exogenous input $w(t)$?

2. How the entrained oscillations $z_k, k = 1, \dots, n$ relate to the exogenous input $w(t)$?

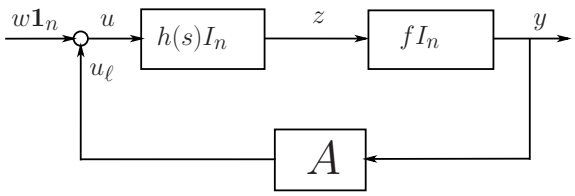

Figure 2.5: Network model of interconnected Goodwin-type oscillators

2.3 Approaches

2.3.1 Design of hierarchical linear dynamical networks

In this section, we briefly introduce our proposed systematic method to design hierarchical feedback controllers for both homogeneous and heterogeneous hierarchical linear dynamical networks. As aforementioned, we only consider two-layer hierarchical networks for simplicity and clarity. Then the method can be straightforwardly extended to hierarchical networks with

more layers. Note that an analysis framework for this type of hierarchical linear dynamical networks has been existed in [14] and [15] but a systematic synthesis approach is still lacking.

As presented earlier, there are two problems in the hierarchical feedback controller design for both homogeneous and heterogeneous hierarchical linear dynamical networks. The primal problem is to design a hierarchical controller to preserve a prescribed hierarchical structure of the network. The next problem is to design a hierarchical controller to selectively shift the undesirable eigenvalues of the subsystems (agents) in the network. Accordingly, this thesis aims to propose a new, systematic method to design hierarchical decentralized optimal controllers for hierarchical dynamical networks based on the LQR approach.

Then the question is under what LQR setting, the desired hierarchical structure of the network can be achieved. In other words, the main focus is how to choose the weighting matrices in the LQR setting to derive a cooperative optimal controller which has a prescribed desirable hierarchical structure. One of the solutions for that question is presented in the thesis where a class of performance indexes is considered which includes both global and local objectives with control input penalty. As a result, the desired structure of the network can be obtained by choosing proper weighting matrices in the performance index.

In the following, we shortly introduce our proposed LQR setting for homogeneous hierarchical linear dynamical networks (2.2). Consider the following performance index

$$J := J_x + J_u \; ; \;\; J_x := J_{x,\mathcal{L}} + J_{x,\mathcal{G}}, \tag{2.8}$$

where J_x relates to the local and global objectives, which is the sum of $J_{x,\mathcal{L}}$ and $J_{x,\mathcal{G}}$, and J_u is a penalty for the control input required to the whole system represented by

$$J_u = \int_0^\infty u(t)^T \mathcal{R} u(t)\, dt, \tag{2.9}$$

where $\mathcal{R}\ (\succ 0) \in \mathbb{R}^{m\times m}$. $J_{x,\mathcal{L}}$ is a local performance index composing of the individual penalties for the states of subsystems represented by

$$J_{x,\mathcal{L}} = \int_0^\infty x(t)^T (I_N \otimes Q_\ell) x(t)\, dt, \tag{2.10}$$

where $Q_\ell (\succeq 0) \in \mathbb{R}^{n_1\times n_1}$. $J_{x,\mathcal{G}}$ corresponds to a global performance index taking into account the information structure of the network captured by a matrix $K \in \mathbb{K}_s$, given by

$$J_{x,\mathcal{G}} = \int_0^\infty x(t)^T (K \otimes Q_g) x(t)\, dt, \tag{2.11}$$

where $Q_g\ (\succeq 0) \in \mathbb{R}^{n_1\times n_1}$, K is a positive semidefinite. Then the performance index can be rewritten as follows,

$$J = \int_0^\infty (x^T \mathcal{Q} x + u^T \mathcal{R} u) dt, \tag{2.12}$$

where

$$\mathcal{Q} = I_N \otimes Q_\ell + K \otimes Q_g. \tag{2.13}$$

It is shown from the optimal control theory [75] that the LQR controller is computed by $u = \mathcal{F}x$, $\mathcal{F} \in \mathbb{R}^{(mN)\times(n_1N)}$ where

$$\mathcal{F} = -\mathcal{R}^{-1}\mathcal{B}^T\mathcal{P},$$

with $\mathcal{P} \in \mathbb{R}^{(n_1N)\times(n_1N)}$ is the unique positive definite solution of the following Riccati equation

$$\mathcal{P}\mathcal{A} + \mathcal{A}^T\mathcal{P} + \mathcal{Q} - \mathcal{P}\mathcal{B}\mathcal{R}^{-1}\mathcal{B}^T\mathcal{P} = 0. \tag{2.14}$$

Consequently, for arbitrary weighting matrix $\mathcal{R}$, the solution $\mathcal{P}$ of the Riccati equation (2.14) is centralized despite a fact that the system matrices $I_{n_2} \otimes A_1, I_{n_2} \otimes B_1$ and the weighting matrix $\mathcal{Q}$ have hierarchical structures. As a result, the controller $\mathcal{F}$ is centralized which is unexpected for our network. *Therefore, the problem now is how to select the weighting matrix $\mathcal{R}$ such that the solution $\mathcal{P}$ of the Riccati equation (2.14) has a hierarchical structure and moreover, the obtained feedback controller $\mathcal{F}$ have a similar hierarchical structure that would result in the prescribed hierarchical structure for the given network.*

The existing distributed LQR designs [16–20, 66, 68] only consider the contexts that the system matrices and weighting matrices belong to some special classes namely operator algebra or semigroups. Nevertheless, in our setting, those matrices do not belong to any operator algebra or semi-groups, and hence the results in [16–20, 66, 68] cannot be applied. *This thesis provides one answer for the problem by choosing the weighting matrix $\mathcal{R}$ under the form $\mathcal{R}^{-1} = I_N \otimes R_\ell + K \otimes R_g$ with one more relation between Q_g and R_g, then it is shown that the derived controller gives the network the prescribed hierarchical structure.*

The figure in the following demonstrates our proposed hierarchical feedback controller design for homogeneous hierarchical dynamical networks. A similar configuration is applied for heterogeneous hierarchical multi-agent networks. The details in the approach and the numerical examples will be given in Chapter 3 and Chapter 4.

2.3.2 Analysis of nonlinear oscillator networks

To analyze the entrainment of nonlinear oscillator networks driven by exogenous periodic inputs, we employ the harmonic balance method to approximate the nonlinear dynamics as linearized gains of the amplitudes of the harmonic components in the network oscillations. Next, by balancing the corresponding harmonic components in the external inputs and network oscillations, we obtain the harmonic equations which shows the relations between the frequency, amplitudes, phases of the induced network oscillations and those of external periodic inputs.

Suppose that the external periodic input including the harmonics up to m-th order as follows,

$$w(t) = \kappa_0 + \kappa_1 \sin(\omega t + \zeta_1) + \ldots + \kappa_m \sin(m\omega t + \zeta_m), \tag{2.15}$$

where $\omega > 0$ is the frequency, $\kappa_0, \kappa_1, \ldots, \kappa_m > 0$ are the bias and amplitudes of harmonic components, $\zeta_1, \ldots, \zeta_m$ are the phases of harmonic components, respectively. Then we first

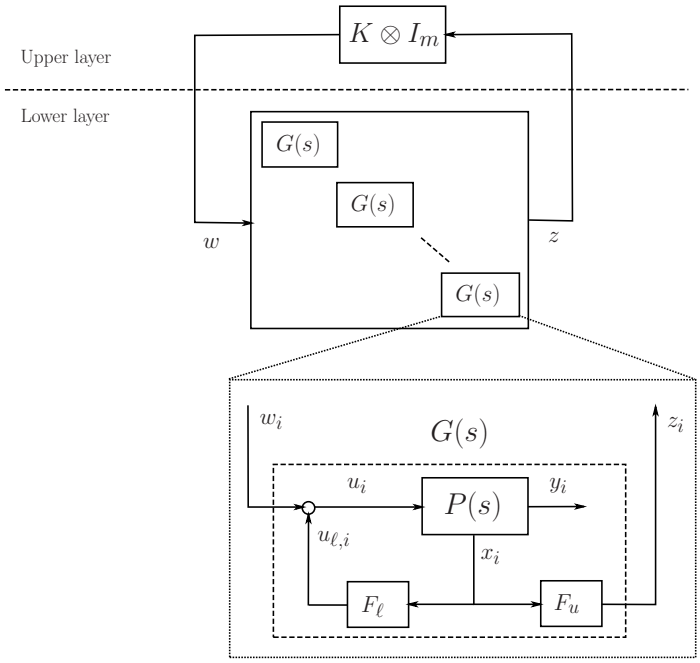

Figure 2.6: Demonstration of a homogeneous hierarchical network and the hierarchical feedback controller design.

assume that the frequency of the induced network oscillations is entrained to the frequency ω of the exogenous input. Subsequently, we approximate the induced network oscillations by

$$\begin{aligned} z_k(t) &= \alpha_{0k} + \alpha_{1k}\sin(\omega t + \varphi_{1k}) + \dots \\ &\quad + \alpha_{mk}\sin(m\omega t + \varphi_{mk}), \\ y_k(t) &= \sigma_{0k}\alpha_{0k} + \sigma_{1k}\alpha_{1k}\sin(\omega t + \varphi_{1k}) + \dots \\ &\quad + \sigma_{mk}\alpha_{mk}\sin(m\omega t + \varphi_{mk}), k = 1, \dots, n, \end{aligned} \tag{2.16}$$

where $\sigma_{0k}, \sigma_{lk}, l = 1, \dots, m$ are describing functions [76]. Based on this approximation, we show how the bias α_{0k} and the amplitudes α_{1k} and the phases φ_{lk} are related to the bias κ_0, the amplitudes κ_l and the phases ζ_l of the external input, $l = 1, \dots, m; k = 1, \dots, n$. Then we propose the condition for the entrainment to occur. Consequently, we further investigate the monotonicity of those relations based on the monotonicity of the nonlinear dynamics. The details in the analysis will be presented in Chapter 5 and Chapter 6.

CHAPTER 3

LQR DESIGN FOR HOMOGENEOUS HIERARCHICAL NETWORKS

3.1 Introduction

The synthesis problem for homogeneous hierarchical multi-agent dynamical networks is studied in this chapter. For simplicity in notation and clarity of results, we only consider two-layer networks but the design for networks with more layers can be executed in a similar manner. A homogeneous two-layer network composes of identical subsystems or groups of agents. In the previous study [14], an analysis framework was proposed to analyze the eigenvalue distribution and the behaviors in these homogeneous hierarchical networks. More specifically, [14] assumed that the the input or output matrices of the subsystems are defined based on the right or left eigenvectors of the interconnection matrix inside each subsystem, then [14] was able to determine the eigenvalue distribution in the whole network as well as the behaviors of the subsystems. This framework is quite general which includes the previous results [10–13,62,63] as special cases and gives a clue for efficiently designing hierarchical networks. Nevertheless, a systematic approach to synthesize this type of hierarchical networks has not been existed so far.

This chapter presents a new systematic method to design hierarchical decentralized optimal controllers for homogeneous dynamical networks based on LQR approach. *As aforementioned, the question is under what LQR setting, the desired hierarchical structure of the network can be achieved.* Note that in [20], an LQR design was introduced for some classes of homogeneous hierarchical networks where the system matrices, the couplings in the network and the weighting matrices in the LQR performance index belong to some special structures namely operator algebras or semi-groups. However, in our class of systems, the assumption of those special structures is not considered and hence the method proposed in [20] cannot be applied.

One of the answers for the given question which is a contribution of this chapter is the employment of a class of performance indexes including both global and local objectives with control input penalty. As a result, the desired structure of the network can be obtained by choosing proper weighting matrices in the performance index.

The second novelty of this chapter is on the ability of the proposed state feedback hierarchical optimal controller to selectively shift the undesirable eigenvalues of the subsystems. Of course, each subsystem can use a local controller to shift its unexpected eigenvalues as in [21–24], however by interacting with other subsystems both global (e.g. low-rank intercon-

nection among subsystems for rapid consensus [10–12]) and local objectives (e.g. selective shift of undesired eigenvalues) in the network can be achieved. Then, by borrowing the ideas in [15] and [21–24] to our proposed hierarchical optimal controller, it is able to selectively shift the undesirable eigenvalues of the subsystems without affecting other eigenvalues.

In the proposed method, we first assume that all the states of agents are measurable then a state feedback hierarchical optimal controller is designed. Next, when only some quantities of the agents' states or outputs of agents can be measured, we introduce local state observers which reduce the output feedback design problem to a state feedback design problem. Then it is proved that the observed states converge to the real states of agents and the objectives of the network are achieved by the proposed output feedback hierarchical controller.

3.2 Problem Formulation

3.2.1 Homogeneous Hierarchical Networked Dynamical Systems

Consider a homogeneous multi-agent dynamical system in which the mathematical model of each agent is as follows,

$$\begin{aligned} \dot{x}_i &= A_1 x_i + B_1 u_i, \\ y_i &= C_1 x_i,\ i = 1, \ldots, N, \end{aligned} \tag{3.1}$$

with $A_1 \in \mathbb{R}^{n_1 \times n_1}$, $B_1 \in \mathbb{R}^{n_1 \times m}$, $0 < m \leq n_1$, $C_1 \in \mathbb{R}^{p \times n_1}$, where $x_i \in \mathbb{R}^{n_1}$ is the state vector of the ith subsystem, and $u_i \in \mathbb{R}^m$ and $y_i \in \mathbb{R}^p$ are the vectors containing all the inputs and measured outputs of the ith subsystem, respectively. Denote $P(s)$ the transfer function of the subsystems, i.e.,

$$P(s) = C_1(sI_{n_1} - A_1)^{-1}B_1.$$

Hence, the initial hierarchical network without controller can be represented by

$$\begin{aligned} \dot{x} &= \mathcal{A}_1 x + \mathcal{B}_1 u, \\ y &= \mathcal{C}_1 x, \end{aligned} \tag{3.2}$$

where $\mathcal{A}_1 = I_N \otimes A_1, \mathcal{B}_1 = I_N \otimes B_1, \mathcal{C}_1 = I_N \otimes C_1$, $x = [x_1^T, \ldots, x_N^T]^T$, $u = [u_1^T, \ldots, u_N^T]^T$, $y = [y_1^T, \ldots, y_N^T]^T$. We here assume that all the states of agents are measurable, i.e., $C_1 = I_{n_1}$ and hence $y_i = x_i$. In the case where only partial state variables are measurable, we can design a stabilizing hierarchical output feedback controller by combining a completely local observer which estimates the local state and the obtained state feedback controller. Due to space limitation, we do not present it in this paper.

The information exchange in the real multi-agent systems controlled with a decentralized fashion is as follows: (i) Each agent sends out a unique aggregated signal to collaborate with other connected agents to realize the global objectives in addition to the local objectives. (ii) Simultaneously, each agent is able to receive the signals sent by other connected agents individually.

Let us denote $\mathcal{G}$ the graph representing the information structure in a multi-agent system, where each node in $\mathcal{G}$ stands for an agent and each edge in $\mathcal{G}$ represents the interconnection between two agents. In this paper, we assume that the communications between agents are bidirectional, i.e., $\mathcal{G}$ is undirected. Then, the information structure in a multi-agent system can be mathematically characterized by a matrix K, where the elements of K stands for the weights on the edges of $\mathcal{G}$, or equivalently the weights for the information exchanges between agents. Denote $\mathcal{E}$ the edge set of $\mathcal{G}$, then the class of K is defined by

$$\mathbb{K}_s := \{K = K^T \in \mathbb{R}^{N\times N} \mid K_{ij} = 0 \text{ if } (i,j) \notin \mathcal{E}\}. \tag{3.3}$$

From the theoretical point of view, such a multi-agent system can be considered as a two-layer hierarchical system, where each agent is cast as a subsystem in the lower layer and those subsystems are interconnected in the upper layer. Accordingly, the interconnection among agents in a multi-agent system can be treated in the associated two-layer hierarchical system as follows. The ith subsystem tries to collaborate with all other subsystems by sending a unique aggregated signal $z_i \in \mathbb{R}^m$, receiving a partial set of aggregated signals $z_j \in \mathbb{R}^m$ from the jth subsystem satisfying $(i,j) \in \mathcal{E}$, and determining a kind of reference command $w_i \in \mathbb{R}^m$ for the global objectives in the simplest way as

$$w_i = \sum_{(i,j)\in\mathcal{E}} K_{ij} z_j,\ i = 1,\ldots,N. \tag{3.4}$$

Moreover, we also allow each subsystem to be implemented with a local controller whose output is denoted by $u_{\ell,i}, i = 1,\ldots,N$. Hence, the control input for each subsystem has the following form

$$u_i = w_i + u_{\ell,i}. \tag{3.5}$$

As a result, the control input for the whole hierarchical network is represented by

$$u = w + u_\ell = (K \otimes I_m)z + u_\ell, \tag{3.6}$$

where $w = \begin{bmatrix} w_1^T & \cdots & w_N^T \end{bmatrix}^T$, $z = \begin{bmatrix} z_1^T & \cdots & z_N^T \end{bmatrix}^T$, $u_\ell = \begin{bmatrix} u_{\ell,1}^T & \cdots & u_{\ell,N}^T \end{bmatrix}^T$. Subsequently, Figure 3.1 describes the whole hierarchical dynamical networked control system, where the interaction among subsystems is represented by the term $K \otimes I_m$, $G(s)$ denotes the transfer function of the locally controlled subsystems (agents).

The question here is how to design $z_i, u_{\ell,i}$ $(i = 1,\ldots,N)$ and $K \in \mathbb{K}_s$ in a systematic way to achieve both the global and local objectives as well as the stabilization of the whole networked system. This is actually our hierarchical decentralized controller design, which will be explained in the next subsection.

3.2.2 Homogeneous Hierarchical Decentralized Design Problem

For the given homogeneous network, there are two design scenarios for hierarchical decentralized controllers namely (i) state feedback design and (ii) output feedback design. If all

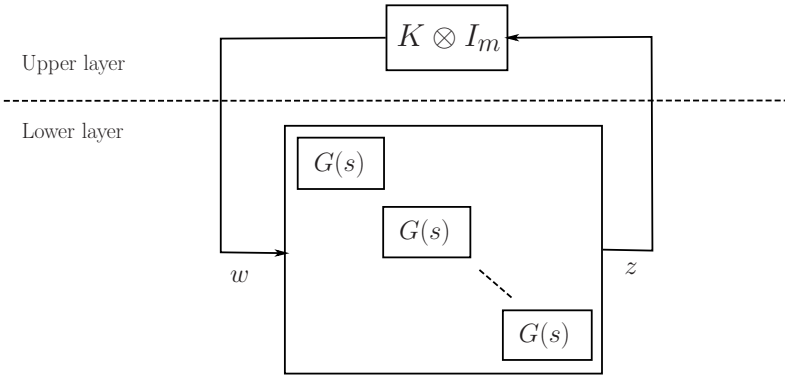

Figure 3.1: Block diagram of homogeneous hierarchical networked control system.

the states of agents, x_i $(i = 1, \ldots, N)$, are available, our goal is to design a hierarchical state feedback controller. On the other hand, in the situation that only partial agents' states, y_i $(i = 1, \ldots, N)$, can be measured, we need to design a hierarchical output feedback controller. Later on, we will prove that utilizing the local observers can reduce the output feedback design problem to the state feedback case.

First, we consider the state feedback design scenario. Figure 3.2 shows the structure of the locally controlled subsystems (agents) in the lower layer where the subsystems (agents) are controlled by local, state feedback controllers.

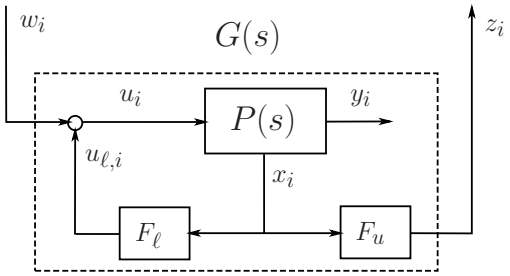

Figure 3.2: Block diagram of state feedback case for homogeneous networks.

Consequently, the state feedback design problem is stated as follows.

State feedback design problem: For the given network $\mathcal{G}$ with (A_1, B_1) controllable, the design problem is to determine the higher level interconnection gain $K \in \mathbb{K}_s$ and the lower layer state feedback gains $F_\ell \in \mathbb{R}^{m \times n_1}$ and $F_u \in \mathbb{R}^{m \times n_1}$, which respectively produce the local feedback signal $u_{\ell,i} = F_\ell x_i$ and the aggregated signal to be sent $z_i = F_u x_i$ for $i = 1, \ldots, N$.

The reference command (3.4) of the ith subsystem and the control input (3.6) yields a state feedback form for $\dot{x} = \mathcal{A}_1 x$ as

$$u = \mathcal{F} x,$$

where $\mathcal{F}$ belongs to the following class:

$$\mathbb{F}_K := \{\mathcal{F} \in \mathbb{R}^{(mN) \times (n_1 N)} \mid \mathcal{F} = I_N \otimes F_\ell + K \otimes F_u\}. \tag{3.7}$$

The first term $I_N \otimes F_\ell$ in the expression of $\mathcal{F}$ is associated with the local feedback signals $u_{\ell,i}, i = 1, \ldots, N$ while the second term $K \otimes F_u$ represents the interactions among subsystems through the aggregated signals $z_i, i = 1, \ldots, N$ since

$$(K \otimes F_u)x = [(K \otimes I_m)(I_N \otimes F_u)]x,$$

Consequently, the sate feedback design problem is reduced to determine F_ℓ, F_u and $K \in \mathbb{K}_s$. In order to do this systematically, we will propose a procedure based on the LQR (Linear Quadratic Regulator) design, which can take the global/local objectives into account, in the next two sections.

Second, we consider the hierarchical output feedback design situation.

Output feedback design problem: For the given network with (A_1, B_1, C_1) controllable and observable, the design problem is to determine a local output feedback controller $L(s)$ such that

$$\begin{bmatrix} u_{\ell,i} \\ z_i \end{bmatrix} = L(s) \begin{bmatrix} y_i \\ u_i \end{bmatrix}, \tag{3.8}$$

which at least stabilizes the whole networked system together with a suitable selection of $K \in \mathbb{K}_s$.

To do so, we introduce the following Luenberger-type local observer for each subsystem

$$\begin{array}{ll} \dot{\hat{x}}_i & = A_1\hat{x}_i + B_1u_i + H_1(\hat{y}_i - y_i), \\ \hat{y}_i & = C_1\hat{x}_i, i = 1, \ldots, N, \end{array} \tag{3.9}$$

where $\hat{x}_i \in \mathbb{R}^{n_1}$, $\hat{y}_i \in \mathbb{R}^p$ are the vectors of estimated state and output of the local observer in the ith subsystem, respectively and $H_1 \in \mathbb{R}^{n_1 \times p}$ is the gain matrix of the local observer such that $A_1 + H_1C_1$ is stable. Summing up all the local observers, we obtain an observer for the given homogeneous subsystems as follows:

$$\begin{array}{ll} \dot{\hat{x}} & = \mathcal{A}_1\hat{x} + \mathcal{B}_1u + \mathcal{H}_1(\hat{y} - y), \\ \hat{y} & = \mathcal{C}_1\hat{x}, \end{array} \tag{3.10}$$

where $\hat{x} = \begin{bmatrix} \hat{x}_1^T & \cdots & \hat{x}_N^T \end{bmatrix}^T$, $\hat{y} = \begin{bmatrix} \hat{y}_1^T & \cdots & \hat{y}_N^T \end{bmatrix}^T$, $\mathcal{H}_1 = I_N \otimes H_1$. It can be clearly seen that the observer (3.10) is fully *decentralized* since it only includes local observers for subsystems.

Subsequently, we denote $e := x - \hat{x}$ the error vector between the real state x and the estimated state $\hat{x}$ and employing the designed stabilizing, hierarchical state feedback controller $u = \mathcal{F}\hat{x}$, as same as the state feedback case, the closed-loop hierarchical network model in this scenario becomes

$$\begin{array}{ll} \dot{x} & = (\mathcal{A}_1 + \mathcal{B}_1\mathcal{F})x - [I_N \otimes (B_1F_\ell) + K \otimes (B_1F_u)]e, \\ \dot{e} & = (\mathcal{A}_1 + \mathcal{H}_1\mathcal{C}_1)e, \end{array} \tag{3.11}$$

Since $\mathcal{A}_1 + \mathcal{B}_1\mathcal{F}$ is stable and we can design $\mathcal{H}_1$ such that $\mathcal{A}_1 + \mathcal{H}_1\mathcal{C}_1$ is stable, the estimated state $\hat{x}(t)$ will converges to the real state $x(t)$ as $t \to \infty$ and the whole hierarchical homogeneous network is stable.

This leads to the state space realization of the local controller $L(s)$ as follows:

$$\begin{aligned}\dot{\hat{x}}_i &= (A_1 + H_1C_1)\hat{x}_i + \begin{bmatrix}B_1 & H_1\end{bmatrix}\begin{bmatrix}u_i\\ y_i\end{bmatrix},\\ \begin{bmatrix}u_{\ell,i}\\ z_i\end{bmatrix} &= \begin{bmatrix}F_\ell & F_u\end{bmatrix}^T \hat{x}_i.\end{aligned}$$

Hence, the design of output feedback case can be reduced to the design of the state feedback case by introducing the local observers (3.9).

3.3 Homogeneous Hierarchical State Feedback LQR Design

3.3.1 Class of Performance Indexes

We introduce in the following the class of quadratic performance indexes in the LQR design, which clearly captures our situation mentioned in the previous section,

$$J := J_x + J_u \;;\;\; J_x := J_{x,\mathcal{L}} + J_{x,\mathcal{G}}, \tag{3.12}$$

where J_x relates to the local and global objectives, which is the sum of $J_{x,\mathcal{L}}$ and $J_{x,\mathcal{G}}$, and J_u is a penalty for the control input required to the whole system represented by

$$J_u = \int_0^\infty u(t)^T \mathcal{R} u(t)\, dt, \tag{3.13}$$

where $\mathcal{R}\ (\succ 0) \in \mathbb{R}^{m\times m}$.

$J_{x,\mathcal{L}}$ is a local performance index composing of the individual penalties for the states of subsystems represented by

$$J_{x,\mathcal{L}} = \int_0^\infty x(t)^T (I_N \otimes Q_\ell) x(t)\, dt, \tag{3.14}$$

where $Q_\ell (\succeq 0) \in \mathbb{R}^{n_1\times n_1}$. $J_{x,\mathcal{G}}$ corresponds to a global performance index taking into account the information structure of the network captured by a matrix $K \in \mathbb{K}_s$, given by

$$J_{x,\mathcal{G}} = \int_0^\infty x(t)^T (K \otimes Q_g) x(t)\, dt, \tag{3.15}$$

where $Q_g\ (\succeq 0) \in \mathbb{R}^{n_1\times n_1}$. We here assume that K in $J_{x,\mathcal{G}}$ is restricted to the class of positive semidefinite interconnection defined by

$$\mathbb{K}_s^+ := \{K \in \mathbb{K}_s \mid K \text{ is positive semidefinite}\}, \tag{3.16}$$

in order to guarantee the positivity of $J_{x,\mathcal{G}}$. Note that $J_{x,\mathcal{G}}$ is employed to improve the control performance, since the elements of K as well as matrix Q_g put some weights on the relative states of subsystems leading to the improvement on the convergence of subsystems' states.

Subsequently, rewriting the performance index (3.12) as follows,

$$J = \int_0^\infty (x^T \mathcal{Q} x + u^T \mathcal{R} u) dt, \tag{3.17}$$

where

$$\mathcal{Q} = I_N \otimes Q_\ell + K \otimes Q_g. \tag{3.18}$$

Motivated by the class of hierarchical decentralized feedback gains (3.7) and the structure of the weighting matrix $\mathcal{Q}$, we select the weighting matrix $\mathcal{R}$ with the following form

$$\mathcal{R}^{-1} = I_N \otimes R_\ell + K \otimes R_g, \tag{3.19}$$

where $R_\ell \in \mathbb{R}^{m\times m}, R_g \in \mathbb{R}^{m\times m}$, $R_\ell \succ 0, R_g \succ 0$. Then we aim at designing a hierarchical decentralized optimal LQR controller for the given hierarchical network (3.2) which minimizes the performance index (3.12).

Employing the following assumptions:

A1: $(\mathcal{A}_1, \mathcal{B}_1)$ is controllable,

A2: $(\mathcal{Q}^{1/2}, \mathcal{A}_1)$ is observable,

it is shown from the optimal control theory [75] that such an LQR controller is computed by $u = \mathcal{F}x$, $\mathcal{F} \in \mathbb{R}^{(mN)\times(n_1N)}$ where

$$\mathcal{F} = -\mathcal{R}^{-1}\mathcal{B}^T\mathcal{P},$$

with $\mathcal{P} \in \mathbb{R}^{(n_1N)\times(n_1N)}$ is the unique positive definite solution of the following Riccati equation

$$\mathcal{P}\mathcal{A}_1 + \mathcal{A}_1^T\mathcal{P} + \mathcal{Q} - \mathcal{P}\mathcal{B}_1\mathcal{R}^{-1}\mathcal{B}_1^T\mathcal{P} = 0. \tag{3.20}$$

In the previous works, it was proved that if $\mathcal{A}_1, \mathcal{B}_1, \mathcal{C}_1, \mathcal{R}, \mathcal{Q}$ belong to some operator algebra [17] or semigroup [20] then the solution $\mathcal{P}$ of the Riccati equation (3.20) also belongs to that algebra or semigroup. As a result, they could prove that the LQR controller gain $\mathcal{F}$ has a similar property. However, in our current setting, $\mathcal{A}_1, \mathcal{B}_1, \mathcal{C}_1, \mathcal{R}, \mathcal{Q}$ do not belong to any operator algebra or semigroup. Therefore, it is not possible to show that with the choice of the weighting matrices as in (3.18) and (3.19), $\mathcal{P}$ has the same structure.

Therefore, in the next subsection, we will propose another way of choosing the weighting matrices $\mathcal{Q}$ and $\mathcal{R}$ of the forms of (3.18) and (3.19), respectively, which completely fits our situation and purpose.

3.3.2 State Feedback Design Procedure

In this subsection, we propose a systematic design procedure for state feedback hierarchical decentralized controllers which consists of four steps. Employing this design procedure, we obtain a hierarchical feedback controller which fulfills the two design requirements in the state feedback design problem.

Here are the steps of the design procedure.

- **Step 1 (Local LQR Design) :**
  Select the weighting matrices for the local objectives, $Q_\ell \in \mathbb{R}^{n_1\times n_1}$ and $R_\ell \in \mathbb{R}^{m\times m}$

such that $(Q_\ell^{1/2}, A_1)$ is observable and $R_\ell \succ 0$, and solve the corresponding local Riccati equations

$$P_\ell A_1 + A_1^T P_\ell - P_\ell B_1 R_\ell B_1^T P_\ell + Q_\ell = 0. \tag{3.21}$$

to obtain the unique positive definite solution $P_\ell \in \mathbb{R}^{n_1 \times n_1}$.

- **Step 2 (Setting Upper Layer Interactions) :**
  Choose a positive semidefinite matrix $K \in \mathbb{K}_s^+$.

- **Step 3 (Global LQR Setting) :**
  Choose $R_g \in \mathbb{R}^{m \times m}, R_g \succ 0$ and set $Q_g \in \mathbb{R}^{n_1 \times n_1}$ as follows:

$$Q_g = P_\ell B_1 R_g B_1^T P_\ell,$$

  where $P_\ell \in \mathbb{R}^{n_1 \times n_1}$ is the solution of the local Riccati equation (3.21).

- **Step 4 (State Feedback Gain Calculation) :**
  Set the state feedback gains F_ℓ and F_u as follows:

$$\begin{aligned} F_\ell &= -R_\ell B_1^T P_\ell, \\ F_u &= -R_g B_1^T P_\ell. \end{aligned}$$

The following theorem clearly shows the validation of the above procedure in which the resultant LQR controller belong to the class $\mathbb{F}_K$ in (3.7) if the weighting matrices are chosen as in the design procedure.

Theorem 3.1. *Consider a set of subsystems represented by (3.1) with (A_1, B_1) controllable for all $i = 1, \ldots, N$. Let K be a matrix in class $\mathbb{K}_s^+$ and the weighting matrices $\mathcal{Q}$ and $\mathcal{R}$ have the forms (3.18) and (3.19) with $R_g \in \mathbb{R}^{m \times m}$ and $Q_g \in \mathbb{R}^{n_1 \times n_1}$ chosen as in Step 3 of the state feedback design procedure in Subsection 3.3.2. Then the optimal hierarchical LQR state feedback gain is given by*

$$\mathcal{F} = I_N \otimes F_\ell + K \otimes F_u, \tag{3.22}$$

where

$$F_\ell = -R_\ell B_1^T P_\ell, F_u = -R_g B_1^T P_\ell. \tag{3.23}$$

The proof of this theorem can be found in the appendix.

3.3.3 Illustrative Example

Consider a network of 3 identical subsystems where each subsystem is described by (3.1) with

$$A_1 = \begin{bmatrix} 0 & 1 \\ -1 & -1 \end{bmatrix}, B_1 = \begin{bmatrix} 0 \\ 1 \end{bmatrix}. \tag{3.24}$$

Then let K be a Laplacian matrix as follows,

$$K = \begin{bmatrix} 1 & -1 & 0 \\ -1 & 1+q & -q \\ 0 & -q & q \end{bmatrix}, q \geq 0. \tag{3.25}$$

This matrix K implies that the 1st and the 2nd subsystems are connected, the 2nd and the 3rd subsystems may be connected while the 1st and the 3rd subsystems are not connected. Subsequently, we can rewrite the global performance index as follows,

$$J_{x,\mathcal{G}} = (x_1 - x_2)^T Q_g (x_1 - x_2) + q(x_2 - x_3)^T Q_g (x_2 - x_3). \tag{3.26}$$

It then can be seen that $J_{x,\mathcal{G}}$ puts a penalty under the form of a quadratic function with a weight matrix Q_g for the difference between the states of subsystems and hence by minimizing J including $J_{x,\mathcal{G}}$, the gaps between the states of subsystems are reduced simultaneously with the decrease of the states. As a result, the convergence speed of the agents' states to zero will be faster as both $J_{x,\mathcal{L}}$ and $J_{x,\mathcal{G}}$ are utilized than when only $J_{x,\mathcal{L}}$ is used. Furthermore, by changing the value of q, the system responses are also changed. The simulation result in Figure 3.3 exhibits the output responses of subsystems without a global peformance index, in which the output of each subsystem is equal to the first state in that subsystem and when a global performance index is employed with $q = 0$, i.e., the 2nd and 3rd subsystems are not connected. Obviously, when the global performance index is employed but $q = 0$, the output of the 1st subsystem converge to the output of the 2nd subsystem before all the outputs of subsystems come to zero. This is because only those subsystems are connected while the 3rd subsystem is not connected to any of them. Next, Figure 3.4 shows the output responses of subsystems when $q = 10$ and $q = 20$. We can observe that the convergence speed in these two cases are faster than in the last cases. Furthermore, the output of the 2nd subsystem rapidly converge to the output of the 3rd subsystem before all the outputs of subsystems come to zero as q increase. This is because a much larger weight is put on the state difference of the 2nd and 3rd subsystems making them converge to each other faster. In other words, by letting q larger the network is divided into two groups of subsystems in which the first group include the 1st subsystem and the second group composes of the 2nd and 3rd subsystems. Thus, the structure of the network is clearly reflected in the interconnection matrix K and changing the elements of K can improve the control performance.

3.4 Selective Pole Shift for Homogeneous Hierarchical Dynamical Networks

This section proposes an approach to selectively shift the undesirable eigenvalues of the subsystems in the network. In fact, each subsystem can be implemented with a local controller to shift its unexpected eigenvalues as in [21–24], however by collaborating with other subsystems both global (e.g. low-rank interconnection among subsystems for rapid consensus [10–12]) and local objectives (e.g. selective shift of undesired eigenvalues) in the network can be achieved. Then, by borrowing the ideas in [15] and [21–24] to our proposed hierarchical optimal controller in Section 3.3, we will show that our hierarchical optimal controller is able to selectively shift the undesirable eigenvalues of the subsystems without affecting other eigenvalues.

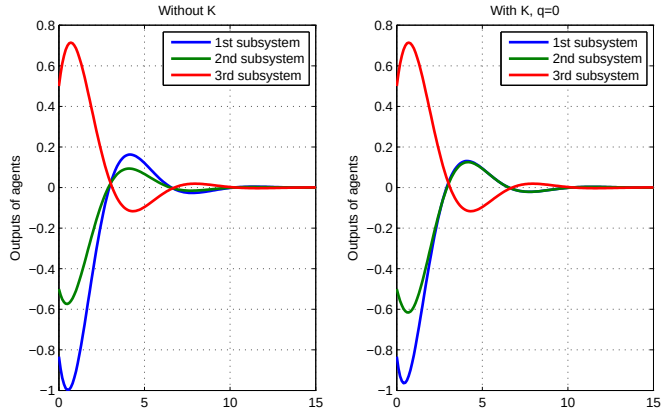

Figure 3.3: System responses without (left) and with (right) a global performance index but $q = 0$.

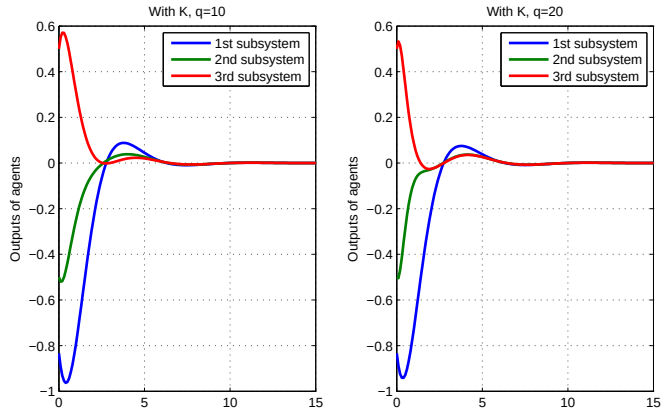

Figure 3.4: System responses with a global performance index as $q = 10$ (left) and $q = 20$ (right).

3.4.1 Selective Pole Shift: Case 1

This subsection describes in details how to further design the LQR controller in Section 3.3 to selectively shift one real, unexpected eigenvalue in each subsystem (agent).

Suppose that λ is a real undesirable eigenvalue of A_1 and ν is the corresponding left eigenvector. We select the sub-weighting matrix Q_ℓ under the form

$$Q_\ell = \nu q_1 \nu^T \tag{3.27}$$

where $q_1 \geq 0$, then the solution P_1 of the Riccati equation (3.21) also has the form

$$P_\ell = \nu p_1 \nu^T \tag{3.28}$$

with a positive real variable p_1. Replacing Q_ℓ and P_ℓ back to (3.21), we obtain

$$p_1\lambda + \lambda p_1 - p_1^2 r_1 + q_1 = 0, \tag{3.29}$$

where

$$r_1 = \nu^T B_1 R_\ell B_1^T \nu. \tag{3.30}$$

Solving the scalar Riccati equation (3.29) gives us

$$p_1 = \frac{\lambda + \sqrt{\lambda^2 + r_1 q_1}}{r_1} \tag{3.31}$$

Hence, to guarantee that $p_1 > 0$, we should select $q_1 > 0$.

Now, we show the eigenvalue distribution of the closed-loop interconnection matrix A in the following proposition.

Theorem 3.2. *With the hierarchical LQR controller (3.22) derived in Theorem 3.1 and the sub-weighting matrix Q_ℓ selected in (3.27), the eigenvalue set the closed-loop interconnection matrix A is determined as follows,*

$$\sigma(A) = \left\{ -\sqrt{\lambda^2 + r_1 q_1} - \gamma r_2 \frac{\lambda + \sqrt{\lambda^2 + r_1 q_1}}{r_1} \middle| \gamma \in \sigma(K) \right\} \bigcup (\sigma(A_1) \backslash \{\lambda\}), \tag{3.32}$$

where

$$r_2 = \nu^T B_1 R_2 B_1^T \nu. \tag{3.33}$$

Proof. Let U be a unitary matrix that transforms K into its Schur form, i.e., UKU^* is an upper triangular matrix with eigenvalues of K on the diagonal. Then

$$(U \otimes I_{n_1}) A (U \otimes I_{n_1}) = I_{n_1} \otimes (A_1 - B_1 R_\ell B_1^T P_\ell) + (UKU^*) \otimes (B_1 R_g B_1^T P_\ell) \tag{3.34}$$

Since the eigenvalues of A and $(U \otimes I_{n_1}) A (U \otimes I_{n_1})$ are similar, we obtain from (3.34) that the eigenvalue set of A is

$$\sigma(A) = \bigcup_{\gamma \in \sigma(K)} \sigma(A_1 - B_1 R_\ell B_1^T P_\ell + \gamma B_1 R_g B_1^T P_\ell) \tag{3.35}$$

Therefore, we only need to show the eigenvalues of $A_1 - B_1(R_\ell + \gamma R_g) B_1^T P_\ell$. Suppose that $\zeta \in \mathbb{R}^{n_1}$ is any right eigenvector of A_1 associated with an eigenvalue $\hat{\lambda}$ different from λ then $\nu^T \zeta = 0$. We have

$$\begin{aligned} [A_1 - B_1(R_\ell + \gamma R_g) B_1^T P_\ell] \zeta &= A_1 \zeta - B_1(R_\ell + \gamma R_g) B_1^T \nu p_1 \nu^T \zeta, \\ &= \hat{\lambda} \zeta. \end{aligned} \tag{3.36}$$

Accordingly, $\hat{\lambda}$ is an eigenvalue of $A_1 - B_1(R_\ell + \gamma R_g) B_1^T P_\ell$ with the corresponding eigenvector ζ. On the other hand,

$$\begin{aligned} \nu^T [A_1 - B_1(R_\ell + \gamma R_g) B_1^T P_\ell] &= \nu^T \lambda - \nu^T B_1(R_\ell + \gamma R_g) B_1^T \nu p_1 \nu^T, \\ &= [\lambda - \nu^T B_1(R_\ell + \gamma R_g) B_1^T \nu p_1] \nu^T. \end{aligned} \tag{3.37}$$

Hence, ν^T is a left eigenvector of $A_1 - B_1(R_\ell + \gamma R_g)B_1^T P_\ell$ asssociated with the eigenvalue $\lambda - \nu^T B_1(R_\ell + \gamma R_g)B_1^T \nu p_1$. In summary, the eigenvalue set of the closed-loop interconnection matrix is

$$\sigma(A) = \left(\bigcup_{\gamma \in \sigma(K)} \xi_\gamma \right) \bigcup (\sigma(A_1) \backslash \{\lambda\}), \tag{3.38}$$

where $\xi_\gamma = \lambda - \nu^T B_1(R_\ell + \gamma R_g)B_1^T \nu p_1$.

Now, utilizing the value of p_1 in (3.31), we have

$$\xi_\gamma = -\sqrt{\lambda^2 + r_1 q_1} - \gamma r_2 \frac{\lambda + \sqrt{\lambda^2 + r_1 q_1}}{r_1}, \tag{3.39}$$

where r_2 is defined in (3.33). Thus, the eigenvalue set of the closed-loop interconnection matrix A can be described as in (3.32). □

Based on the result of Theorem 3.2, the eigenvalue set of the closed-loop interconnection matrix A is completely determined by the eigenvalues of the local interconnection matrix A_1 and the interconnection matrix K between the subsystems in the upper layer. The following theorem shows a systematic way to select the matrices K and R_g to stabilize the closed-loop interconnection matrix A.

3.4.2 Selective Pole Shift: Case 2

In this subsection, we present a technique to further design the LQR controller in Section 3.3 such that two unexpected eigenvalues in each subsystem (agent) are selectively shifted. For the circumstance of selective shifting of more eigenvalues in each subsystem (agent), a similar method can be straightforwardly obtained or the method in this subsection and the previous subsection can be repetitively employed.

Suppose that (λ_1, λ_2) are undesirable eigenvalues of A_1 and ν_1^*, ν_2^* are the associated left eigenvectors. We select the sub-weighting matrix Q_ℓ under the form

$$Q_\ell = \begin{bmatrix} \nu_1 & \nu_2 \end{bmatrix} Q_1 \begin{bmatrix} \nu_1^* \\ \nu_2^* \end{bmatrix} \tag{3.40}$$

where $Q_1 \succeq 0$ then the solution P_ℓ of the Riccati equation (3.21) also has the form

$$P_\ell = \begin{bmatrix} \nu_1 & \nu_2 \end{bmatrix} P_1 \begin{bmatrix} \nu_1^* \\ \nu_2^* \end{bmatrix} \tag{3.41}$$

with a positive definite matrix P_1. Replacing Q_ℓ and P_ℓ back to (3.21), we obtain

$$P_1\Gamma + \Gamma^* P_1 - P_1 R_1 P_1 + Q_1 = 0, \tag{3.42}$$

where

$$\begin{aligned} \Gamma &= \begin{bmatrix} \lambda_1 & 0 \\ 0 & \lambda_2 \end{bmatrix}, \\ R_1 &= \begin{bmatrix} \nu_1^* \\ \nu_2^* \end{bmatrix} B_1 R_\ell B_1^T \begin{bmatrix} \nu_1 & \nu_2 \end{bmatrix}. \end{aligned} \tag{3.43}$$

Solving the 2×2 Riccati equation (3.42) gives us matrix P_1 and then P_ℓ is calculated from (3.41). Therefore, to ensure that (3.21) has a unique solution, (3.42) must have a unique solution as well.

Denote

$$E = B_1^T \begin{bmatrix} \nu_1 & \nu_2 \end{bmatrix}, E \in \mathbb{R}^{m \times 2}. \tag{3.44}$$

We show the eigenvalue distribution of the closed-loop interconnection matrix A in the following theorem.

Theorem 3.3. *With the LQR feedback controller $u = \mathcal{F}x$ defined in Theorem 3.1 and the sub-weighting matrix Q_ℓ selected in (3.40), the eigenvalue set the closed-loop interconnection matrix A is determined as follows,*

$$\sigma(A) = \left(\bigcup_{\gamma \in \sigma(K)} \sigma(\Xi_\gamma) \right) \bigcup (\sigma(A_1) \backslash \{\lambda_1, \lambda_2\}), \tag{3.45}$$

where Ξ_γ is a 2×2 matrix defined by

$$\Xi_\gamma = \Gamma - E^*(R_\ell + \gamma R_g) E P_\ell, \tag{3.46}$$

and E is defined in (3.44).

Proof. Similarly to the proof of Proposition 3.2, we obtain that the eigenvalue set of the closed-loop interconnection matrix A is

$$\sigma(A) = \bigcup_{\gamma \in \sigma(K)} \sigma(A_1 - B_1(R_\ell + \gamma R_g) B_1^T P_\ell) \tag{3.47}$$

Moreover, all the eigenvalues of A_1 except λ_1, λ_2 are eigenvalues of $A_1 - B_1(R_\ell + \gamma R_g) B_1^T P_\ell$ and hence are eigenvalues of A.

Denote $\hat{\lambda}_1, \hat{\lambda}_2$ the two other eigenvalues of $A_1 - B_1(R_\ell + \gamma R_g) B_1^T P_\ell$. Suppose that $\hat{\lambda}_1, \hat{\lambda}_2 \notin \sigma(A_1) \backslash \{\lambda_1, \lambda_2\}$ then the eigenvectors corresponding to $\hat{\lambda}_1, \hat{\lambda}_2$ must lie in the subspace spanned by ν_1, ν_2. Let w_1^*, w_2^* are left eigenvectors of $A_1 - B_1(R_\ell + \gamma R_g) B_1^T P_\ell$ associated with $\hat{\lambda}_1, \hat{\lambda}_2$, respectively. Then

$$w_k^* = \alpha_k \nu_1^* + \beta_k \nu_2^*, k = 1, 2. \tag{3.48}$$

As a result,

$$\begin{aligned}
& w_k^*[A_1 - B_1(R_\ell + \gamma R_g) B_1^T P_\ell] \\
= & \begin{bmatrix} \alpha_k^* & \beta_k^* \end{bmatrix} \begin{bmatrix} \nu_1^* \\ \nu_2^* \end{bmatrix} A_1 - \begin{bmatrix} \alpha_k^* & \beta_k^* \end{bmatrix} \begin{bmatrix} \nu_1^* \\ \nu_2^* \end{bmatrix} B_1(R_\ell + \gamma R_g) B_1^T \begin{bmatrix} \nu_1 & \nu_2 \end{bmatrix} P_1 \begin{bmatrix} \nu_1^* \\ \nu_2^* \end{bmatrix}, \\
= & \begin{bmatrix} \alpha_k^* & \beta_k^* \end{bmatrix} \left(\Gamma - \begin{bmatrix} \nu_1^* \\ \nu_2^* \end{bmatrix} B_1(R_\ell + \gamma R_g) B_1^T \begin{bmatrix} \nu_1 & \nu_2 \end{bmatrix} P_1 \right) \begin{bmatrix} \nu_1^* \\ \nu_2^* \end{bmatrix}, \\
= & \begin{bmatrix} \alpha_k^* & \beta_k^* \end{bmatrix} \Xi_\gamma \begin{bmatrix} \nu_1^* \\ \nu_2^* \end{bmatrix}.
\end{aligned} \tag{3.49}$$

Therefore,

$$\begin{bmatrix}\alpha_k^* & \beta_k^*\end{bmatrix}(\Xi_\gamma - \hat{\lambda}_k I_2)\begin{bmatrix}\nu_1^* \\ \nu_2^*\end{bmatrix} = 0, k = 1, 2. \tag{3.50}$$

Note that ν_1^*, ν_2^* are linearly independent, so we obtain

$$\begin{bmatrix}\alpha_k^* & \beta_k^*\end{bmatrix}(\Xi_\gamma - \hat{\lambda}_k I_2) = 0, k = 1, 2. \tag{3.51}$$

This implies that $\hat{\lambda}_k$ is an eigenvalue of Ξ_γ associated with the left eigenvector $\begin{bmatrix}\alpha_k^* & \beta_k^*\end{bmatrix}$, $k = 1, 2$. Hence, the eigenvalues of Ξ_γ are also eigenvalues of $A_1 - B_1(R_\ell + \gamma R_g)B_1^T P_\ell$. As a result, the eigenvalue set of the closed-loop interconnection matrix can be represented by (3.45). □

Thanks to Theorem 3.3, we can determine the eigenvalue spectrum of the closed-loop interconnection matrix A based on the eigenvalues of the local interconnection matrix A_1 and the matrix Ξ_γ. Although the eigenvalues of Ξ_γ are not analytically obtained but Ξ_γ is a 2×2 matrix, so its eigenvalues can be easily calculated.

3.4.3 Example 3.1: Homogeneous network of single integrator dynamics

Consider a network of 50 agents whose dynamics are described by the integrator $1/s$. Then this network is divided into 10 groups and each group has 5 agents. Suppose that the local interconnection structure in each group is given by

$$A_1 = \begin{bmatrix}0 & 0 & 1 & 0 & 0 \\ 1 & 0 & 0 & 1 & 0 \\ 0 & 2 & 0 & 0 & 0 \\ 0 & 0 & 0 & 0 & -2 \\ 1 & 0 & 1 & 0 & 0\end{bmatrix}. \tag{3.52}$$

The eigenvalues of A_1 are $1.2249 \pm 0.8516i, -0.8716 \pm 1.3358i, -0.7065$ displayed in Figure 3.5, in which $1.2249 \pm 0.8516i$ are unstable. Consequently, the whole network has two unstable eigenvalues, each one has the multiplicity equals to 10.

In the example in Section 3.3, we have introduce an example to show the role of the global performance index, in particular the interconnection matrix K, but we have not yet present another element in the global performance index which is the weighting matrix Q_g. Hence, this example aims at showing how the changes of Q_g could affect to the control performance of the network.

Suppose that all the states of the agents are measurable and we can freely choose but fix the interconnection matrix between the subsystems. Consequently, $C_i = I_5$ and $y_i = x_i$ for all $i = 1, \ldots, 10$. Now, we apply our proposed design procedure to design the stabilizing feedback controller such that the network's hierarchical structure is preserved and the undesirable eigenvalues are properly shifted. In the first step, we choose $m = 1$ and

$$B_1 = \begin{bmatrix}1 & 0 & 1 & 0 & 1\end{bmatrix}^T. \tag{3.53}$$

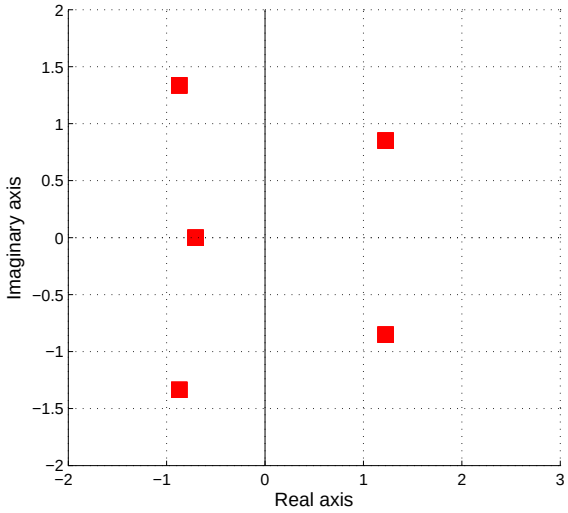

Figure 3.5: Eigenvalue distribution of A_1.

Moreover, let $\lambda_1 = 1.2249 - 0.8516i, \lambda_2 = 1.2249 + 0.8516i$ then the left eigenvectors of A_1 corresponding to λ_1 and λ_2 are

$$\begin{aligned} \nu_1^* &= \begin{bmatrix} 0.3830 - 0.1098i & 0.5468 & 0.3349 - 0.2328i & 0.3010 + 0.2092i & -0.1711 - 0.4606i \end{bmatrix}, \\ \nu_2^* &= \begin{bmatrix} 0.3830 + 0.1098i & 0.5468 & 0.3349 + 0.2328i & 0.3010 - 0.2092i & -0.1711 + 0.4606i \end{bmatrix}. \end{aligned} \tag{3.54}$$

Next, we choose $Q_1 = \begin{bmatrix} 2 & 1 \\ 1 & 2 \end{bmatrix}$ and $R_\ell = 1$ then

$$\begin{aligned} R_1 &= \begin{bmatrix} \nu_1^* \\ \nu_2^* \end{bmatrix} B_1 R_\ell B_1^T \begin{bmatrix} \nu_1 & \nu_2 \end{bmatrix}, \\ &= \begin{bmatrix} 0.9442 & -0.3462 - 0.8784i \\ -0.3462 + 0.8784i & 0.9442 \end{bmatrix}. \end{aligned} \tag{3.55}$$

Consequently, solving the Riccati equation (3.21) gives us

$$P_1 = \begin{bmatrix} 15.7432 & -0.7244 + 13.7802i \\ -0.7244 - 13.7802i & 15.7432 \end{bmatrix}. \tag{3.56}$$

Therefore, we can compute P_ℓ to be

$$\begin{aligned} P_\ell &= \begin{bmatrix} \nu_1 & \nu_2 \end{bmatrix} P_1 \begin{bmatrix} \nu_1^* \\ \nu_2^* \end{bmatrix}, \\ &= \begin{bmatrix} 2.4864 & 4.6374 & 1.2237 & 4.0048 & -4.6489 \\ 4.6374 & 8.9819 & 1.9916 & 8.0968 & -9.7532 \\ 1.2237 & 1.9916 & 0.8563 & 1.4228 & -1.3424 \\ 4.0048 & 8.0968 & 1.4228 & 7.6338 & -9.5293 \\ -4.6489 & -9.7532 & -1.3424 & -9.5293 & 12.2137 \end{bmatrix}. \end{aligned} \tag{3.57}$$

Let $R_g = 1$ and K be a Laplacian matrix which satisfies the positive semidefiniteness in

Theorem 3.1 as follows,

$$K = \begin{bmatrix} 2 & -1 & 0 & 0 & 0 & 0 & 0 & 0 & 0 & -1 \\ -1 & 1 & 0 & 0 & 0 & 0 & 0 & 0 & 0 & 0 \\ 0 & 0 & 2 & 0 & -1 & 0 & 0 & 0 & -1 & 0 \\ 0 & 0 & 0 & 2 & 0 & -1 & 0 & 0 & -1 & 0 \\ 0 & 0 & -1 & 0 & 2 & 0 & 0 & -1 & 0 & 0 \\ 0 & 0 & 0 & -1 & 0 & 1 & 0 & 0 & 0 & 0 \\ 0 & 0 & 0 & 0 & 0 & 0 & 1 & -1 & 0 & 0 \\ 0 & 0 & 0 & 0 & -1 & 0 & -1 & 2 & 0 & 0 \\ 0 & 0 & -1 & -1 & 0 & 0 & 0 & 0 & 3 & -1 \\ -1 & 0 & 0 & 0 & 0 & 0 & 0 & 0 & -1 & 2 \end{bmatrix}. \tag{3.58}$$

Figure 3.6 displays a demonstration for the designed homogeneous hierarchical network including the structure of the interconnection matrix K.

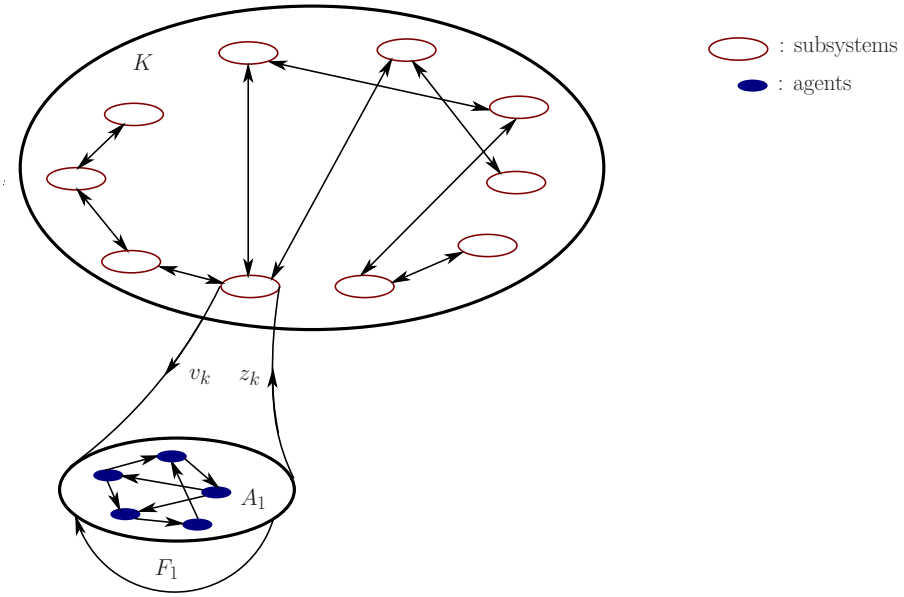

Figure 3.6: Illustration of the designed homogeneous hierarchical dynamical network in Example 2.

Then the eigenvalues of the closed-loop interconnection matrix A and the states of all agents are exhibited in Figure 3.7. We can see that all the eigenvalues of closed-loop system belong to the left-haft complex plane, moreover only unstables eigenvalues are changed while the other stable eigenvalues remain unaltered. As a result, the states of all agents converge to 0 as observed in the subplot on the right hand side.

It should be noted that the aggregation matrix $F_u = -R_g B_1^T P_\ell$ is computed to be

$$F_u = \begin{bmatrix} -0.9388 & -3.1242 & 0.7376 & -4.1018 & 6.2223 \end{bmatrix}. \tag{3.59}$$

Thus, the aggregated signal z_k of the k-th subsystem is a scalar value which is equal to the weighted sum of the outputs of agents in that subsystem with the weights shown in

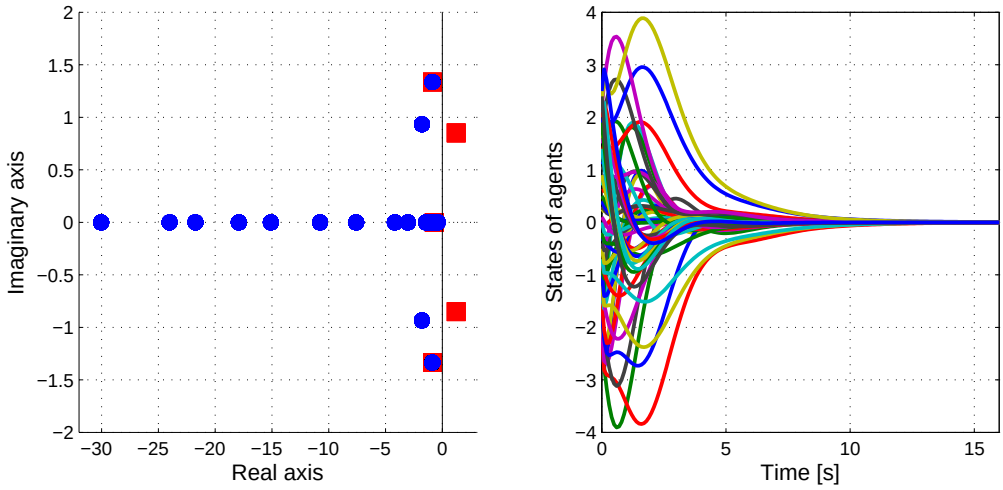

Figure 3.7: States of all agents in the designed two-layer hierarchical network.

(3.59). Accordingly, the communication between subsystems in the upper layer uses only scalar values resulting in very low computational cost and fast speed. On the other hand, the input signal from the upper layer to the ith subsystem, $i = 1, \ldots, 10$ is described as follows,

$$w_i = -\sum_{j=1}^{10} K(i,j) R_g B_1^T P_\ell (x_j - x_i), \tag{3.60}$$

where x_i, x_j are the state vectors of the i-th and j-th subsytems, respectively; $K(i,j)$ is the element of K at ith row and jth column.

In the following, we attempt to verify the effects on the selections of weighting matrices Q_ℓ, i.e., Q_1 and Q_g, i.e., R_g to the response of the designed hierarchical network. To do so, K is chosen and fix as above. Note here that in the example in Section 3.3, Q_ℓ is free to choose since each subsystem is stable, however in this example each subsystem is unstable and hence Q_ℓ has less freedom because it is chosen based on the left eigenvectors associated with unstable eigenvalues. We are able to change Q_ℓ by varying the sub-weighting matrix Q_1 as follows

$$Q_1 = \eta I_2, \tag{3.61}$$

with $\eta > 0$ and increases from 1 to 5 while remaining other matrices. Then the outputs of subsystems which are equal to the averages of the states inside subssytems are plotted in Figure 3.8. It reveals that as Q_ℓ becomes larger but not to much, the closed-loop system is faster stabilized. This is because the eigenvalues of the closed-loop system are pushed further to the left half complex plane as we increase Q_ℓ. Nevertheless, there are unchanged eigenvalues of the network by the proposed method, so we cannot get faster convergence rate if the change of Q_ℓ let the shifted eigenvalues further to the imaginary axis than the unchanged eigenvalues. Actually, this is illustrated in the lower subplots in Figure 3.8. The similar situation also happen with Q_g. Thus, we need to be careful when choosing the weighting

matrices.

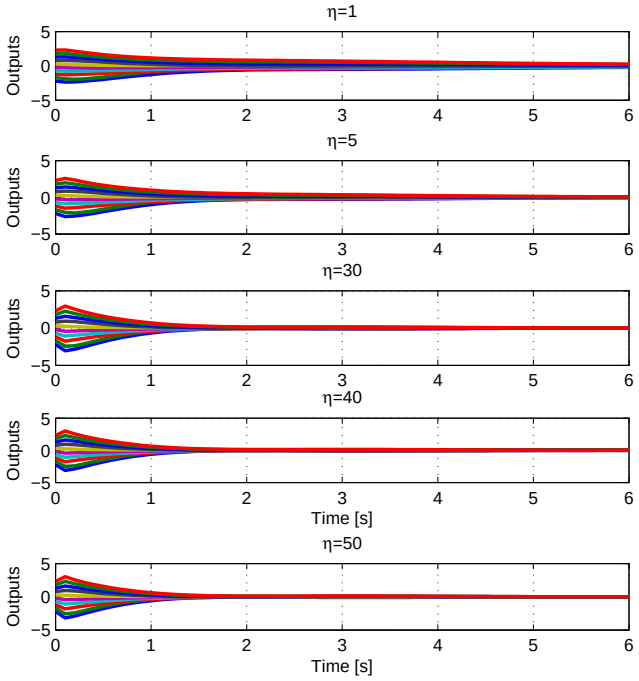

Figure 3.8: Outputs of the closed-loop system as Q_1 changes.

3.4.4 Example 3.2: Homogeneous network of hormonal oscillators

Consider a network of 10 oscillators describing the hormone secretion oscillations in which each oscillator is described by the following Goodwin model [52, 77, 78],

$$\begin{aligned} \dot{R} &= f(T) - b_1 R, \\ \dot{L} &= g_1 R - b_2 L, \\ \dot{T} &= g_2 L - b_3 T, \end{aligned} \tag{3.62}$$

where R, L, T are concentrations of GnRH (LHRH), LH and T(Testosterone) hormones, respectively; g_1, g_2, b_1, b_2, b_3 are positive constants; $f(T) = \dfrac{K}{1+\beta T^n}, K > 0, \beta > 0, n$ is a positive integer called the Hill coefficient. The diagram for the secretion of Testosterone is described in Figure 3.9. Then the oscillator (3.62) can be cast as a subsystem consisting of 3 integrators, each integrator represents the dynamics of GnRH, LH and T hormones, and those integrators are interconnected as seen in (3.62). Suppose that (R_0, L_0, T_0) is an equilibrium point of (3.62), then we have

$$f(T_0) = b_1 R_0, g_1 R_0 = b_2 L_0, g_2 L_0 = b_3 T_0.$$

Denote $f'(T_0)$ the value of the derivative of $f(T)$ with respect to T at T_0, then the linearized model of the oscillator is as follows,

$$\begin{aligned} \dot{R} &= f'(T_0) T - b_1 R, \\ \dot{L} &= g_1 R - b_2 L, \\ \dot{T} &= g_2 L - b_3 T, \end{aligned} \tag{3.63}$$

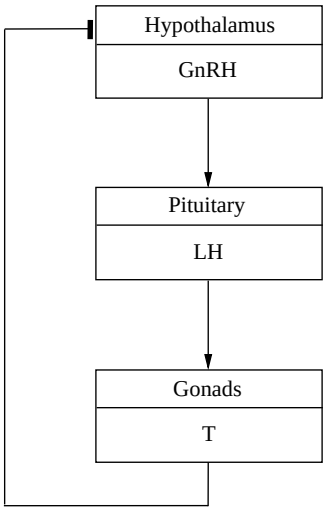

Figure 3.9: Diagram for Testosterone secretion control in men

Hence, each linearized oscillator is a subsystem in the oscillator network described by

$$\dot{x}_i = A_1 x_i, i = 1, \ldots, 10, \tag{3.64}$$

where

$$A_1 = \begin{bmatrix} -b_1 & 0 & f'(T_0) \\ g_1 & -b_2 & 0 \\ 0 & g_2 & -b_3 \end{bmatrix}. \tag{3.65}$$

Note that A_1 is unstable since the original model (3.62) is oscillating. Consequently, we assume that the oscillators are interconnected by receiving the hormone secretion from other oscillators through the serum and affect to the release of Testosterone hormone, i.e., the last equation in (3.63). This implies that the input matrix B_1 of each linearized oscillator is $B_1 = \begin{bmatrix} 0 & 0 & 1 \end{bmatrix}^T$. Furthermore, the hormonal oscillators are assumed to communicate in a cyclic manner as illustrated in Figure 3.10, i.e., the interconnection matrix between the oscillators are required to be a cyclic matrix with non-zero elements in the main diagonal, in the first diagonals above and below the main diagonal, and at the upper right and lower left conners. This interconnection matrix means that each hormonal oscillator communicates with two neighbouring oscillators by comparing its output with the outputs of other hormonal oscillators and hence K is also a Laplacian matrix.

Then the dynamics of each linearized oscillator is

$$\dot{x}_i = A_1 x_i + B_1 u_i, i = 1, \ldots, 10, \tag{3.66}$$

where u_i is the input of ith oscillator.

Denote

$$\begin{aligned} x &= \begin{bmatrix} x_1^T & \cdots & x_{10}^T \end{bmatrix}^T, \\ u &= \begin{bmatrix} u_1 & \cdots & u_{10} \end{bmatrix}^T. \end{aligned} \tag{3.67}$$

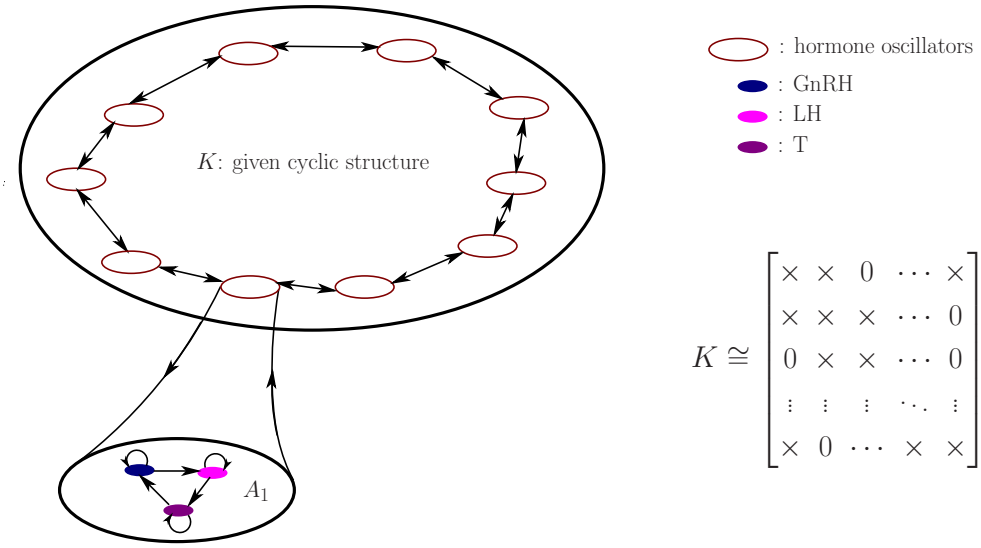

Figure 3.10: Structure of the hormonal oscillator network.

Suppose that all the states of hormonal oscillators are measurable, i.e., all the secretions of GnRH, LH and T hormones can be measured. Employing our proposed method, we design a static feedback controller $u = \mathcal{F}x$ such that the whole linearized hormone oscillator network is stable due to a fact that the hormone oscillators should be synchronized and only unstable eigenvalues of A_1 are moved while the other eigenvalues remain unchanged. Furthermore, the communication between oscillators are low rank. To do so, we first adopt the parameters for hormone secretion oscillations in [77] as follows, $b_1 = 1.29, b_2 = 0.97, b_3 = 1.39, g_1 = 10, g_2 = 0.7$. Let the Hill coefficient $n = 15$ then we can easily compute the equilibrium value of Testosterone concentration is $T_0 = 1.07$ and $f'(T_0) = -2.7352$. Subsequently, the local interconnection matrix in each subsystem is

$$A_1 = \begin{bmatrix} -1.2900 & 0 & -2.7352 \\ 10.0000 & -0.9700 & 0 \\ 0 & 0.7000 & -1.3900 \end{bmatrix}. \tag{3.68}$$

The eigenvalues of A_1 are $0.1239 \pm 2.3115i, -3.8978$ displayed in Figure 3.11, in which $0.1239 \pm 2.3115i$ are unstable. Therefore, the whole homogeneous hierarchical network has two unstable eigenvalues with multiplicity 10. Utilizing our proposed design procedure, we will design a state feedback controller which selectively shift those two undesirable eigenvalues.

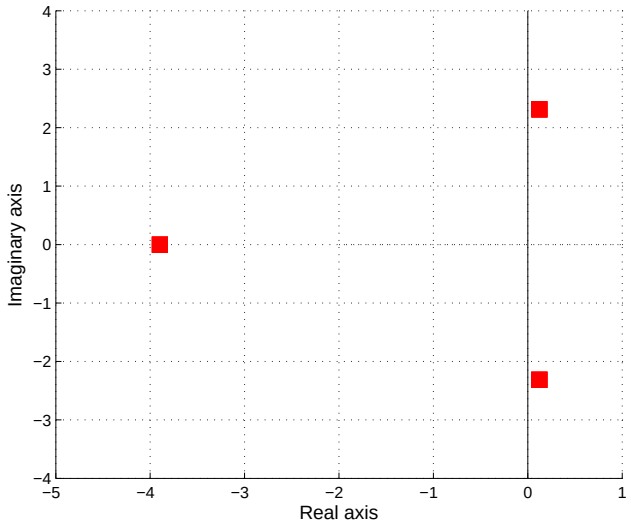

Figure 3.11: Eigenvalue distribution of A_1.

Next, we choose $Q_\ell = 1$, $R_\ell = 1$ and $R_g = 1$, then let K be as follows,

$$K = \begin{bmatrix} 2 & -1 & 0 & 0 & 0 & 0 & 0 & 0 & 0 & -1 \\ -1 & 2 & -1 & 0 & 0 & 0 & 0 & 0 & 0 & 0 \\ 0 & -1 & 2 & -1 & 0 & 0 & 0 & 0 & 0 & 0 \\ 0 & 0 & -1 & 2 & -1 & 0 & 0 & 0 & 0 & 0 \\ 0 & 0 & 0 & -1 & 2 & -1 & 0 & 0 & 0 & 0 \\ 0 & 0 & 0 & 0 & -1 & 2 & -1 & 0 & 0 & 0 \\ 0 & 0 & 0 & 0 & 0 & -1 & 2 & -1 & 0 & 0 \\ 0 & 0 & 0 & 0 & 0 & 0 & -1 & 2 & -1 & 0 \\ 0 & 0 & 0 & 0 & 0 & 0 & 0 & -1 & 2 & -1 \\ -1 & 0 & 0 & 0 & 0 & 0 & 0 & 0 & -1 & 2 \end{bmatrix}. \tag{3.69}$$

It can be verified that the weighting matrices $\mathcal{Q} = I_{10} \otimes Q_\ell + K \otimes Q_g$ and $\mathcal{R}^{-1} = I_{10} \otimes R_\ell + K \otimes R_g$ are semi postive definite and positive definite, respectively. In addition, all the eigenvalues of the closed-loop interconnection matrix A belong to the left-haft complex plane as exhibited in Figure 3.12 in which only the unstable eigenvalue $\lambda_1 = 1.4647$ of A_1 are changed while the other eigenvalues remain unaltered. Furthermore, all states of linearized oscillators are stabilized as seen in the right hand side plot.

The aggregation matrix $F_u = -R_g B_1^T P_\ell$ of each subsystem, i.e., each linearized hormone oscillator is computed to be

$$F_u = \begin{bmatrix} -1.1478 & 0.1210 & 1.6374 \end{bmatrix}. \tag{3.70}$$

Thus, the information of each subsystem is aggregated through a scalar value z_k which is equal to a weighted sum of the oscillator states, i.e., a weighted sum of the concentrations of the GnRH, LH and T hormones in that subsystem with the weights shown in (3.70). Then those scalar values are sent to other subsystems, i.e., oscillators with the interconnection strengths

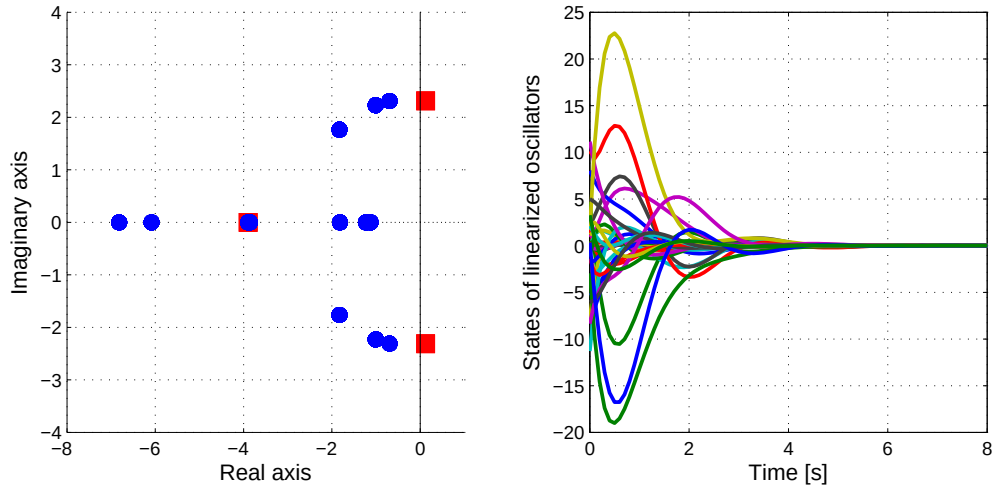

Figure 3.12: States of all linearized hormonal oscillators in the designed oscillator network.

$K_{ij}, i, j = 1, \ldots, 10$. Finally, each subsystem, i.e., oscillator receive the information from other oscillators through the input matrix $B_1 = \begin{bmatrix} 0 & 0 & 1 \end{bmatrix}^T$ which only sends the information to the third state, i.e., the secretion of Testosterone hormone.

Next, we consider the case that not all secretions of GnRH, LH and T hormones are measurable but instead only the secretion of Testosterone hormone in the serum can be measured, i.e., we are able to measure the following output of each oscillator $y_i = C_1 x_i$ where

$$C_1 = \begin{bmatrix} 0 & 0 & 1 \end{bmatrix}. \tag{3.71}$$

Then an observer needs to be designed to approximate the real states of the linearized oscillators. Note that we can easily check the observability of (C_1, A_1). Then we first find a matrix H_1 such that $A_1 + H_1 C_1$ is stable. Let us select

$$H_1 = \begin{bmatrix} -20 & -20 & -20 \end{bmatrix}, \tag{3.72}$$

which makes $A_1 + H_1 C_1$ stable with eigenvalues $-1.2782 \pm 2.8348i, -21.0936$. Consequently, the state feedback controller $u = \mathcal{F}\hat{x}$ with $\mathcal{F}$ designed in the previous part and the observed state $\hat{x}$ is utilized for the linearized hormonal oscillator network. Figure 3.13 reveals that the observed states converge to the real states of linearized oscillators and Figure 3.14 shows that the outputs of linearized hormonal oscillator network are stable.

3.5 Summary

We have presented in this chapter a new systematic method to design hierarchical state feedback optimal LQR controllers for homogeneous multi-agent dynamical networks. The interconnection structure in the upper layer is taken into account in a global performance index which reflects our global control objective for the whole network. The proposed design

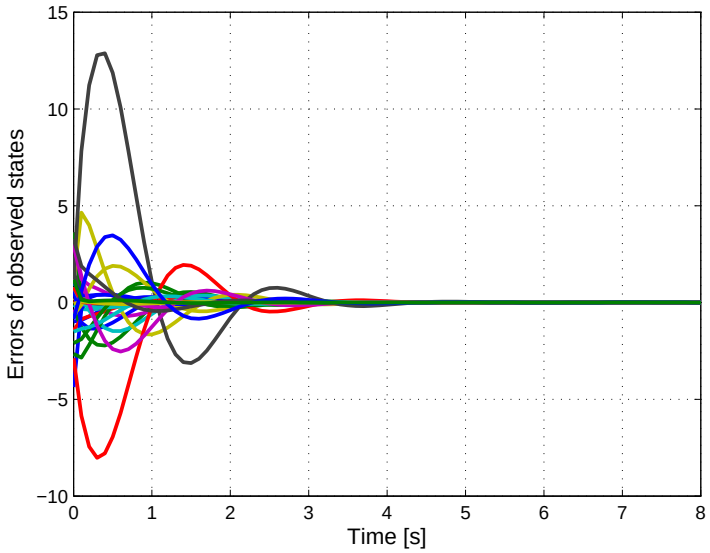

Figure 3.13: Errors between real and observed states in the oscillator network with the designed output feedback controller.

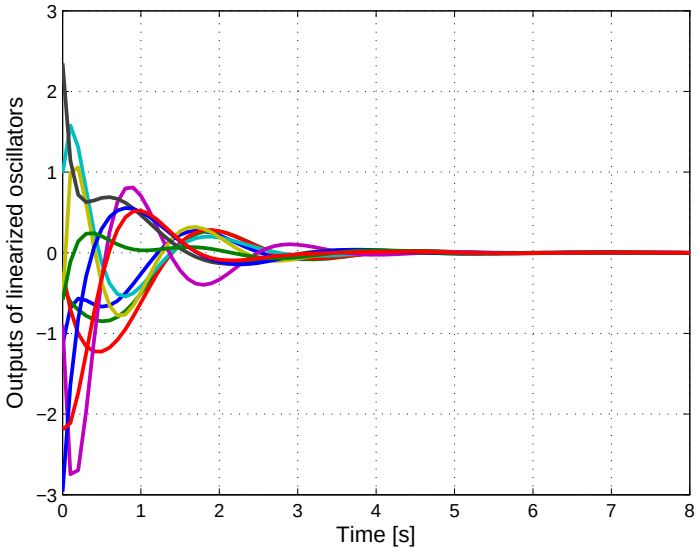

Figure 3.14: Outputs of all linearized hormonal oscillators with the designed output feedback controller.

method has two novel features namely the preservation of a prescribed desirable hierarchical structure which does not belong to any operator algebra or semigroups and the ability to selectively shift the unexpected eigenvalues of the subsystems in the network.

In case that only some quantities of states can be measured, we propose to use local state observers to reduce the output feedback hierarchical design problem to a state feedback hierarchical design problem. An advantage in our approach is that the state observers are

fully decentralized.

Finally, several examples are introduced to demonstrate the theoretical results. The first example illustrates the effects of elements of the interconnection matrix to the responses of the subsystems. The second example shows the effects of the weighting matrices and the last example deals with a practical model of linearized Testosterone hormonal oscillation networks and both state and output feedback controllers are designed to stabilize the linearized model of the hormonal oscillator network.

3.6 Appendix: Proof of Theorem 3.1

We first show that Assumptions **A1** and **A2** are satisfied in our setting. Assumption **A1** is obvious since it is equivalent to the controllability of (A_1, B_1) for all $i = 1, \ldots, N$. Similarly, we readily see that Assumption **A2** holds when $Q_g = 0$. Note that the second term of $\mathcal{Q}$, or $K \otimes Q_g$, is positive semidefinite, because both matrices K and Q_g are positive semidefinite. Therefore, introduction of this extra term in $\mathcal{Q}$ does not break the observability condition, and hence Assumption **A2** holds even for any $Q_g \succeq 0$. In addition, $R_\ell \succ 0$ leading to $I_N \otimes R_\ell \succ 0$. This yields $\mathcal{R}^{-1} = I_N \otimes R_\ell + K \otimes R_g \succ 0$, i.e., $\mathcal{R} \succ 0$. Consequently, we see that there exists a unique positive definite solution of (3.20).

Next, substituting $\mathcal{P} = I_N \otimes P_\ell$ and $\mathcal{Q}, \mathcal{R}$ back to the Riccati equation (3.20), we obtain

$$\begin{aligned} 0 &= I_N \otimes (P_\ell A_1 + A_1^T P_\ell - P_\ell B_1 R_\ell B_1^T P_\ell + Q_\ell) \\ &\quad + K \otimes (Q_g - P_\ell B_1 R_g B_1^T P_\ell). \end{aligned} \tag{3.73}$$

This is always true with $Q_g = P_\ell B_1 R_g B_1^T P_\ell$ and P_ℓ is the solution of (3.21). Hence, $\mathcal{P} = I_N \otimes P_\ell$ is a solution of (3.20). Since we have assumed the uniqueness of the solution of (3.20), that matrix $\mathcal{P}$ is the unique solution. Accordingly, the LQR controller is calculated as follows,

$$\begin{aligned} \mathcal{F} &= -\mathcal{R}^{-1}\mathcal{B}^T\mathcal{P}, \\ &= -(I_N \otimes R_\ell + K \otimes R_g)(I_N \otimes B_1^T)(I_N \otimes P_\ell), \\ &= -I_N \otimes (R_\ell B_1^T P_\ell) - K \otimes (R_g B_1^T P_\ell). \end{aligned}$$

Thus, the LQR controller gains F_ℓ and F_u are determined by (3.22).

CHAPTER 4

LQR DESIGN FOR HETEROGENEOUS HIERARCHICAL NETWORKS

4.1 From Homogeneous to Heterogeneous Networks: Similarities and Differences

In chapter 3, we have presented a systematic method to design hierarchical optimal controllers for homogeneous multi-agent dynamical networks. This chapter introduces a systematic design approach based on LQR method for a more general and complex class of networks, namely heterogeneous multi-agent dynamical networks. For simplicity and clarity, the results are presented only for two-layer hierarchical networks. The heterogeneous hierarchical networks differ from homogeneous multi-agent dynamical networks that the models of agents in the network are distinct. As a result, to represent homogeneous multi-agent dynamical networks we can use the Kronecker product but to describe heterogeneous multi-agent networks we need the Khatri-Rao product.

Similarly to chapter 3, the question here is under what LQR setting, a prescribed hierarchical structure of the heterogeneous multi-agent dynamical network can be achieved. Note that, the design in this chapter is essentially different from the design in chapter 3 since the hierarchical structure of a feedback controller for a heterogeneous hierarchical network is much more complex than for a homogeneous hierarchical network due to a fact that the dimensions of the agents could be distinct. It is therefore unable to straightforwardly extend the approach proposed in chapter 3 to this chapter.

Fortunately, one answer for the provided question can be obtained by introducing a class of performance indexes for heterogeneous multi-agent dynamical networks consisting of both global and local objectives with control input penalty. This results in a hierarchical optimal decentralized controller which is able to make the desired hierarchical structure of the network achievable by choosing appropriate weighting matrices in the performance index.

The heterogeneous multi-agent dynamical networks were studied in [15, 65] but they focused on the analysis problem and a systematic synthesis approach is still lacking. This chapter on the other hand focuses on the synthesis problem and accordingly propose a systematic method to design hierarchical optimal feedback controllers for that type of networks. It should be emphasized that there are important features in our work which have not been considered in [15, 65]. First, the dimensions of input and output matrices of the agents are assumed to be the same in [15, 65] but we consider here a more general context where the dimensions of those matrices are different. As a result, the class of heterogeneous multi-

agent dynamical networks in our work is broader than in [15, 65]. Second, the numbers of undesirable eigenvalues for the agents are distinct whereas they are assumed to be the same in [15, 65]. Thus, our networks are more general than the networks in [15, 65].

4.2 Problem formulation

4.2.1 Heterogeneous Hierarchical Networked Dynamical Systems

Consider a multi-agent system having N agents whose model is represented by

$$\begin{aligned} \dot{x}_i &= A_i x_i + B_i u_i, \\ y_i &= C_i x_i,\ i = 1, \ldots, N, \end{aligned} \tag{4.1}$$

where $A_i \in \mathbb{R}^{n_i \times n_i}$, $B_i \in \mathbb{R}^{n_i \times m_i}$, $0 < m_i \leq n_i$, $C_i \in \mathbb{R}^{p_i \times n_i}$, $x_i \in \mathbb{R}^{n_i}$ is the state vector of the ith subsystem, and $u_i \in \mathbb{R}^{m_i}$ and $y_i \in \mathbb{R}^{p_i}$ are the vectors containing all the inputs and measured outputs of the ith subsystem, respectively. Denote $P_i(s)$ the transfer function of the ith subsystem, i.e.,

$$P_i(s) = C_i(sI_{n_i} - A_i)^{-1}B_i.$$

To simplify the presentation of results, we consider a class of systems having $m_i = \mu\, \forall i = 1, \ldots, N$, i.e., all subsystems have the same number of inputs. Then denote $m = \mu N$, $p = p_1 + \cdots + p_N$, the heterogeneous hierarchical network model is

$$\begin{aligned} \dot{x} &= \mathcal{A}x + \mathcal{B}u, \\ y &= \mathcal{C}x, \end{aligned} \tag{4.2}$$

where $x = \begin{bmatrix} x_1^T, & \ldots, & x_N^T \end{bmatrix}^T \in \mathbb{R}^n$, $u = \begin{bmatrix} u_1^T, & \ldots, & u_N^T \end{bmatrix}^T \in \mathbb{R}^m$, $y = \begin{bmatrix} y_1^T, & \ldots, & y_N^T \end{bmatrix}^T \in \mathbb{R}^p$; $\mathcal{A} = \mathrm{diag}\{A_i\}_{k=1,\ldots,N} \in \mathbb{R}^{n \times n}$, $\mathcal{B} = \mathrm{diag}\{B_i\}_{i=1,\ldots,N} \in \mathbb{R}^{n \times m}$, $\mathcal{C} = \mathrm{diag}\{C_i\}_{k=1,\ldots,N} \in \mathbb{R}^{p \times n}$.

The information exchange in the real multi-agent systems controlled with a decentralized fashion is as follows: (i) Each agent sends out a unique aggregated signal to collaborate with other connected agents to realize the global objectives in addition to the local objectives. (ii) Simultaneously, each agent is able to receive the signals sent by other connected agents individually.

Let us denote $\mathcal{G}$ the graph representing the information structure in a multi-agent system, where each node in $\mathcal{G}$ stands for an agent and each edge in $\mathcal{G}$ represents the interconnection between two agents. In this paper, we assume that the communications between agents are bidirectional, i.e., $\mathcal{G}$ is undirected. Then, the information structure in a multi-agent system can be mathematically characterized by a matrix K, where the elements of K stands for the weights on the edges of $\mathcal{G}$, or equivalently the weights for the information exchanges between agents. Denote $\mathcal{E}$ the edge set of $\mathcal{G}$, then the class of K is defined by

$$\mathbb{K}_s := \{K = K^T \in \mathbb{R}^{N \times N} \mid K_{ij} = 0 \text{ if } (i, j) \notin \mathcal{E}\}. \tag{4.3}$$

From the theoretical point of view, such a multi-agent system can be considered as a two-layer hierarchical system, where each agent is cast as a subsystem in the lower layer and

those subsystems are interconnected in the upper layer. Accordingly, the interconnection among agents in a multi-agent system can be treated in the associated two-layer hierarchical system as follows. The ith subsystem tries to collaborate with all other subsystems by sending a unique aggregated signal $z_i \in \mathbb{R}^\mu$, receiving a partial set of aggregated signals $z_j \in \mathbb{R}^\mu$ from the jth subsystem satisfying $(i,j) \in \mathcal{E}$, and determining a kind of reference command $w_i \in \mathbb{R}^\mu$ for the global objectives in the simplest way as

$$w_i = \sum_{(i,j)\in\mathcal{E}} K_{ij} z_j,\ i = 1, \ldots, N. \tag{4.4}$$

Moreover, we also allow each subsystem to be implemented with a local controller whose output is denoted by $u_{\ell,i}, i = 1, \ldots, N$. Hence, the control input for each subsystem has the following form

$$u_i = w_i + u_{\ell,i}. \tag{4.5}$$

Figure 4.1 shows the structure of the locally controlled subsystems (agents) in the lower layer where $G_i(s)$ denotes the transfer function of the controlled ith subsystem (agent) and $L_i(s)$ denotes the local controller.

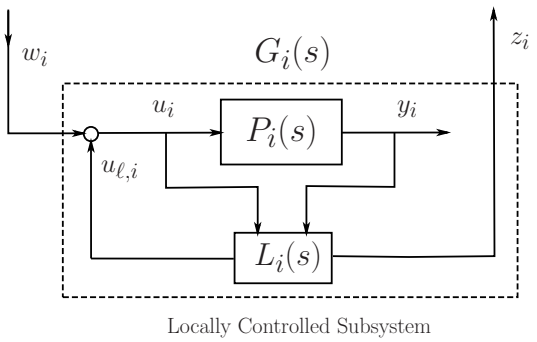

Figure 4.1: Block diagram of locally controlled subsystems (agents)

As a result, the control input for the whole hierarchical network is represented by

$$u = w + u_\ell = (K \otimes I_\mu) z + u_\ell, \tag{4.6}$$

where $w = \begin{bmatrix} w_1^T & \cdots & w_N^T \end{bmatrix}^T$, $z = \begin{bmatrix} z_1^T & \cdots & z_N^T \end{bmatrix}^T$, $u_\ell = \begin{bmatrix} u_{\ell,1}^T & \cdots & u_{\ell,N}^T \end{bmatrix}^T$. Subsequently, Figure 4.2 describes the whole hierarchical dynamical networked control system, where the interaction among subsystems is represented by the term $K \otimes I_\mu$.

The question here is how to design $z_i, u_{\ell,i}$ $(i = 1, \ldots, N)$ and $K \in \mathbb{K}_s$ in a systematic way to achieve both the global and local objectives as well as the stabilization of the whole networked system. This is actually our hierarchical decentralized controller design, which will be explained in the next subsection.

4.2.2 Heterogeneous Hierarchical Decentralized Design Problem

There are two design circumstances of hierarchical decentralized controllers for the given heterogeneous network, namely (i) state feedback design and (ii) output feedback design. If

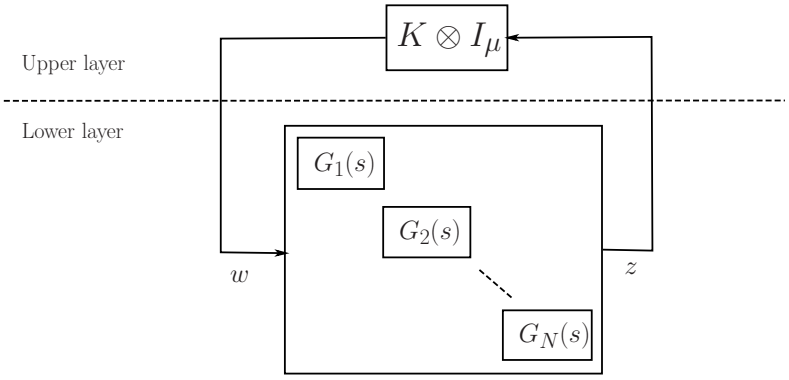

Figure 4.2: Block diagram of heterogeneous hierarchical networked control system.

all the states of agents, x_i $(i = 1, \ldots, N)$, are available, our purpose is to design a hierarchical state feedback controller. On the other hand, in the case that only partial agents' states, y_i $(i = 1, \ldots, N)$, can be measured, we need to design a hierarchical output feedback controller. We will show that introducing the local observers can reduce the design problem to the state feedback case.

First, we consider the design problem for the state feedback case of which the situation is seen in Figure 4.3 describing the whole hierarchical dynamical networked control system, where the interaction among subsystems is represented by the term $K \otimes I_\mu$.

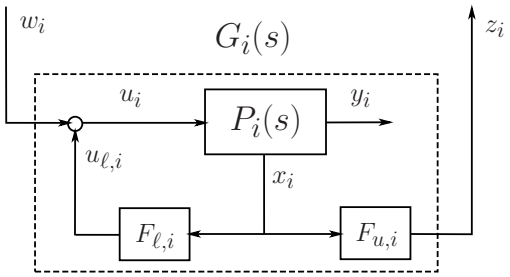

Figure 4.3: Block diagram of state feedback case for heterogeneous networks.

State feedback design problem: For the given network $\mathcal{G}$ with $(A_i, B_i), i = 1, \ldots, N$ controllable, the design problem is to determine the higher level interconnection gain $K \in \mathbb{K}_s$ and the lower layer state feedback gains $F_{\ell,i} \in \mathbb{R}^{\mu \times n_i}$ and $F_{u,i} \in \mathbb{R}^{\mu \times n_i}$, which respectively produce the local feedback signal $u_{\ell,i} = F_{\ell,i} x_i$ and the aggregated signal to be sent $z_i = F_{u,i} x_i$ for $i = 1, \ldots, N$.

Since the reference command of the ith subsystem w_i is determined by (4.4) and hence we have (4.6) , the determination of $F_{\ell,i}$ and $F_{u,i}$ for $i = 1, \ldots, N$ together with $K \in \mathbb{K}_s$ yields a state feedback form for $\dot{x} = \mathcal{A}x$ as

$$u = \mathcal{F}x,$$

where $\mathcal{F}$ belongs to the following class:

$$\mathbb{F}_K := \{\mathcal{F} \in \mathbb{R}^{m\times n} \mid \mathcal{F} = I_N \odot F_\ell + K \odot F_u\}, \tag{4.7}$$

with $F_\ell \in \mathbb{F}_\ell$ and $F_u \in \mathbb{F}_u$, where the class of local feedback gains $\mathbb{F}_\ell$ is defined by

$$\mathbb{F}_\ell := \{F_\ell \in \mathbb{R}^{m\times n} \mid F_\ell = \mathrm{diag}\{F_{\ell,i}\}_{i=1,\ldots,N}\} \tag{4.8}$$

the class of the global feedback gains $\mathbb{F}_u$ is defined by

$$\mathbb{F}_u = \{F_u \in \mathbb{R}^{m\times n} \mid F_u = [(\mathbf{1}_N\mathbf{1}_N^T) \otimes I_\mu]\mathrm{diag}\{F_{u,i}\}_{i=1,\ldots,N}, F_{u,i} \in \mathbb{R}^{\mu\times n_i}\}.$$

The requirement of $F_\ell \in \mathbb{F}_\ell$ is trivial. Noting that

$$(K \odot F_u)x = [(K \otimes I_\mu)\mathrm{diag}\{F_{u,i}\}_{i=1,\ldots,N}]x,$$

the requirement of $F_u \in \mathbb{F}_u$ can be confirmed by

$$\begin{aligned}(K \odot F_u)x &= [(K \otimes I_\mu)\mathrm{diag}\{F_{u,i}\}_{i=1,\ldots,N}]x \\ &= [(K \otimes I_\mu) \odot \mathrm{diag}\{F_{u,i}\}_{i=1,\ldots,N}]x \\ &= [K \odot [(\mathbf{1}_N\mathbf{1}_N^T) \otimes I_\mu] \odot \mathrm{diag}\{F_{u,i}\}_{i=1,\ldots,N}]x.\end{aligned}$$

Consequently, the sate feedback design problem is reduced to determine $F_\ell \in \mathbb{F}_\ell$, $F_u \in \mathbb{F}_u$ and $K \in \mathbb{K}_s$. In order to do this systematically, we will propose a procedure based on the LQR (Linear Quadratic Regulator) design, which can take the global/local objectives into account, in the next two sections.

Next, we consider the design problem for the output feedback case.

Output feedback design problem: For the given network $\mathcal{G}$ with $(A_i, B_i, C_i), i = 1, \ldots, N$ controllable and observable, the design problem is to determine local output feedback controllers $L_i(s)$ in Figure 4.1, i.e.,

$$\begin{bmatrix} u_{\ell,i} \\ z_i \end{bmatrix} = L_i(s) \begin{bmatrix} y_i \\ u_i \end{bmatrix}, \tag{4.9}$$

which at least stabilizes the whole networked system together with an appropriate choice of $K \in \mathbb{K}_s$.

Let us introduce the following Luenberger-type local observer for each subsystem

$$\begin{aligned}\dot{\hat{x}}_i &= A_i\hat{x}_i + B_iu_i + H_i(\hat{y}_i - y_i), \\ \hat{y}_i &= C_i\hat{x}_i, i = 1, , \ldots, N,\end{aligned} \tag{4.10}$$

where $\hat{x}_i \in \mathbb{R}^{n_i}$, $\hat{y}_i \in \mathbb{R}^{p_i}$ are the vectors of estimated state and output of the local observer in the ith subsystem, respectively and $H_i \in \mathbb{R}^{n_i\times p_i}$ is the gain matrix of the local observer such that $A_i + H_iC_i$ is stable. Summing up all the local observers, we obtain an observer for the given heterogeneous subsystems as follows:

$$\begin{aligned}\dot{\hat{x}} &= \mathcal{A}\hat{x} + \mathcal{B}u + \mathcal{H}(\hat{y} - y), \\ \hat{y} &= \mathcal{C}\hat{x},\end{aligned} \tag{4.11}$$

where $\hat{x} = \begin{bmatrix}\hat{x}_1^T & \cdots & \hat{x}_N^T\end{bmatrix}^T$, $\hat{y} = \begin{bmatrix}\hat{y}_1^T & \cdots & \hat{y}_N^T\end{bmatrix}^T$, $\mathcal{H} = \mathrm{diag}\{H_i\}_{i=1,\ldots,N}$. It can be clearly seen that the observer (4.11) is fully *decentralized*, since it only includes local observers for subsystems. Note that the order of the local observers may be different due to the different orders of the subsystems and that certain reduced-order observers are possible to be implemented.

Then, by introducing the error vector between the real state x and the estimated state $\hat{x}$. $e := x - \hat{x}$ and employing the designed stabilizing, hierarchical state feedback controller $u = \mathcal{F}\hat{x}$, as same as the standard case, the closed-loop hierarchical network model in this case becomes

$$\begin{aligned} \dot{x} &= (\mathcal{A} + \mathcal{B}\mathcal{F})x - [I_N \odot (\mathcal{B}F_\ell) + K \odot (\mathcal{B}F_u)]e, \\ \dot{e} &= (\mathcal{A} + \mathcal{H}\mathcal{C})e, \end{aligned} \tag{4.12}$$

Since $\mathcal{A} + \mathcal{B}\mathcal{F}$ is stable and we can design $\mathcal{H}$ such that $\mathcal{A} + \mathcal{H}\mathcal{C}$ is stable, the estimated state $\hat{x}(t)$ will converges to the real state $x(t)$ as $t \to \infty$ and the whole hierarchical heterogeneous network is stable.

This combination leads to the state space realization of the local controller $L_i(s)$ as follows:

$$\begin{aligned} \dot{\hat{x}}_i &= (A_i + H_i C_i)\hat{x}_i + \begin{bmatrix}B_i & H_i\end{bmatrix}\begin{bmatrix}u_i \\ y_i\end{bmatrix}, \\ \begin{bmatrix}u_{\ell,i} \\ z_i\end{bmatrix} &= \begin{bmatrix}F_{\ell,i} & F_{u,i}\end{bmatrix}^T \hat{x}_i. \end{aligned}$$

This shows that the design of output feedback case can be reduced to the design of the state feedback case by introducing the local observers (4.10).

4.3 Heterogeneous Hierarchical State Feedback LQR Design

4.3.1 Class of Performance Indexes

We first define the class of quadratic performance indexes to be minimized, which clearly captures our situation mentioned in the previous section. Consider the following performance index:

$$J := J_x + J_u \; ; \;\; J_x := J_{x,\mathcal{L}} + J_{x,\mathcal{G}}, \tag{4.13}$$

where J_x relates to the local and global objectives, which is the sum of $J_{x,\mathcal{L}}$ and $J_{x,\mathcal{G}}$, and J_u is a penalty for the control input required to the whole system represented by

$$J_u = \int_0^\infty u(t)^T \mathcal{R} u(t)\, dt, \tag{4.14}$$

where $\mathcal{R}\ (\succ 0) \in \mathbb{R}^{m\times m}$.

$J_{x,\mathcal{L}}$ is a local performance index composing of the individual penalties for the states of subsystems represented by

$$J_{x,\mathcal{L}} = \int_0^\infty x(t)^T (I_N \odot Q_\ell) x(t)\, dt, \tag{4.15}$$

where $Q_\ell = \text{diag}\{Q_i\}_{i=1,\dots,N}$ $(\succeq 0) \in \mathbb{R}^{n\times n}$ with Q_i $(\succeq 0) \in \mathbb{R}^{n_i\times n_i}$. $J_{x,\mathcal{G}}$ corresponds to a global performance index taking into account the information structure of the network captured by a matrix $K \in \mathbb{K}_s$, and it is given by

$$J_{x,\mathcal{G}} = \int_0^\infty x(t)^T (K \odot Q_g) x(t)\, dt, \tag{4.16}$$

where Q_g $(\succeq 0) \in \mathbb{R}^{n\times n}$. We here assume that K in $J_{x,\mathcal{G}}$ is restricted to the class of positive semidefinite interconnection defined by

$$\mathbb{K}_s^+ := \{K \in \mathbb{K}_s \mid K \text{ is positive semidefinite}\}, \tag{4.17}$$

in order to guarantee the positivity of $J_{x,\mathcal{G}}$. Note that $J_{x,\mathcal{G}}$ is employed to improve the control performance, since the elements of K as well as matrix Q_g put some weights on the relative states of subsystems leading to the improvement on the convergence of subsystems' states.

Subsequently, we can rewrite the performance index (4.13) as

$$J = \int_0^\infty (x(t)^T \mathcal{Q} x(t) + u(t)^T \mathcal{R} u(t)) dt, \tag{4.18}$$

where

$$\mathcal{Q} = I_N \odot Q_\ell + K \odot Q_g. \tag{4.19}$$

Following the form of $\mathcal{Q}$ above, we select the weighting matrix $\mathcal{R}$ with the following form:

$$\mathcal{R}^{-1} = I_N \odot R_\ell + K \odot R_g, \tag{4.20}$$

where $R_\ell = \text{diag}\{R_i\}_{i=1,\dots,N}$ $(\succ 0) \in \mathbb{R}^{m\times m}$ with R_i $(\succ 0) \in \mathbb{R}^{\mu\times\mu}$.

Employing the two standard assumptions, namely

[A1] $(\mathcal{A}, \mathcal{B})$ is controllable and

[A2] $(\mathcal{Q}^{1/2}, \mathcal{A})$ is observable,

it is shown from the optimal control theory [75] that the LQR optimal state feedback control is given by $u = \mathcal{F}x$ with

$$\mathcal{F} = -\mathcal{R}^{-1}\mathcal{B}^T\mathcal{P} \in \mathbb{R}^{m\times n},$$

where $\mathcal{P} \in \mathbb{R}^{n\times n}$ is the unique positive definite solution of the following Riccati equation:

$$\mathcal{P}\mathcal{A} + \mathcal{A}^T\mathcal{P} + \mathcal{Q} - \mathcal{P}\mathcal{B}\mathcal{R}^{-1}\mathcal{B}^T\mathcal{P} = 0. \tag{4.21}$$

It was proved in the previous works that if $\mathcal{A}, \mathcal{B}, \mathcal{C}, \mathcal{Q}, \mathcal{R}$ belong to some operator algebra [17] or semigroup [20] then the solution $\mathcal{P}$ of the Riccati equation (4.21) also belongs to that algebra or semigroup. As a result, they could prove that the LQR state feedback gain $\mathcal{F}$ has a similar property. However, in our setting in this paper, the Khatri-Rao product does not satisfy the properties of any operator algebra or semigroup, and hence it is not possible to show that with the choice of the weighting matrices as in (4.19) and (4.20), $\mathcal{P}$ has the same structure.

Therefore, in the next subsection, we will propose another way of choosing the weighting matrices $\mathcal{Q}$ and $\mathcal{R}$ of the forms of (4.19) and (4.20), respectively, which completely fits our situation and purpose.

4.3.2 State Feedback Design Procedure

In this subsection, we propose a systematic design procedure for hierarchical decentralized state feedback which consists of four steps.

- **Step 1 (Local LQR Design) :**
  Select the weighting matrices for the local objectives, $Q_i \in \mathbb{R}^{n_i \times n_i}$ and $R_i \in \mathbb{R}^{\mu \times \mu}$ such that $(Q_i^{1/2}, A_i)$ is observable and $R_i \succ 0$ for $i = 1, \ldots, N$, and solve the corresponding local Riccati equations

  $$P_i A_i + A_i^T P_i - P_i B_i R_i B_i^T P_i + Q_i = 0, \tag{4.22}$$

  to obtain the unique positive definite solution $P_i \in \mathbb{R}^{n_i \times n_i}$.

- **Step 2 (Setting Upper Layer Interactions) :**
  Choose a positive semidefinite matrix $K \in \mathbb{K}_s^+$ so that it properly reflects the global objective.

- **Step 3 (Global LQR Setting) :**
  Set the weighting matrices for $R_g \in \mathbb{R}^{m \times m}$ and $Q_g \in \mathbb{R}^{n \times n}$ for $J_{x,\mathcal{G}}$ as follows:

  $$R_g = r_{g1}(\mathbf{1}_N \mathbf{1}_N^T) \otimes I_\mu + r_{g2} I_m, \tag{4.23}$$
  $$Q_g = P_\ell \mathcal{B} R_g \mathcal{B}^T P_\ell, \tag{4.24}$$

  where $r_{g2} > 0$, $r_{g1} > 0$,

  $$P_\ell := \mathrm{diag}\{P_i\}_{i=1,\ldots,N} \succ 0 \tag{4.25}$$

  and $P_i \in \mathbb{R}^{n_i \times n_i}$ are the positive definite solutions of (4.22).

- **Step 4 (State Feedback Gain Calculation) :**
  Set the state feedback gains $F_{\ell,i}$ and $F_{u,i}$ for $i = 1, \ldots, N$ as follows:

  $$F_{\ell,i} = -(R_{\ell,i} + r_{g2} K_{ii} I_\mu) B_i^T P_i, \tag{4.26}$$
  $$F_{u,i} = -r_{g1} B_i^T P_i. \tag{4.27}$$

The validation of the procedure can be clearly made by the following theorem, which shows that the resultant LQR controller will belong to the class $\mathbb{F}_K$ in (4.7) if the weighting matrices are chosen as in the design procedure above.

Theorem 4.1. *Consider a set of subsystems represented by (4.1) with (A_i, B_i) controllable for all $i = 1, \ldots, N$. Let K be a matrix in class $\mathbb{K}_s^+$ and the weighting matrices $\mathcal{Q}$ and $\mathcal{R}$ have the forms (4.19) and (4.20) with $R_g \in \mathbb{R}^{m \times m}$ and $Q_g \in \mathbb{R}^{n \times n}$ chosen as in Step 3 of the state feedback design procedure in Subsection 4.3.2. Then the optimal hierarchical LQR state feedback gain is given by*

$$F = I_N \odot F_\ell + K \odot F_u, \tag{4.28}$$

where

$$\begin{array}{rl} F_\ell & = -\mathrm{diag}\{(R_{\ell,i} + r_{g2}K_{ii}I_\mu)B_i^T P_i\}_{i=1,\ldots,N} \quad \in \mathbb{F}_\ell, \\ F_u & = -[(\mathbf{1}_N\mathbf{1}_N^T) \otimes I_\mu]\mathrm{diag}\{r_{g1}B_i^T P_i\}_{i=1,\ldots,N} \quad \in \mathbb{F}_u. \end{array} \tag{4.29}$$

(See the appendix for the proof.)

There are a couple of remarks on the proposed design procedure.

- To make the cooperation among subsystems (agents) stronger, we may increase the value of R_g due to a fact that it will increase the value of Q_g as well. As a result, $\mathcal{Q}$ is increase while $\mathcal{R}$ is decreased since R^{-1} is proportional to R_g. Thus, the global performance index $J_{x,\mathcal{G}}$ is emphasized whereas the penalty for the control input $u^T\mathcal{R}u$ is reduced. Especially, the increase of r_{g1} is dominant to emphasize the cooperation, since r_{g2} is introduced only to make R_g non-singular. This feature will be demonstrated by an illustrated example in the next subsection.

- There are two ways of the implementation. The first one is a distributed manner, where the ith agent sends out the aggregated signal z_i to all the connected agent and computes its own reference command w_i by receiving information from the jth agents for j satisfying $(i,j) \in \mathcal{E}$. The second one is a hierarchical decentralized manner, where the ith agent sends out the aggregated signal z_i to the upper layer and the upper layer computes the reference commands w_i for all $i = 1, \ldots, N$ and sends the corresponding command to all the agents.

4.3.3 Example 4.1: Illustrative Example

Consider a network of 3 distinct subsystems whose transfer functions are given by

$$h_i(s) = \frac{1}{s^2 + \zeta_i s - 3} \quad (i = 1, 2, 3). \tag{4.30}$$

We use the following state-space realization of the form (3.1) for each subsystem.

$$A_i = \begin{bmatrix} 0 & 1 \\ 3 & -\zeta_i \end{bmatrix}, B_i = \begin{bmatrix} 0 \\ 1 \end{bmatrix}. \tag{4.31}$$

The parameter are set as $\zeta_1 = 4, \zeta_2 = 4.5, \zeta_3 = 5$ in the simulation. We observe that each matrix A_i has one unstable eigenvalue. Then by employing our design procedure, we can design a stabilizing hierarchical decentralized LQR controller for this network as follows.

We first choose $Q_1 = Q_2 = Q_3 = I_2$ and $R_1 = R_2 = R_3 = 1$ and solve the local Riccati equations (4.22) to obtain P_i $(i = 1, \ldots, 3)$. We then select $R_g = 10\mathbf{1}_3\mathbf{1}_3^T + I_3$ and $Q_g = P_\ell \mathcal{B} R_g \mathcal{B}^T P_\ell$ as in Step 3 of the design procedure to make each subsystem send a unique aggregated signal to cooperate with other two subsystems. Next, for the cooperation, let K be a Laplacian matrix as

$$K = \begin{bmatrix} 1 & -1 & 0 \\ -1 & 1+q & -q \\ 0 & -q & q \end{bmatrix}, \quad q \geq 0. \tag{4.32}$$

This matrix K implies that the 1st and the 2nd subsystems are connected, the 2nd and the 3rd subsystems may be connected depending on q while the 1st and the 3rd subsystems are not connected. Subsequently, we can rewrite the global performance index as follows,

$$\begin{aligned} & x^T(K \odot Q_g)x \\ = \; & r_{g1}[(B_1^T P_1 x_1 - B_2^T P_2 x_2)^T (B_1^T P_1 x_1 - B_2^T P_2 x_2) \\ & +q(B_2^T P_2 x_2 - B_3^T P_3 x_3)^T (B_2^T P_2 x_2 - B_3^T P_3 x_3)] \\ & +r_{g2}[P_1 B_1 B_1^T P_1 x_1^T x_1 + (1+q) P_2 B_2 B_2^T P_2 x_2^T x_2 \\ & +qP_3 B_3 B_3^T P_3 x_3^T x_3]. \end{aligned}$$

It can be seen that $J_{x,\mathcal{G}}$ puts a penalty under the form of a quadratic function with some weights for the difference between the states of subsystems and hence by minimizing J including $J_{x,\mathcal{G}}$, the gaps between the states of the 2nd and 3rd subsystems are reduced simultaneously with the decrease of the state of each subsystem. As a result, the convergence speed of the states of the 2nd and 3rd subsystems will be faster than that of the 1st subsystem. This means the obtained hierarchical LQR controller is designed not only for stabilization but also for cooperation among subsystems as they converge to zero.

The left hand side of plot in Figure 4.4 exhibits the output responses of subsystems without a global performance index. We can see that three subsystems independently converge to 0. When a global performance index is employed but $q = 0$, i.e., the 2nd and 3rd subsystems are not connected, the right hand side of plot tn the figure shows that the output of the 3rd subsystem is still the same with the left plot but the outputs of the 1st and 2nd subsystems make closer to each other before all the outputs of subsystems come to zero. This is because only the 1st and 2nd subsystems are connected while the 3rd subsystem is not connected to any of them.

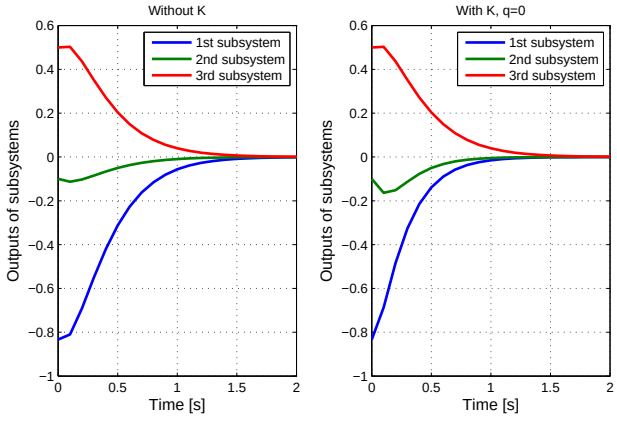

Figure 4.4: System responses when there is no global performance index and with a global performance index but $q = 0$.

Next, Figure 4.5 illustrates the outputs of subsystems when $q = 2$ and $q = 20$. We can observe that the convergence speed in these cases are faster than in the last cases.

Furthermore, the output of the 2nd subsystem rapidly converges to the output of the 3rd subsystem before all the outputs of subsystems come to zero as q increases. It is due to a much larger weight is put on the difference between the states of the 2nd and 3rd subsystems making them converge to each other faster. In other words, by letting q larger the network is divided into two groups of subsystems in which the first group include the 1st subsystem and the second group composes of the 2nd and 3rd subsystems. Thus, the structure of the network is clearly reflected in the interconnection matrix K and changing the elements of K with in class $\mathbb{K}_s^+$ can improve the control performance.

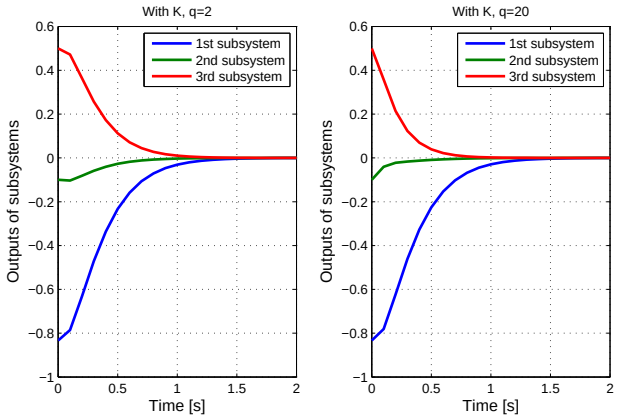

Figure 4.5: System responses when there is a global performance index with $q = 2$ and $q = 20$.

4.3.4 Example 4.2: Heterogeneous network of two-mass-spring systems

In the following, we investigate networks of two-mass-spring systems used to describe many industrial applications such as vibration in mechanical systems, with the model given in [1]. Figure 4.6 illustrates the considered two-mass-spring systems with their parameters and variables.

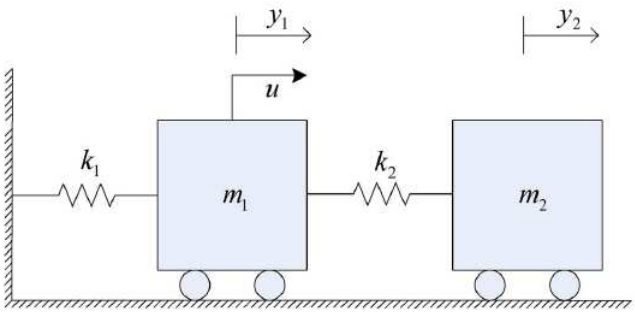

Figure 4.6: Two-mass-spring systems [1].

For simplicity, we consider a network of 6 distinct two-mass-spring systems, each one

is represented by the following state-space model,

$$\dot{x}_i = A_i x_i + B_i u_i, i = 1, \ldots, 6, \tag{4.33}$$

where

$$x_i = \begin{bmatrix} y_{1i} \\ \dot{y}_{1i} \\ y_{2i} \\ \dot{y}_{2i} \end{bmatrix}, A_i = \begin{bmatrix} 0 & 1 & 0 & 0 \\ \frac{-k_{1i}-k_{2i}}{m_{1i}} & 0 & \frac{k_{2i}}{m_{1i}} & 0 \\ 0 & 0 & 0 & 1 \\ \frac{k_{2i}}{m_{2i}} & 0 & \frac{-k_{2i}}{m_{2i}} & 0 \end{bmatrix}, B_i = \begin{bmatrix} 0 \\ \frac{1}{m_{1i}} \\ 0 \\ 0 \end{bmatrix}, \tag{4.34}$$

with m_{1i} and m_{2i} are two masses, k_{1i} and k_{2i} are spring constants; x_i is the state vector including the displacement of two masses and their derivatives, u_i is the force input for the mass 1 in each system.

Assuming that the two-mass-spring systems can bidirectionally exchange the information on their states then this network of two-mass-spring systems can be cast as a heterogeneous hierarchical network of integrators where each two-mass-spring system is a subsystem. We can see that the given two-mass-spring systems are unstable which may be the source for vibration in mechanical systems, then the control objective is to design a hierarchical controller for stabilizing the given network of two-mass-spring systems, i.e. for suppressing the vibration, and preserving the hierarchical structure of the network.

In this example, $m_{1i} = 0.8 + 0.1 * i$ kg, $m_{2i} = 0.6 + 0.1 * i$ kg, $k_{1i} = 1.2 + 0.1 * i$ N/m, $k_{2i} = 0.7 + 0.1 * i$ N/m. Consequently, all eigenvalues of 6 two-mass-spring systems lie in the imaginary axis which implies that the states in the two-mass-spring systems are oscillating. Indeed, Figure 4.7 shows the oscillating behaviors in the given two-mass-spring systems which may cause unexpected vibrations in mechanical systems.

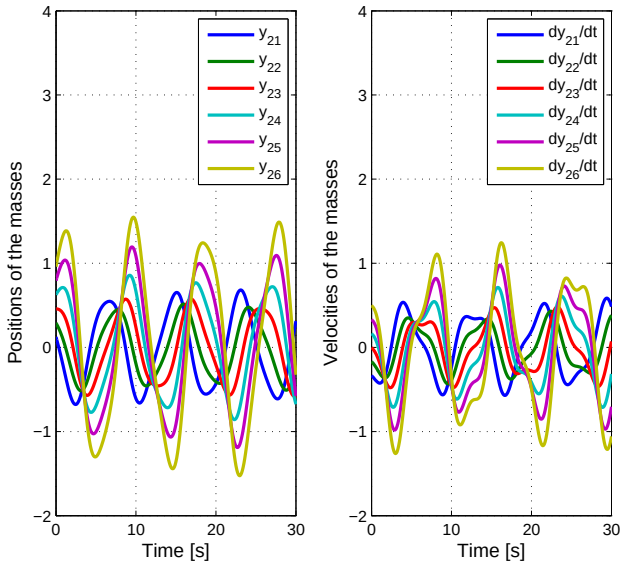

Figure 4.7: Oscillating behaviors of two-mass-spring systems without controller.

Utilizing our proposed design procedure, we design a hierarchical LQR controller for stabilizing the given heterogeneous network of two-mass-spring systems. Then, we have to utilize all left eigenvectors of A_i to construct the weighting matrix Q_i, $i = 1, \ldots, 6$ since all eigenvalues of each two-mass-spring system are unstable. Let us choose

$$\mathcal{Q}_i = 2I_4, R_i = 1, i = 1, \ldots, 6. \tag{4.35}$$

Subsequently, we can compute the weighting matrices Q_i and $\mathcal{R}_i$, $i = 1, \ldots, 6$ as in (4.38) and solve the Riccati equations (4.40) to obtain the matrices $\mathcal{P}_{1i}$, $i = 1, \ldots, 6$. Hence, we calculate P_i, $i = 1, \ldots, 6$ as in (4.39).

Next, assuming that the two-mass-spring systems are connected in a cyclic manner, i.e., K is cyclic, we select

$$R_g = \begin{bmatrix} 2 & 1 & 1 & 1 & 1 \\ 1 & 2 & 1 & 1 & 1 \\ 1 & 1 & 2 & 1 & 1 \\ 1 & 1 & 1 & 2 & 1 \\ 1 & 1 & 1 & 1 & 2 \end{bmatrix}, K = \begin{bmatrix} 2 & -1 & 0 & 0 & 0 & -1 \\ -1 & 2 & -1 & 0 & 0 & 0 \\ 0 & -1 & 2 & -1 & 0 & 0 \\ 0 & 0 & -1 & 2 & -1 & 0 \\ 0 & 0 & 0 & -1 & 2 & -1 \\ -1 & 0 & 0 & 0 & -1 & 2 \end{bmatrix}. \tag{4.36}$$

It can be verified that R_g is positive definite and K is positive semidefinite. Then the optimal hierarchical controller for the given heterogeneous network of two-mass-spring systems is built as in (4.28). The simulation result in Figure 4.8 shows that all eigenvalues of the closed-loop interconnection matrix A of the two-mass-spring network with designed controller lie in the left-half complex plane. Thus, the designed two-mass-spring network is stabilized as illustrated in Figure 4.9 where we only plot the positions and velocities of the second masses in the two-mass-spring systems since they are more difficult to control than the first masses.

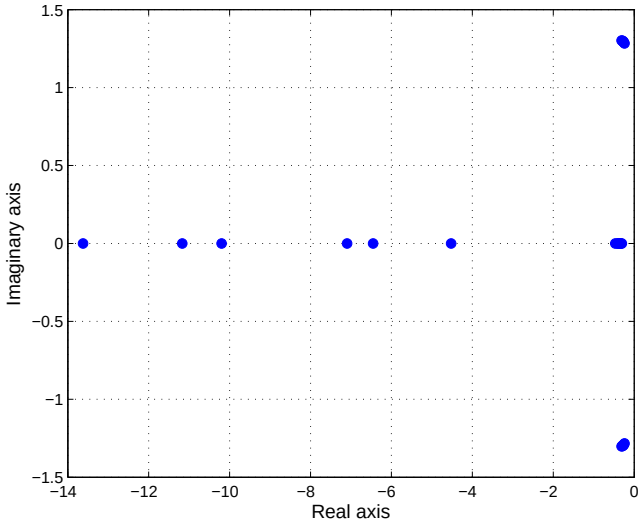

Figure 4.8: Eigenvalue distribution of the two-mass-spring network with designed controller.

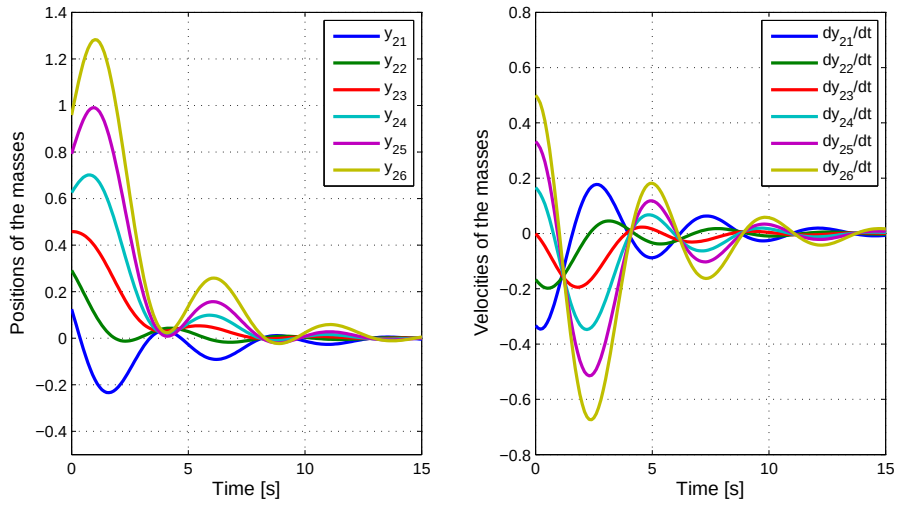

Figure 4.9: Time plot of states in the cyclic two-mass-spring network.

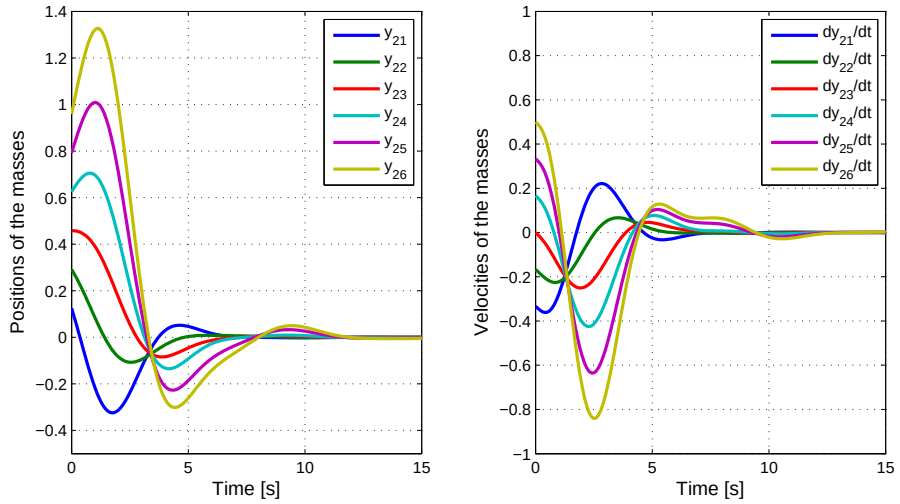

Figure 4.10: Time plot of the two connected groups of two-mass-spring systems when $q = 10$.

To verify the effect of communication structure among the subsystems to the response of the network, we try K with different structures as follows. The network is divided into two groups, the 1st group contains the 1st, 2nd and 3rd two-mass-spring systems while the 2nd group includes the 4th, 5th and 6th two-mass-spring systems. Moreover, these two groups are connected by the connection between the 3rd two-mass-spring system in the first group and the 4th two-mass-spring system in the second group. Accordingly, the interconnection

matrix K is

$$K = \begin{bmatrix} 2 & -1 & -1 & 0 & 0 & 0 \\ -1 & 2 & -1 & 0 & 0 & 0 \\ -1 & -1 & 2+q & -q & 0 & 0 \\ 0 & 0 & -q & 2+q & -1 & -1 \\ 0 & 0 & 0 & -1 & 2 & -1 \\ 0 & 0 & 0 & -1 & -1 & 2 \end{bmatrix}, q \geq 0. \tag{4.37}$$

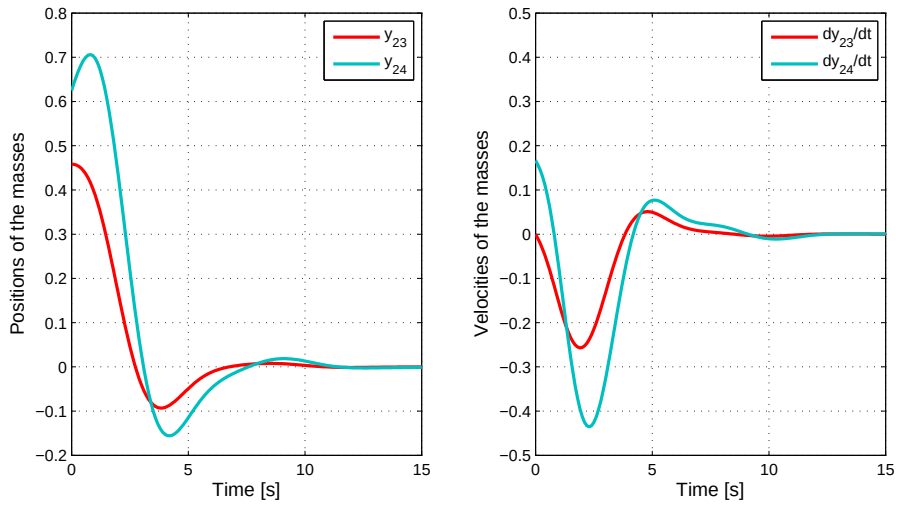

Figure 4.11: Time plot of the 3rd and 4th two-mass-spring systems when $q = 10$.

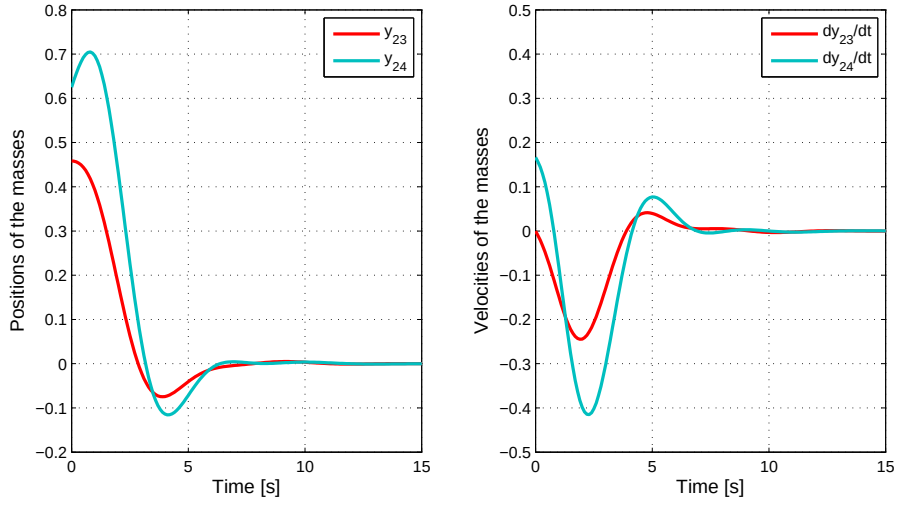

Figure 4.12: Time plot of the 3rd and 4th two-mass-spring systems when $q = 20$.

Figure 4.10 reveals that the positions and velocities of the 3rd and 4th two-mass-spring systems converge to each other faster than to other two-mass-spring systems as $q = 10$. Moreover, the convergence rate is faster than in cyclic structure. Consequently, we increase q to be 20 to see how it affects to the convergence speed of the positions and velocities of the

3rd and 4th two-mass-spring systems. The simulation results in Figure 4.11 and Figure 4.12 display the positions and velocities of the 3rd and 4th two-mass-spring systems as $q = 10$ and $q = 20$, respectively. It can be seen that the convergence speed in the case of $q = 20$ is faster than in the case of $q = 10$. The reason for such behaviors is that we increase q, i.e., put more weights on the state differences between the 3rd and 4th two-mass-spring systems in the global performance index.

4.4 Selective Pole Shift for Heterogeneous Hierarchical Dynamical Networks

This section introduces an approach to further design the LQR controller in Section 4.3 such that the undesirable eigenvalues in each subsystem (agent) are selectively shifted. The key point here is to choose the proper matrices Q_i based on the left eigenvectors of $A_i, i = 1, \ldots, N$ associated with the undesired eigenvalues.

For $i = 1, \ldots, N$, suppose that $(\lambda_{1i}, \ldots, \lambda_{l_i i})$ are undesirable eigenvalues of A_i and $\nu_{1i}^*, \ldots, \nu_{l_i i}^*$ are the associated left-eigenvectors; l_i is the number of undesirable eigenvalues in the ith subsystem. We select the weighting matrix Q_i under the form

$$Q_i = V_i \mathcal{Q}_i V_i^*, \tag{4.38}$$

where $V_i = \begin{bmatrix} \nu_{1i} & \cdots & \nu_{l_i i} \end{bmatrix}$, $\mathcal{Q}_i \succeq 0$, then the solution P_i of the Riccati equation (4.22) also has the form

$$P_i = V_i \mathcal{P}_i V_i^*, \tag{4.39}$$

with a positive definite matrix $\mathcal{P}_i \in \mathbb{R}^{l_i \times l_i}$. Substituting Q_i and P_i back to (4.22), we obtain

$$\mathcal{P}_i \Gamma_i + \Gamma_i \mathcal{P}_i - \mathcal{P}_i \mathcal{R}_i \mathcal{P}_i + \mathcal{Q}_i = 0, \tag{4.40}$$

where

$$\Gamma_i = \text{diag}\{\lambda_{ji}\}_{j=1,\ldots,l_i}, \mathcal{R}_i = V_i^* B_i R_i B_i^T V_i. \tag{4.41}$$

Therefore, solving the $l_i \times l_i$ Riccati equation (4.40) gives us matrix $\mathcal{P}_i$ and then P_i is calculated from (4.39).

Denote

$$E_i = B_i^T V_i, E_i \in \mathbb{R}^{\mu \times l_i}, i = 1, \ldots, N. \tag{4.42}$$

Once we obtain $P_i, i = 1, \ldots, N$, the eigenvalue spectrum of the closed-loop interconnection matrix A in the whole heterogeneous hierarchical network can be determined as in the following theorem.

Theorem 4.2. *With the hierarchical decentralized LQR state feedback controller $u = \mathcal{F}x$ designed in Theorem 4.1 and the sub-weighting matrix Q_ℓ selected in (4.38), the eigenvalue set the closed-loop interconnection matrix A is*

$$\sigma(A) = \bigcup_{i=1}^{N} (\sigma(A_i) \backslash \{\lambda_{1i}, \ldots, \lambda_{l_i i}\}) \bigcup \sigma(\Xi), \tag{4.43}$$

where Ξ *is defined by*

$$\Xi = \Gamma - \Psi_1 - (K \odot \Psi_2), \tag{4.44}$$

and $\Gamma = \text{diag}\{\Gamma_i\}_{i=1,\ldots,N}$, $\Psi_1 = \text{diag}\{\Psi_{1i}\}_{i=1,\ldots,N}$, $\Psi_2 = [\Psi_2(i,j)]_{i,j=1,\ldots,N}$ *in which*

$$\begin{aligned} \Psi_{1i} &= E_i^* R_i E_i \mathcal{P}_i, \\ \Psi_2(i,j) &= E_i^* R_g(i,j) E_j \mathcal{P}_j. \end{aligned} \tag{4.45}$$

Proof. Consider any right eigenvector η_i of A_i corresponding to an eigenvalue $\lambda_i \in \sigma(A_k)\backslash\{\lambda_{1i}, \ldots, \lambda_{l_i i}\}$. Denote $\hat{\eta}_i \in \mathbb{X}_{\Delta_1}^N$ the vector whose ith block is η_i and other blocks are zero. Then

$$\begin{aligned} A\hat{\eta}_i &= [I_N \odot \mathcal{A}]\hat{\eta}_i - [I_N \odot (\mathcal{B}R_\ell \mathcal{B}^T P_\ell)]\hat{\eta}_i \\ &\quad -[K \odot (\mathcal{B}R_g \mathcal{B}^T P_\ell)]\hat{\eta}_i. \end{aligned} \tag{4.46}$$

The ith block of the second term on the right-hand side of (4.46) is $B_i R_i E_i \mathcal{P}_i V_i^* \eta_k$ which is equal to 0 since $\nu_{ji}^* \eta_i = 0 \; \forall \; j = 1, \ldots, l_i$. Similarly, the third term on the right-hand side of (4.46) is also equal to 0. On the other hand, the first term on the right-hand side of (4.46) is a vector in $\mathbb{X}_{\Delta_1}^N$ whose ith block is equal to $A_i \mu_i = \lambda_i \eta_i$. Accordingly, $[I_N \odot \mathcal{A}]\hat{\eta}_i = \lambda_i \hat{\eta}_i$. Therefore, λ_i is an eigenvalue of A with the associated right eigenvector $\hat{\eta}_i$. This leads to

$$\bigcup_{i=1}^{q} (\sigma(A_i)\backslash\{\lambda_{1i}, \ldots, \lambda_{l_i i}\}) \subset \sigma(A) \tag{4.47}$$

Now, denote $V = \text{diag}\,\{V_i\}_{i=1,\ldots,N}$. We have

$$\begin{aligned} V^* A &= V^*[I_m \odot (\mathcal{A} - \mathcal{B}R_\ell \mathcal{B}^T P_\ell) - K \odot (\mathcal{B}R_g \mathcal{B}^T P_\ell)] \\ &= \text{diag}\,\{\Gamma_i - E_i^* R_i E_i \mathcal{P}_i\}_{i=1,\ldots,N} V^* \\ &\quad -V^*[K \odot (\mathcal{B}R_g \mathcal{B}^T P_\ell)] \\ &= (\Gamma - \Psi_1)V^* - V^*[K \odot (\mathcal{B}R_g \mathcal{B}^T P_\ell)] \end{aligned} \tag{4.48}$$

The (i,j) block of the second term on the right-hand side of (4.48) is

$$V_i^* K_{ij} B_i R_g(i,j) B_j^T P_j V_j^* \tag{4.49}$$

$$\begin{aligned} &= K_{ij} V_i^* B_i R_g(i,j) B_j^T V_j \mathcal{P}_j V_j^* \\ &= K_{ij} \Psi_2(i,j) V_j^* \end{aligned} \tag{4.50}$$

Hence, the second term on the right-hand side of (4.48) is indeed $(K \odot \Psi_2)V^*$. As a result,

$$V^* A = [\Gamma - \Psi_1 - K \odot \Psi_2]V^*. \tag{4.51}$$

Let ρ^* is any left eigenvector of $\Gamma - \Psi_1 - K \odot \Psi_2$ and γ is the associated eigenvalue. Then multiplying both sides of (4.51) with ρ^* we obtain

$$\begin{aligned} \rho^* V^* A &= \rho^*[\Gamma - \Psi_1 - K \odot \Psi_2]V^* \\ &= \gamma \rho^* V^* \end{aligned} \tag{4.52}$$

This means γ is also an eigenvalue of A with the corresponding left eigenvector $(V\rho)^*$. Accordingly,

$$\sigma(\Gamma - \Psi_1 - K \odot \Psi_2) \subset \sigma(A) \tag{4.53}$$

Thus, combining (4.47) and (4.53) gives us (4.43). □

Thanks to Theorem 4.2, only undesirable eigenvalues are selectively moved. Furthermore, we can determine the eigenvalue spectrum of the closed-loop interconnection matrix A based on the eigenvalues of the local interconnection matrices $A_i, i = 1, \ldots, N$ and the matrix Ξ.

4.5 Application to Vehicle Platoons

In this section, we aim at applying the designed hierarchical optimal LQR stabilizing controller for solving the velocity consensus problem in heterogeneous vehicle platoons. By heterogeneous, we mean that the dynamics of vehicles are different since the vehicles running on the roads are made by different companies with different technical specifications such as length, weights, torques, etc. One of the fundamental problems for building an automated highway is that the cars should run at the same velocity and the distance between a car with its predecessor in a lane should be constant, minimum but positive, i.e., without collision, such that the throughput of the highway is better. This configuration of a vehicle network is usually called a vehicle string or a vehicle platoon. The simplest communication topology among the vehicles in a platoon is that a vehicle is connected with its preceding and following ones, i.e., each vehicle only regulate its velocity based on the relative positions and relative velocities with its preceding and following vehicles. There may also be more complex scenarios such as the sensor range in a vehicle is wide enough to sense the relative positions and relative velocities with other vehicles in the platoon rather than its two nearest vehicles, or the vehicles in different lanes can intercommunicate instead of only connecting to others in the same lane. However, we only consider the string communication topology as aforementioned for simplicity.

Suppose that the vehicle network composes of $N+1$ different vehicles and the position vector of vehicles is denoted by $x = \begin{bmatrix} x_0, \ldots, x_N \end{bmatrix}^T$. Following the work in [79], we consider the following model for vehicles

$$h_i(s) = \frac{a_i}{s(s + b_i)}, i = 0, \ldots, N, \tag{4.54}$$

where a_i, b_i are parameters depending on the length, weight and other characteristics of the ith vehicle. Note here that in [79], the dynamics of vehicles are homogeneous and the vehicles were assumed to connect to other vehicles with string topology and consequently, the stability of the whole vehicle network was analyzed. However, in this work, we consider independent vehicles, i.e., they are not connected at first, then we would like to design a controller for

them so that their velocities become consensus and they are communicated through a string topology. Furthermore, we will consider the 0th vehicle as a leader for the network, i.e., it is freely running and other vehicles must follow it.

Figure 4.13 describes a vehicle platoon with related variables where $r_i = y_{i-1} - y_i - \gamma_i, i = 1, \ldots, N$ are the vehicles' headway distances, $\gamma_i, i = 1, \ldots, N$ are constants representing the lengths of vehicles plus safety margins of headway distances as stopping [79]. Subsequently, our objective is to the design a controller for this vehicle platoon such that all the velocities of vehicles are consensus to the velocity of the leading vehicle and the headway distances become zero so that the distances among vehicles are minimum. In the following, we will assume that $\gamma_1 = \cdots = \gamma_N = \gamma$ for simplicity in representing the results.

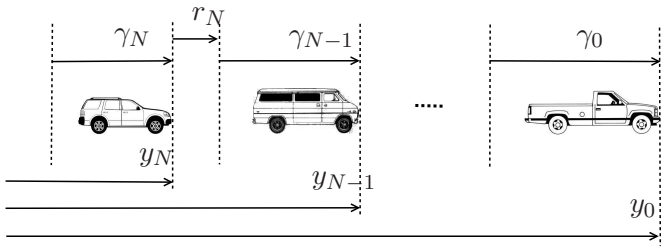

Figure 4.13: Demonstration of a vehicle platoon.

The state-space model of the transfer functions $h_i(s), i = 1, \ldots, N$ are as follows,

$$\dot{\xi}_i = A_i \xi_i + B_i u_i, \tag{4.55}$$

where $\xi_i = \begin{bmatrix} y_i & \dot{y}_i \end{bmatrix}^T$ is the vector of the position and velocity of the ith vehicle, u_i is the control input, and

$$A_i = \begin{bmatrix} 0 & 1 \\ 0 & -b_i \end{bmatrix}, B_i = \begin{bmatrix} 0 \\ a_i \end{bmatrix}. \tag{4.56}$$

Let us define a new state vector $x_i = \begin{bmatrix} y_i - (N-i)\gamma & \dot{y}_i \end{bmatrix}^T, i = 1, \ldots, N$ then we obtain the state-space model for the new state variables as follows,

$$\dot{x}_i = A_i x_i + B_i u_i. \tag{4.57}$$

Accordingly, the velocities of all vehicles will reach consensus and the distances between two nearest vehicles will become γ if x_i comes to zero for all $i = 1, \ldots, N$. Then, we treat $h_i(s), i = 1, \ldots, N$ as subsystems and employing our method proposed in Section 4.3, we design an optimal hierarchical LQR state feedback controller for the speed consensus problem in the vehicle platoon.

To illustrate the consensus design, we consider the following example.

Example. Consider a platoon of 8 different vehicles with parameters $a_i, b_i, i = 1, \ldots, 7$ are randomly chosen in the intervals $[1, 2]$ and $(0, 1]$, respectively. Then we choose $Q_i = 1, i = 1, \ldots, 7$, $R_i = 1, i = 1, \ldots, 7$ and

$$R_g = \mathbf{1}_7\mathbf{1}_7^T + I_7, K = \begin{bmatrix} 1 & -1 & 0 & 0 & 0 & 0 & 0 \\ -1 & 2 & -1 & 0 & 0 & 0 & 0 \\ 0 & -1 & 2 & -1 & 0 & 0 & 0 \\ 0 & 0 & -1 & 2 & -1 & 0 & 0 \\ 0 & 0 & 0 & -1 & 2 & -1 & 0 \\ 0 & 0 & 0 & 0 & -1 & 2 & -1 \\ 0 & 0 & 0 & 0 & 0 & -1 & 1 \end{bmatrix}.$$

Then we obtain matrices $P_i, i = 1, \ldots, 4$ and hence the hierarchical LQR state feedback controller $\mathcal{F}$. The simulation result in Figure 4.14 displays the positions of all vehicles as the 0th vehicle, i.e., the leading vehicle keeps its velocity constant at 2 m/s. At the initial condition, the distances between the 1st and 0th vehicles, between the 3rd and 2nd, and between the 6th and 5th vehicles are quite large whereas the distances between the 2nd and 1st vehicles, between the 5th and 4th and 3rd vehicles, and between the 7th and 6th vehicles are quite small. This configuration means that the vehicle network has three groups including the (1st, 2nd); (3rd, 4th, 5th); and (6th, 7th) vehicles; respectively. Then Figure 4.14 shows that the distances among the vehicles are regulated to be as desired and the velocities of all vehicles converge to the velocity of the leading vehicle, i.e., the velocities of vehicles are consensus.

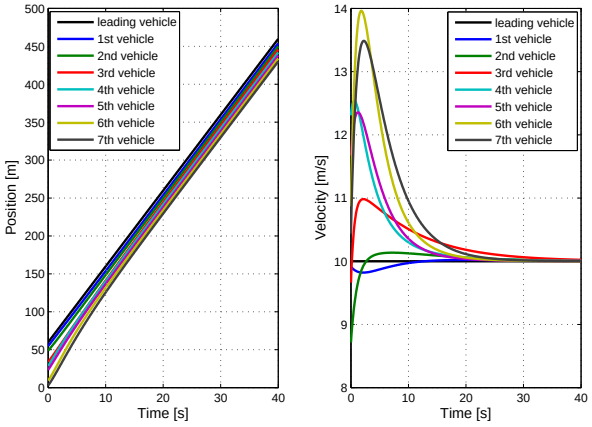

Figure 4.14: Consensus of vehicles's velocities with the designed hierarchical optimal LQR controller.

Next, we verify how are the responses of the vehicle platoon as the leading vehicle changes its velocity. Assuming that the velocity of the leading vehicle changes as a sinusoidal signal $4 + 2\sin(t)$, then Figure 4.15 reveals that the speed of all following cars are still consensus with the velocity of the leading vehicle and the distances between each vehilce and its predecessor come to desired values.

In another situation, we assume that there exist constant disturbances to the vehicle platoon after the platoon is run for 20 s. The disturbance to each vehicle is represented by an additional term $E_i d$ in the state space model (4.55) where $E_i = \begin{bmatrix} 0 & 1 \end{bmatrix}^T, i = 1, \ldots, 7$ and

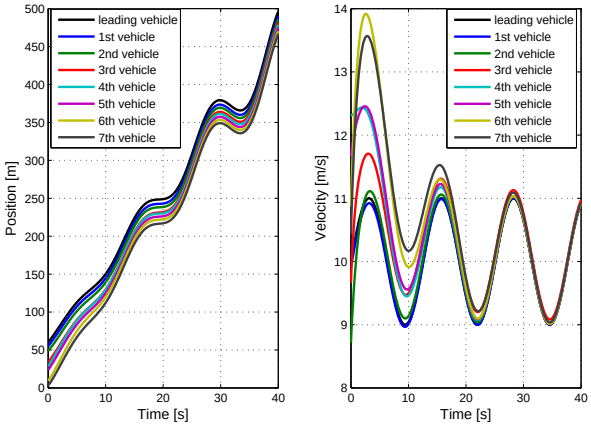

Figure 4.15: Consensus of vehicles's velocities as the leading vehicle changes its speed.

$d = 0.5$. Figure 4.16 displays the simulation results for this case. We can observe that as soon as the disturbances affect to the vehicle platoon, the velocities of vehicles exhibit some transient responses before converging to the velocity of the leader again. Thus, the proposed controller still work well in the presence of constant disturbance.

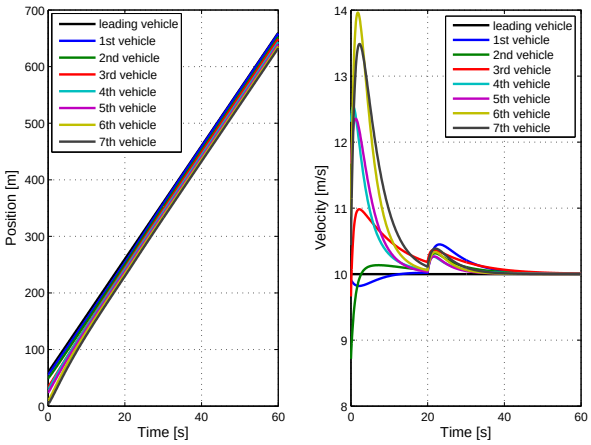

Figure 4.16: Consensus of vehicles's velocities with the designed hierarchical optimal LQR controller.

4.6 Summary

This chapter has proposed a systematic method to design state and output feedback hierarchical, optimal LQR controllers for heterogeneous hierarchical multi-agent dynamical networks. There are two novelties in our synthesis method. First, the hierarchical LQR controller preserves a prescribed hierarchical structure of the heterogeneous network. This is due to the selection of the weighting matrices with proper hierarchical structures. Second, the hierar-

chical LQR controller is able to selectively shift the undesired eigenvalues of subsystems in the network by choosing the weighting matrices based on the left eigenvectors associated with those undesirable eigenvalues. Note that the number of undesirable eigenvalues in a subsystem may be different from that of other subsystems.

The next contribution of this chapter is to employ the proposed design method for an application in vehicle platoons where the velocities of vehicles are expected to be the same and the distances among the vehicles are as desired. This actually raises up a consensus problem for vehicle platoons. Consequently, by considering the models for the headway distances among vehicles which are heterogeneous, we are able to design a state feedback hierarchical optimal controller for such system using our proposed method. As a result, the headway distances are controlled to be zero leading to the consensus on the velocities of vehicles and the desired distances among them.

4.7 Appendix

4.7.1 Khatri-Rao product

Definition 4.1. *Consider an interval $I = [0, n]$ where n is a positive integer. Denote Δ a partition dividing I into $N \leq n$ intervals by the points $0 = \zeta_0 < \zeta_1 < \cdots < \zeta_N = n$. Denote the length of I by $\rho(\Delta)$, the length of smaller intervals $[\zeta_{i-1}, \zeta_i]$ by $\delta^i, i = 1, \ldots, N$, the number of partitions by $\sharp(\Delta)$. Next, define the set of $M \times N$ block matrices*

$$\mathbb{X}^{M\times N}(\Delta_1, \Delta_2) = \{ X \in \mathbb{R}^{\rho(\Delta_1)\times\rho(\Delta_2)} \Big| X_{ij} \in \mathbb{R}^{\delta_1^i \times \delta_2^j} \}, \tag{4.58}$$

where partitions Δ_1 and Δ_2 satisfy $\sharp(\Delta_1) = M$ and $\sharp(\Delta_2) = N$, respectively and X_{ij} represents the (i, j) block matrix of X. Then, the Khatri-Rao product is a binary operator

$$\odot : \mathbb{R}^{M\times N} \times \mathbb{X}^{M\times N}(\Delta_1, \Delta_2) \to \mathbb{X}^{M\times N}(\Delta_1, \Delta_2)$$

such that for all matrices $A = [a_{ij}] \in \mathbb{R}^{M\times N}, B = [B_{ij}] \in \mathbb{X}^{M\times N}(\Delta_1, \Delta_2)$,

$$A \odot B = C \in \mathbb{X}^{M\times N}(\Delta_1, \Delta_2), C_{ij} = a_{ij} B_{ij}. \tag{4.59}$$

4.7.2 Proof of Theorem 4.1

We first show that Assumptions **A1** and **A2** are satisfied in our setting. Assumption **A1** is trivially satisfied, because it is equivalent to the controllability of (A_i, B_i) for all $i = 1, \ldots, N$. Similarly, we readily see that Assumption **A2** holds when $Q_g = 0$. Note that the second term of $\mathcal{Q}$, or $K \odot Q_g$, is positive semidefinite, because both matrices K and Q_g are positive semidefinite. Therefore, introduction of this extra term in $\mathcal{Q}$ does not break the observability condition, and hence Assumption **A2** holds even for any $Q_g \succeq 0$. In addition, $R_\ell \succ 0$ leading to $I_N \odot R_\ell \succ 0$. This yields $\mathcal{R}^{-1} = I_N \odot R_\ell + K \odot R_g \succ 0$, i.e., $\mathcal{R} \succ 0$. Consequently, we see that there exists a unique positive definite solution of (4.21).

Next, substituting $\mathcal{P} = I_N \odot P_\ell$ and $\mathcal{Q}, \mathcal{R}$ back to the Riccati equation (4.21), we obtain

$$\begin{aligned} 0 &= I_N \odot (P_\ell \mathcal{A} + \mathcal{A}^T P_\ell - P_\ell \mathcal{B} R_\ell \mathcal{B}^T P_\ell + Q_\ell) \\ &\quad + K \odot (Q_g - P_\ell \mathcal{B} R_g \mathcal{B}^T P_\ell) \end{aligned} \tag{4.60}$$

This is always true with $Q_g = P_\ell \mathcal{B} R_g \mathcal{B}^T P_\ell$ and $P_\ell = \mathrm{diag}\{P_i\}_{i=1,\ldots,N}$, where P_i $(i = 1, \ldots, N)$ are positive definite solutions of (4.22). Hence, $\mathcal{P} = I_N \odot P_\ell$ is the unique positive definite solution of (4.21). Accordingly, the LQR controller is calculated as follows,

$$\begin{aligned} \mathcal{F} &= -\mathcal{R}^{-1} \mathcal{B}^T \mathcal{P}, \\ &= -(I_N \odot R_\ell + K \odot R_g)(I_N \odot \mathcal{B}^T)(I_N \odot P_\ell), \\ &= -I_N \odot (R_\ell \mathcal{B}^T P_\ell) - K \odot (R_g \mathcal{B}^T P_\ell), \\ &= -\mathrm{diag}\{(R_{\ell,i} + r_{g2} K_{ii} I_\mu) B_i^T P_i\}_{i=1,\ldots,N} \\ &\quad -K \odot ([(\mathbf{1}_N \mathbf{1}_N^T) \otimes I_\mu] \mathrm{diag}\{r_{g1} B_i^T P_i\}_{i=1,\ldots,N}). \end{aligned}$$

Consequently, the LQR controller gains F_ℓ and F_u are determined by (4.28). This completes the proof.

CHAPTER 5

SYNCHRONIZATION IN NETWORKS OF GENERALIZED GOODWIN-TYPE OSCILLATORS

5.1 Introduction

In this chapter, the oscillations in the networks of generalized Goodwin oscillators driven by exogenous periodic inputs are analyzed. Generalized Goodwin oscillators are nonlinear oscillators containing a high-order linear transfer function in series with a nonlinear function. This type of networks has been used to describe the biochemical processes with negative feedbacks. So far, the researches on nonlinear oscillator networks mostly focus on the natural oscillations occur in the networks but there are real situations that these networks are driven by some exogenous periodic signals, for instance circadian networks driven by zeitgebers [29, 70–72]. It has been reported in many researches, e.g. [80–82] that there are several sleep disorder syndromes related to circadian rhythms such as delayed/advanced sleep phase, seasonal affective disorder (SAD), shift work, jet lag, etc, which may have clinical treatments by using bright light or melatonin. The bright light or melatonin actually are external sources which are employed to adjust the phases of circadian rhythms in patients. From a system point of view, this is fit into the problem of driven nonlinear oscillator networks considered in this chapter and the next chapter. Therefore, the study of oscillations in the networks excited by external periodic inputs has a significant importance which is closely related to practical applications. Analyzing how the profiles of the network oscillations including the frequency, phases and amplitudes depend on the profile of exogeneous input reveals the dynamical behaviors of the network and hence would give us the clues to regulate the network oscillations by external inputs.

The contribution of this chapter is to provide an analysis framework for the nonlinear oscillator networks, in particular generalized Goodwin oscillator networks where a condition for the synchronization of network oscillations by the external input is proposed. Furthermore, the analytical expressions showing the relations between the profiles of network oscillations and external inputs are revealed, and the monotonicity of those relations is figured out. From a broader view, this chapter and the next chapter propose an analysis approach for the leader-follower consensus problems for nonlinear systems where the external signal is the leader and the oscillators in the network are the followers. In addition, more insights on the relations of the leader and the followers are revealed showing the roles of the external input as a command signal to not only reach consensus in the network but also shift the profile of network oscillations.

The analysis approach we employ in this chapter and the next chapter is the harmonic balance approach. For a given periodic driving signal, the induced oscillations in the network are assumed to contain the harmonic components up to the same order as the harmonic components in the driving signal. Consequently, balancing the harmonic components gives us the harmonic balance equations which show the dependence of the profiles of induced network oscillations to the profile of the exciting periodic signal. Then the relations between network oscillations and the external signal are figured out to be monotonic under some additional assumptions and conditions. Finally, a numerical example is introduced to illustrate the theoretical results.

5.2 Goodwin-type Nonlinear Oscillator Networks

5.2.1 Model of a Goodwin-type Nonlinear Oscillator

In this paper, we consider a class of nonlinear oscillators networks consisting of so called generalized Goodwin-type oscillators of qth-order ($q \geq 2$) expressed as

$$\begin{cases} \dfrac{dX_1}{d\tau} &= k_1 \dfrac{K^p}{K^p + X_q^p} - k_{q+1} X_1, \\ \dfrac{dX_2}{d\tau} &= k_2 X_1 - k_{q+2} X_2, \\ &\vdots \\ \dfrac{dX_q}{d\tau} &= k_q X_{q-1} - k_{2q} X_q. \end{cases} \tag{5.1}$$

This model is a generalization of the classical 3rd-order Goodwin model in [25, 26, 60, 61] to represent a process with nonlinear negative feedback which may be found for instance in biochemical networks. The physical meanings of variables and parameters may be explained as follows. $X_1, X_2, \ldots, X_q$ are the concentrations of chemicals; $k_1, k_2, \ldots, k_{2q}$ are the rates of reactions; the Hill function $\dfrac{K^p}{K^p + X_q^p}$ represents a nonlinear effect of the last chemical to the first one, and K is a constant. Then, introducing new variables as

$$\begin{aligned} &\eta = \sqrt[q]{\frac{K}{k_1 k_2 \cdots k_q}}, b_1 = \eta k_{q+1}, \ldots, b_q = \eta k_{2q}, \\ &x_1 = \frac{\eta^{q-1} k_2 \cdots k_q X_1}{K}, x_2 = \frac{\eta^{q-2} k_3 \cdots k_q X_2}{K}, \\ &\ldots, x_q = \frac{X_q}{K}, t = \frac{\tau}{\eta}, \end{aligned} \tag{5.2}$$

leads to the dimensionless mathematical model of a single Goodwin-type oscillator as follows,

$$\begin{cases} \dfrac{dx_1}{dt} &= f(x_q) - b_1 x_1, \quad f(x_q) = \dfrac{1}{1 + x_q^p}, \\ \dfrac{dx_2}{dt} &= x_1 - b_2 x_2, \\ &\vdots \\ \dfrac{dx_q}{dt} &= x_{q-1} - b_q x_q. \end{cases} \tag{5.3}$$

Using the Laplace transform, we further rewrite the dimensionless Goodwin-type oscillator as

$$\begin{cases} z &= h(s)u, \\ u &= f(z), \end{cases} \tag{5.4}$$

where z is used to denote x_q and

$$h(s) = \frac{1}{(s+b_1)(s+b_2)\cdots(s+b_q)}. \tag{5.5}$$

5.2.2 Model of Oscillator Networks

Assuming now that the oscillator network includes n interconnected Goodwin-type oscillators, where the input of kth oscillator is given by

$$u_k = \sum_{1\le j\le n} A_{kj} f(z_j) + w, k = 1, \ldots, n, \tag{5.6}$$

where $A_{kj}, k, j = 1, \ldots, n$ are coupling weights between oscillator k and other oscillators. This means that the input of each oscillator is the summation of a linear combination of the output of other oscillators $y_j = f(z_j)$ and the external input w. Figure 5.1 shows the block diagram of the network described above.

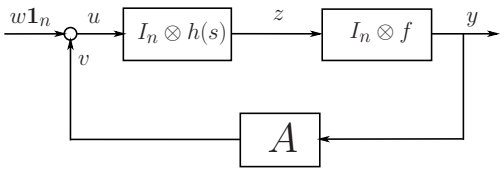

Figure 5.1: Network model of interconnected Goodwin-type oscillators

Consequently, under the effect of the same external input w, the whole network model is described as follows,

$$\begin{cases} z &= H(s)u, \\ y &= \mathcal{F}z, \\ u &= Ay + w\mathbf{1}_n, \end{cases} \tag{5.7}$$

where $H(s) = h(s)I_n, \mathcal{F} = fI_n$ and

$$\begin{aligned} u &= \begin{bmatrix} u_1 & u_2 & \ldots & u_n \end{bmatrix}^T, \\ y &= \begin{bmatrix} y_1 & y_2 & \ldots & y_n \end{bmatrix}^T, \\ z &= \begin{bmatrix} z_1 & z_2 & \ldots & z_n \end{bmatrix}^T. \end{aligned}$$

5.3 Entrainment in Goodwin-type Oscillator Networks

5.3.1 Periodic Oscillations, Synchronization and Entrainment

We here present the definitions of periodic oscillations, synchronization and entrainment used in this paper so that they are clearly distinguished.

Definition 5.1. *(**Periodically oscillating signal**) A signal $x(t)$, at steady state, is called a periodically oscillating signal with a period $T(>0)$ if $\lim_{t\to\infty}\{x(t+T)-x(t)\}=0$. Moreover, $\omega = 2\pi/T$ is called the frequency of that oscillation.*

Definition 5.2. *(**Synchronization**) A network system represented by (5.7) is said to be synchronized if all the outputs $y_k(t)$, $k = 1,\ldots,n$ are periodically oscillating signals with same frequency, phase, and amplitude.*

Definition 5.3. *(**Entrainment**) A network system represented by (5.7), which is excited by an external, periodically oscillating input $w(t)$, is said to be entrained by $w(t)$, if it is synchronized and the frequency is equal to that of $w(t)$.*

The definition of synchronization from Definition 2 is sometime called full synchronization in some other papers. That is because they consider "weaker synchronizing" scenarios where only the frequencies or frequencies and phases of oscillators are the same. On the other hand, from Definition 2 and 3, synchronization and entrainment are different. A network of periodic oscillators need not to be synchronized but they are still able to be entrained by an external, periodically oscillating signal.

Therefore, in this paper, we attempt to find the properties of the entrainment and the conditions for non-synchronized interconnected oscillators such that they are entrained by an exogenous input.

5.3.2 Motivating Example

In order to make the goals of this paper more clear we here illustrate a motivating numerical example, in which the autonomous oscillations in the network are asynchronous and then the network oscillations are entrained under the excitation of an external periodic input.

Consider a network (5.7) of 50 5th-order Goodwin-type oscillators with the dimensionless parameters $b_1 = b_2 = b_3 = b_4 = b_5 = 1, p = 10$ and a randomly generated interconnection matrix A such that it admits $\mathbf{1}_{50}$ as one of its eigenvectors. Figure 5.2 shows the autonomous oscillations in this network, which are asynchronous. In addition, the intrinsic frequency of the autonomous oscillations is 0.69.

Consequently, suppose that each 5th-order Goodwin-type oscillator is excited by a common periodic signal with higher order harmonics as follows,

$$w(t) = 5 + 4\sin(0.5t) + 7\sin(t + \frac{4\pi}{11}) + 9\sin(1.5t + \frac{6\pi}{7}).$$

Here, the frequency of external input is close to the autonomous frequency of network oscillations and the amplitudes of harmonic components in the external input are high. Then, the resulting oscillations in the network are displayed in Figure 5.3. We can observe that the induced oscillations not only synchronize at the frequency 0.5 of external signal but also contain higher order harmonics instead of having only zero and first order harmonics.

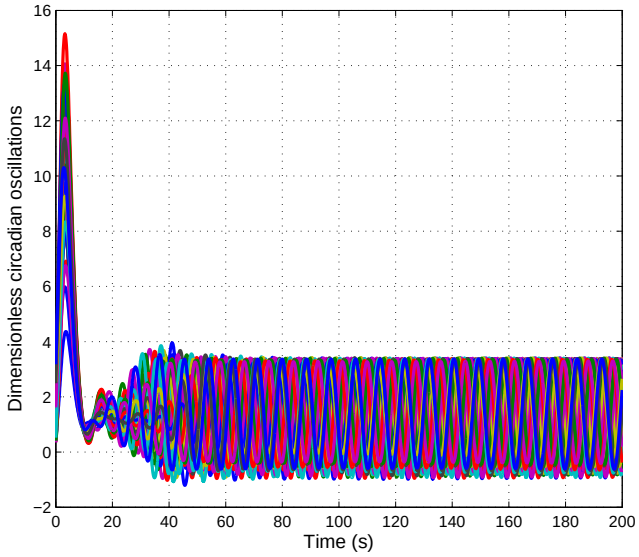

Figure 5.2: Autonomous oscillations in a randomly interconnected network of 5th-order Goodwin-type oscillators.

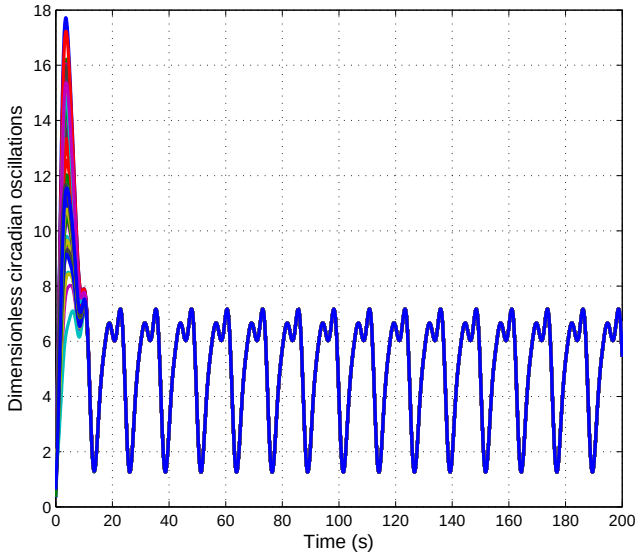

Figure 5.3: Entrainment in a randomly interconnected network of 5th-order Goodwin-type oscillators by a periodic input with higher order harmonics.

Now, we consider another situation where the elements of above matrix A are randomly perturbed which has no longer an eigenvector $\mathbf{1}_{50}$. However, the external input is kept the same as above. Then Figure 5.4 shows that the forced oscillations in the network are not synchronized.

From these simulation results, a couple of questions raise up. First, how to explain

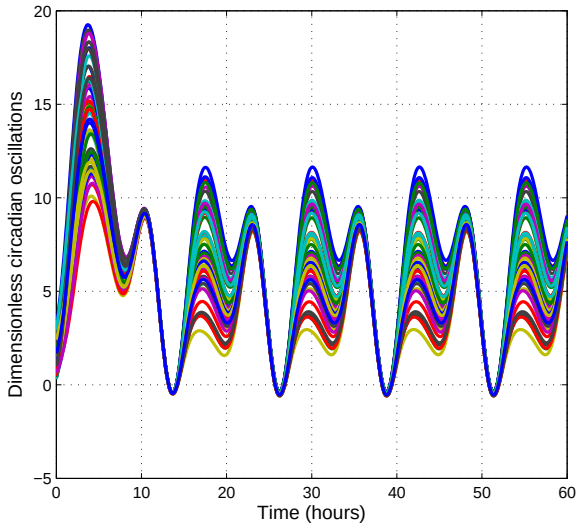

Figure 5.4: No entrainment in a 5th-order Goodwin-type oscillators if A does not has an eigenvector $\mathbf{1}_{50}$.

the entrainment of network oscillations in the presence of the external periodic input, or in other words what are the conditions for the entrainment of the oscillator network by an external periodic input? Second, how to evaluate or compute the entrained oscillations in the network? The answers for those questions will be sequentially given in the succeeding sections.

5.4 Entrainment Condition

This section is devoted to the conditions for occurring the entrainment.

Let us consider the external periodic input including the harmonics up to mth order represented by

$$w(t) = \kappa_0 + \kappa_1 \sin(\omega t + \zeta_1) + \ldots + \kappa_m \sin(m\omega t + \zeta_m), \tag{5.8}$$

where $\omega > 0$ is the frequency; $\kappa_0, \kappa_1, \ldots, \kappa_m > 0$ are the bias and amplitudes of harmonic components; $\zeta_1, \ldots, \zeta_m$ denote the phases of harmonic components. Accordingly, assume that the frequency of induced oscillations in the Goodwin-type oscillator network is entrained to ω, and the induced oscillations $z_k(t)$ and $y_k(t)$ can be approximated by the following periodic signals composing of higher-order harmonic components up to mth order,

$$\begin{aligned} z_k^{(m)}(t) &\approx \alpha_{0k} + \alpha_{1k} \sin(\omega t + \varphi_{1k}) + \ldots \\ &\quad + \alpha_{mk} \sin(m\omega t + \varphi_{mk}), \\ y_k^{(m)}(t) &\approx \sigma_{0k}\alpha_{0k} + \sigma_{1k}\alpha_{1k} \sin(\omega t + \varphi_{1k}) + \ldots \\ &\quad + \sigma_{mk}\alpha_{mk} \sin(m\omega t + \varphi_{mk}), k = 1, \ldots, n, \end{aligned} \tag{5.9}$$

where σ_{0k} and $\sigma_{jk}, j = 1, \ldots, m$ are describing functions which can be calculated [76] by

$$\begin{aligned}\sigma_{0k} &= \frac{1}{2\pi\alpha_{0k}} \int_0^{2\pi} f(\alpha_{0k} + \ldots + \alpha_{mk}\sin(mt))dt,\\ \sigma_{jk} &= \frac{1}{\pi\alpha_{jk}} \int_0^{2\pi} f(\alpha_{0k} + \ldots + \alpha_{mk}\sin(mt))\sin(jt)dt.\end{aligned}$$

Denote

$$\left\{\begin{array}{ll}\alpha_0 &= \left[\alpha_{01}, \ldots, \alpha_{0n}\right]^T,\\ \alpha_j &= \left[\alpha_{j1}e^{i\varphi_{11}}, \ldots, \alpha_{1n}e^{i\varphi_{jn}}\right]^T, j = 1, \ldots, m,\\ \Sigma_0 &= \operatorname{diag}\left(\sigma_{0k}\right)_{k=1,\ldots,n},\\ \Sigma_j &= \operatorname{diag}\left(\sigma_{jk}\right)_{k=1,\ldots,n}, j = 1, \ldots, m.\end{array}\right. \tag{5.10}$$

Then, we can represent the signals $z^{(m)}(t), y^{(m)}(t)$ and $w(t)$ by phasor vectors as follows:

$$\left\{\begin{array}{ll}z^{(m)} &= \alpha_0 + \alpha_1 + \ldots + \alpha_m,\\ y^{(m)} &= \Sigma_0\alpha_0 + \Sigma_1\alpha_1 + \ldots + \Sigma_m\alpha_m,\\ w &= \kappa_0 + \kappa_1 e^{i\zeta_1} + \ldots + \kappa_m e^{i\zeta_m}.\end{array}\right. \tag{5.11}$$

Introducing $\phi(s) := 1/h(s)$, which is the generalized frequency variable [40], then we have

$$\phi(i\omega) = (i\omega)^q + \beta_1(i\omega)^{q-1} + \cdots + \beta_{q-1}(i\omega)^1 + \beta_q, \tag{5.12}$$

where

$$\beta_k = \sum_{i_1, i_2, \ldots, i_k \in \{1,2\ldots,q\}} b_{i_1} b_{i_2} \cdots b_{i_k}; k = 1, 2 \ldots, q.$$

Consequently, substituting (5.11) into (5.7) and balancing harmonic components, we can obtain the following harmonic balance equations:

$$\left\{\begin{array}{ll}\left[\phi(0)I_n - A\Sigma_0\right]\alpha_0 &= \kappa_0\mathbf{1}_n,\\ \left[\phi(ij\omega)I_n - A\Sigma_j\right]\alpha_j &= \kappa_j e^{i\zeta_j}\mathbf{1}_n, j = 1, \ldots, m.\end{array}\right. \tag{5.13}$$

Then, the following proposition shows a necessary condition for entrainment in the network (5.7).

Proposition 5.1. *If the entrainment occurs in network (5.7) and harmonic balance equation (5.13) is satisfied then the interconnection matrix A representing the couplings among Goodwin-type oscillators must have an eigenvector $\mathbf{1}_n$.*

Proof. As the entrainment occur, (5.13) leads to

$$\left\{\begin{array}{ll}\left[\phi(0)I_n - A\hat{\sigma}_0\right]\hat{\alpha}_0\mathbf{1}_n &= \kappa_0\mathbf{1}_n,\\ \left[\phi(ij\omega)I_n - A\hat{\sigma}_j\right]\hat{\alpha}_j e^{i\hat{\varphi}_j}\mathbf{1}_n &= \kappa_j e^{i\zeta_j}\mathbf{1}_n, j = 1, \ldots, m,\end{array}\right. \tag{5.14}$$

where $\sigma_{01} = \cdots = \sigma_{0n} = \hat{\sigma}_0, \sigma_{k1} = \cdots = \sigma_{kn} = \hat{\sigma}_k, k = 1, \ldots, m$; $\alpha_{01} = \cdots = \alpha_{0n} = \hat{\alpha}_0$, $\alpha_{j1} = \cdots = \alpha_{jn} = \hat{\alpha}_j$, $\varphi_{j1} = \cdots = \varphi_{jn} = \hat{\varphi}_j, j = 1, \ldots, m$. This is in turn equivalent to the following equations:

$$\left\{\begin{array}{ll}A\hat{\sigma}_0\hat{\alpha}_0\mathbf{1}_n &= \left[\phi(0)\hat{\alpha}_0 - \kappa_0\right]\mathbf{1}_n,\\ A\hat{\sigma}_j\hat{\alpha}_j e^{i\hat{\varphi}_j}\mathbf{1}_n &= \left[\phi(ij\omega)\hat{\alpha}_j e^{i\hat{\varphi}_j} - \kappa_j e^{i\zeta_j}\right]\mathbf{1}_n, j = 1, \ldots, m.\end{array}\right. \tag{5.15}$$

It can immediately deduce from (5.15) that $\mathbf{1}_n$ is an eigenvector of A. □

Unfortunately, we can not show the sufficiency for the entrainment. However, we may raise in the following a conjecture by employing similar ideas in [50] for single oscillators forced by periodic inputs.

Conjecture 5.1. *If the frequency of the external periodic input $w(t)$ is close to the natural frequency of network oscillations, the amplitude of the external input is sufficiently large, and the interconnection matrix A has an eigenvector $\mathbf{1}_n$, then the network (5.7) is entrained by the external input $w(t)$.*

Some simulation results presented in Section 6.4 provide an evidence for supporting this conjecture.

5.5 Properties of Entrainment

Suppose that the network (5.7) is entrained by the external periodic input $w(t)$. Let λ be the eigenvalue of A corresponding to the eigenvector $\mathbf{1}_n$, then we obtain from (5.15) that

$$\begin{cases} [\phi(0) - \lambda\hat{\sigma}_0]\,\hat{\alpha}_0 & = \kappa_0, \\ [\phi(ij\omega) - \lambda\hat{\sigma}_j]\,\hat{\alpha}_j e^{i\hat{\varphi}_j} & = \kappa_j e^{i\zeta_j}, j = 1, \ldots, m. \end{cases} \tag{5.16}$$

It is generally hard to solve the harmonic balance equations in (5.16). Nevertheless, we will show in Subsection 5.5.1 that an explicit estimation for the entrained network oscillations could be obtained in a certain situation. For other cases, Subsection 5.5.2 reveals the monotonic dependence of network oscillations on the external input, which bring useful information on entrained oscillations, though we could not explicitly approximate them.

5.5.1 Case 1: A has an eigen-pair $(0, \mathbf{1}_n)$

In this case, the harmonic balance equations in (5.16) becomes

$$\begin{cases} \phi(0)\hat{\alpha}_0 & = \kappa_0, \\ \phi(ij\omega)\hat{\alpha}_j e^{i\hat{\varphi}_j} & = \kappa_j e^{i\zeta_j}, j = 1, \ldots, m. \end{cases} \tag{5.17}$$

Let us denote $\rho_j = \hat{\varphi}_j - \zeta_j$ the phase shifts between the jth-order harmonics in the network oscillations and the external input, and $\phi_{\mathrm{R},j}, \phi_{\mathrm{I},j}$ the real and imaginary parts of $\phi(ij\omega)$, $i, j = 1, \ldots, m$, respectively, then (5.17) is equivalent to

$$\begin{cases} \phi(0)\hat{\alpha}_0 & = \kappa_0, \\ [(\phi_{\mathrm{R},j} + i\phi_{\mathrm{I},j}]\,\hat{\alpha}_j e^{i\rho_j} & = \kappa_j, j = 1, \ldots, m. \end{cases} \tag{5.18}$$

The following proposition gives us an estimation of the entrained network oscillations.

Proposition 5.2. *Suppose that network (5.7) is entrained by the external input of the form (5.8) and the network oscillations can be approximated as in (5.9). Then their amplitudes and phases can be estimated as follows:*

$$\hat{\alpha}_j = \frac{\kappa_j}{\sqrt{\phi_{R,j}^2 + \phi_{I,j}^2}}, j = 1, \ldots, m. \tag{5.19}$$

$$\hat{\varphi}_j = \zeta_j - \mathrm{atan}(\phi_{I,j}/\phi_{R,j}), j = 1, \ldots, m. \tag{5.20}$$

Proof. Note that $\phi_{\mathrm{R},j}$ and $\phi_{\mathrm{I},j}$ can be easily calculated from (5.12) for every $j = 1, \ldots, m$. Subsequently, (5.18) are equivalent to

$$\begin{aligned} \left[\phi_{\mathrm{R},j}^2 + \phi_{\mathrm{I},j}^2\right] \hat{\alpha}_j^2 &= \kappa_j^2, \\ -\frac{\phi_{\mathrm{I},j}}{\phi_{\mathrm{R},j}} &= \tan(\rho_j), \end{aligned} \tag{5.21}$$

which lead to (5.19) and (5.20). □

Since $\sqrt{\phi_{\mathrm{R},j}^2 + \phi_{\mathrm{I},j}^2} > 0$, we immediately obtain the following corollary from Proposition 5.2.

Corollary 5.1. *The following two statements hold.*

(i). The amplitude $\hat{\alpha}_j$ of the jth-order harmonic components in the entrained network oscillations is a monotonically increasing function of the amplitude κ_j of the jth-order harmonic component in the external driving signal.

(ii). The phase shift ρ_j between the jth-order harmonic components in the entrained network oscillations and in the exciting input is a constant with respect to the changes of the amplitude κ_j.

Proposition 5.2 theoretically contributes an explicit estimation for the profile of any harmonic order in the network oscillations as they are entrained by the external input (5.8) within the context that the interconnection matrix A has an eigen-pair $(0, \mathbf{1}_n)$. This analysis result would give us a strong basic for designing oscillator networks in real applications.

5.5.2 Case 2: A has an eigen-pair $(\lambda, \mathbf{1}_n)$, $\lambda \neq 0$

In this scenario, we are not able to obtain an explicit estimation of the entrained network oscillations as in the previous case. Hence, we aim at verifying the monotonic dependence of the entrained oscillations to the external input as it is varying. As a result, even though we do not know precisely the profile of entrained oscillations but at least we may know how they change with respect to the external input.

For simplicity, we only consider the case of sinusoidal external inputs, i.e.,

$$w(t) = \kappa_0 + \kappa_1 \sin(\omega t + \zeta_1).$$

Subsequently, under some mathematical manipulations, the describing function $\hat{\sigma}_1$ can be rewritten as

$$\begin{aligned} \hat{\sigma}_1 &= \frac{1}{\pi \hat{\alpha}_1} \int_0^{2\pi} f\left(\hat{\alpha}_0 + \hat{\alpha}_1 \sin(t)\right) \sin(t) dt, \\ &= \frac{1}{\pi \hat{\alpha}_1} \int_0^{\pi} \left[f\left(\hat{\alpha}_0 + \hat{\alpha}_1 \sin(t)\right) - f\left(\hat{\alpha}_0 - \hat{\alpha}_1 \sin(t)\right)\right] \sin(t) dt. \end{aligned}$$

Note that $\hat{\alpha}_0$ should be greater than or equal to $\hat{\alpha}_1$ to guarantee that $\hat{\alpha}_0 + \hat{\alpha}_1 \sin(t)$ and $\hat{\alpha}_0 - \hat{\alpha}_1 \sin(t)$ are non-negative since the Hill function is only defined in the interval $[0, +\infty)$.

Therefore, we can see from the above equation that $\hat{\sigma}_1 < 0$, since $\hat{\alpha}_0 + \hat{\alpha}_1 \sin(t) > \hat{\alpha}_0 - \hat{\alpha}_1 \sin(t) > 0$ with $t \in [0, \pi]$ and the Hill function f is monotonically decreasing.

Consider the harmonic balance equation in (5.16) associated with the 1st harmonic component,

$$[\phi(i\omega) - \lambda\hat{\sigma}_1]\,\hat{\alpha}_1 e^{i\hat{\varphi}_1} = \kappa_1 e^{i\zeta_1}. \tag{5.22}$$

Then (5.22) is equivalent to

$$[\phi_{\mathrm{R},1} - \lambda\hat{\sigma}_1 + i\phi_{\mathrm{I},1}]\,\hat{\alpha}_1 e^{i\rho_1} = \kappa_1. \tag{5.23}$$

Note that $\phi_{\mathrm{R},1}$ and $\phi_{\mathrm{I},1}$ can be easily calculated from (5.12), and hence (5.23) is equivalent to

$$\left[(\phi_{\mathrm{R},1} - \lambda\hat{\sigma}_1)^2 + \phi_{\mathrm{I},1}^2\right]\hat{\alpha}_1^2 \quad = \kappa_1^2, \tag{5.24}$$

$$-\frac{\phi_{\mathrm{I},1}}{\phi_{\mathrm{R},1} - \lambda\hat{\sigma}_1} = \tan(\rho_1). \tag{5.25}$$

The proposition below shows the second monotonic property of the entrainment in the Goodwin-type oscillator networks under the following assumption.

- **Assumption 1.** The integral in the describing function $\hat{\sigma}_1$ is a monotonically decreasing function of $\hat{\alpha}_0$ and $\hat{\alpha}_1$.

Proposition 5.3. *Suppose that Assumption 1* [1] *is satisfied. Then, the amplitude $\hat{\alpha}_1$ of the 1st harmonic components in the entrained network oscillations is a monotonically increasing function of the amplitude κ_1 of the 1st harmonic component in the driving signal if the following condition holds,*

C1. $\phi_{R,1}\lambda > 0$.

Proof. We obtain from Assumption 1 that the describing function $\hat{\sigma}_1$ is a monotonically decreasing function of $\hat{\alpha}_1$ since $\dfrac{1}{\hat{\alpha}_1}$ is positive and monotonically decreasing with respect to $\hat{\alpha}_1$.

Accordingly, the following two cases occur if the condition C1 is satisfied.
Case 1: $\phi_{\mathrm{R},1} > 0$ and $\lambda > 0$: We can deduce from Assumption 1 that $-\lambda\hat{\sigma}_1\hat{\alpha}_1$ is positive and monotonically increasing with respect to $\hat{\alpha}_1$, and hence $[\phi_{\mathrm{R},1} - \lambda\hat{\sigma}_1]\,\hat{\alpha}_1$ is monotonically increasing with respect to $\hat{\alpha}_1$. Moreover, we have

$$\max_{\hat{\alpha}_1 \in [0,+\infty)} [\phi_{\mathrm{R},1} - \lambda\hat{\sigma}_1]\,\hat{\alpha}_1 = +\infty, \min_{\hat{\alpha}_1 \in [0,+\infty)} [\phi_{\mathrm{R},1} - \lambda\hat{\sigma}_1]\,\hat{\alpha}_1 = 0.$$

Case 2: $\phi_{\mathrm{R},1} < 0$ and $\lambda < 0$: We see that $[\phi_{\mathrm{R},1} - \lambda\hat{\sigma}_1]\,\hat{\alpha}_1$ is monotonically decreasing with respect to $\hat{\alpha}_1$. Computing similarly to Case 1, we have

$$\min_{\hat{\alpha}_1 \in [0,+\infty)} [\phi_{\mathrm{R},1} - \lambda\hat{\sigma}_1]\,\hat{\alpha}_1 = -\infty, \max_{\hat{\alpha}_1 \in [0,+\infty)} [\phi_{\mathrm{R},1} - \lambda\hat{\sigma}_1]\,\hat{\alpha}_1 = 0.$$

[1] See the Appendix for the validation of this assumption.

Thus, we can conclude from both Case 1 and Case 2 that $[(\phi_{\mathrm{R},1} - \lambda\hat{\sigma}_1)]^2\,\hat{\alpha}_1^2$ is monotonically increasing with respect to $\hat{\alpha}_1$ in $[0, +\infty)$. In addition, we have

$$\max_{\hat{\alpha}_1 \in [0,+\infty)} \left[(\phi_{\mathrm{R},1} - \lambda\hat{\sigma}_1)^2\right] \hat{\alpha}_1^2 = +\infty,$$
$$\min_{\hat{\alpha}_1 \in [0,+\infty)} \left[(\phi_{\mathrm{R},1} - \lambda\hat{\sigma}_1)^2\right] \hat{\alpha}_1^2 = 0.$$

On the other hand, $\phi_{\mathrm{I},1}^2\hat{\alpha}_1^2$ is always a monotonically increasing function of $\hat{\alpha}_1$ in $[0, +\infty)$. Thereupon, if condition C1 is satisfied, $\kappa_1^2 = \left[(\phi_{\mathrm{R},1} - \lambda\hat{\sigma}_1)^2 + \phi_{\mathrm{I},1}^2\right] \hat{\alpha}_1^2$ is monotonically increasing with respect to $\hat{\alpha}_1$, i.e., $\hat{\alpha}_1$ is a monotonically increasing function of κ_1. This completes the proof. □

Example 1: Consider the same network (5.7) of 50 5th-order Goodwin-type oscillators as in the motivating example. We here attempt to verify the monotonicity of the amplitude $\hat{\alpha}_1$ on the amplitude κ_1 of the first harmonic components in the network oscillations and the external signal. Let the external signal be

$$w(t) = 7 + \kappa_1 \sin(0.5t),$$

where κ_0 is fixed at 7 and κ_1 is increased from 1 to 7. We then measure the amplitude $\hat{\alpha}_1$ of the induced network oscillations and illustrate the dependence of $\hat{\alpha}_1$ on κ_1 in Figure 5.5. It is seen that $\hat{\alpha}_1$ is monotonically increasing with respect to κ_1. We also observe that $\hat{\alpha}_0$ is almost constant in the simulation, in particular $\hat{\alpha}_0 \approx 4$. Moreover, these values of $\hat{\alpha}_0$ and $\hat{\alpha}_1$ belong to the region plotted in Figure 5.6 in the appendix.

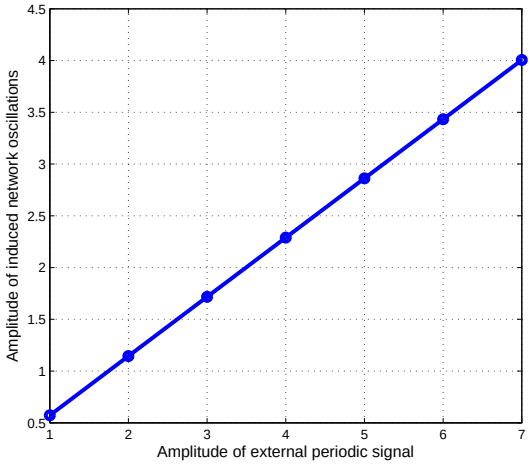

Figure 5.5: Monotonicity of the amplitude of network oscillations to the amplitude of exciting signal.

Next, we introduce the third monotonic property of the entrainment in the Goodwin-type oscillator networks.

Proposition 5.4. *Suppose that Assumption 1 is satisfied. Then the phase shift* ρ_1 *of the* 1*st harmonic component in the entrained network oscillations is a monotonic function of the amplitude* κ_1 *of the* 1*st harmonic component in the external driving signal as indicated in the following table, where* $-$ *and* $+$ *mean negative and positive, respectively;* $\uparrow$ *and* $\downarrow$ *mean monotonically increasing and decreasing, respectively.*

Table 5.1: Monotonic dependence of the phase shift to the external input in networks of generalized Goodwin-type oscillators.

λ	$\phi_{\mathrm{R},1}$	$\phi_{\mathrm{I},1}$	ρ_1
$-$	$-$	$-$	$-\uparrow$
$-$	$-$	$+$	$+\downarrow$
$-$	$+$	$-$	$+\uparrow$
$-$	$+$	$+$	$-\downarrow$
$+$	$-$	$-$	$-\downarrow$
$+$	$-$	$+$	$+\uparrow$
$+$	$+$	$-$	$+\downarrow$
$+$	$+$	$+$	$-\uparrow$

Proof. It is seen from the proof of Proposition 5.3 that the describing function is negative and monotonically decreasing with respect to $\hat{\alpha}_1$. On the other hand, $\tan(\rho_1)$ is a monotone function of ρ_1, hence it can be deduced from (5.25) that ρ_1 is a monotonic function of $\hat{\alpha}_1$ and whether that function is increasing or decreasing depends on the signs of $\phi_{\mathrm{R},1}$, $\phi_{\mathrm{I},1}$ and λ. Then, making a sign table yields the results as in Table 1. □

5.6 Summary

This chapter has contributed a framework for analyzing the entrainment in the networks of generalized Goodwin oscillators driven by an external periodic input. Utilizing the harmonic balance method, a condition for the synchronization of network oscillations by a driving periodic input is proposed. Moreover, the relations between the phases and amplitudes of the harmonic components in the induced network oscillations and those of the external input are revealed. Subsequently, those relations are shown to be monotone under an additional assumption and some conditions. This further result gives us a deeper understanding on the dynamical behaviors of the induced network oscillations under the drive of an external periodic input.

APPENDIX

- **Assumption 1.** The integral in the describing function $\hat{\sigma}_1$ is a monotonically decreasing function of $\hat{\alpha}_0$ and $\hat{\alpha}_1$.

This assumption seems to be conservative from a theoretical point of view but we observe from many simulations that this assumption is satisfied with the bias $\hat{\alpha}_0$ and the amplitude of the 1st-order harmonic $\hat{\alpha}_1$ in some intervals. An example of such an interval of $\hat{\alpha}_0$ and $\hat{\alpha}_1$ is shown in Figure 5.6 where $\hat{\alpha}_0$ and $\hat{\alpha}_1$ belong to the interval $[0, 10]$ and the Hill coefficient p is taken to be 9. We can observe that there exist some regions of $\hat{\alpha}_0$ and $\hat{\alpha}_1$ such that in which $\hat{\sigma}_1$ is monotonically decreasing, for instance near the upper right corner in the figure. Hence, Assumption 1 is employed in for analysis in this paper.

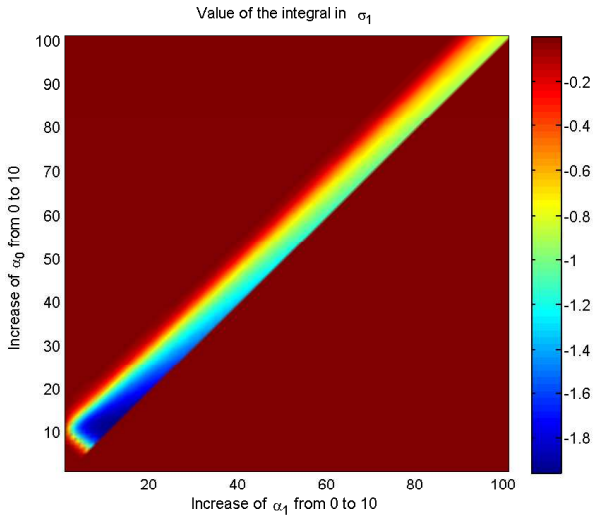

Figure 5.6: An example of the describing function $\hat{\sigma}_1$ calculated with $\hat{\alpha}_0, \hat{\alpha}_1 \in [0, 10]$.

CHAPTER 6

SYNCHRONIZATION BEHAVIORS IN 3rd-ORDER GOODWIN OSCILLATOR NETWORKS

6.1 Introduction

In this chapter, we investigate a more specific model of oscillator networks than the model in Chapter 5, namely 3rd-order Goodwin oscillator networks. This model has been utilized to study the circadian oscillations [25,26,83] but only the autonomous circadian oscillations have been considered, i.e., without the effect of an external signal. Nevertheless, it is known that the period of autonomous circadian oscillations is not precisely 24 hours and which make the period of circadian oscillation to be 24 hours is some external timing cues called zeitgebers [29,70,71]. Furthermore, the phases of circadian rhythms can be adjusted by external signals for example the bright light or melatonin [80–82]. Therefore, it is really important to conduct the researches on the analysis of circadian oscillations driven by the zeitgebers. The phase models have been used to study that problem, for example [59, 84], but the phase models usually contain little information about the biological parameters and do not completely represent the oscillation profile. On the other hand, the 3rd-order Goodwin model describes processes with negative feedbacks which were proved to be one of the core mechanisms for circadian networks [28, 29, 53–55]. Moreover, the 3rd-order Goodwin model is represented by ordinary differential equations which includes parameters representing biological values. Thus, investigating the 3rd-order Goodwin oscillator networks would give more biological insights to the circadian rhythms driven by Light-Dark signals and hence may be helpful for clinical applications of light to treat some diseases related to circadian rhythms, e.g., delayed/advanced sleep phase, seasonal affective disorder (SAD), shift work, jet lag, etc [80–82].

This chapter contributes the analysis of the synchronization and entrainment in the 3rd-order Goodwin oscillator networks driven by periodic zeitgebers. The approach used in this chapter is similar to the approach in Chapter 5 and hence the results obtained here basically agree with the results in Chapter 5 but more specific so that we obviously see the meanings of the parameters in the model. On the other hand, there is one important result on the monotonic dependence of the phase shift of induced network oscillations to the period of the zeitgeber which has not been derived in Chapter 5. Furthermore, the obtained results in this chapter show some degrees of agreement with the biological observations on the circadian rhythms. Therefore, the analysis results in this chapter not only contribute to the theoretical knowledge about the dynamical behaviors of nonlinear oscillator networks but also be useful

and closed to the practical systems.

6.2 Circadian Networks

In this section, we particularly pay attention to circadian networks in which the circadian oscillators are reprsented by the classical 3rd-order Goodwin model [60,61] to study the effects of zeitgebers to circadian oscillations. The critical point here is that although the model is simple but it captures the essential features that benefit the study of the entrainment of circadian oscillations such as the containment of a negative feedback loop and the simplification of formulation [84] .

A network of 3rd-order Goodwin oscillators is represented by

$$\begin{cases} z &= H(s)u, \\ y &= \mathcal{F}z, \\ u &= Ay + w\mathbf{1}_n, \end{cases} \tag{6.1}$$

where

$$h(s) = \frac{1}{(s+b_1)(s+b_2)(s+b_3)}. \tag{6.2}$$

Since the 3rd-order Goodwin oscillator network is a special case of the generalized model (5.7), all results derived in the previous sections are also applied here. However, we still recall the important results with details for 3rd-order Goodwin model and introduce an important property of the entrainment which has not been addressed for generalized Goodwin-type oscillator networks. In addition, a practical model of circadian rhythm in *Neurospora crassa* adopted from [31] is employed in the simulation to clearly demonstrate the theoretical results.

For simplicity, let us consider the zeitgeber to be sinusoidal, i.e.,

$$w(t) = \kappa_0 + \kappa_1 \sin(\omega t + \zeta_1), \tag{6.3}$$

and suppose that the circadian network is entrained by the zeitgeber (6.3). Consequently, the harmonic balance equations for entrained oscillations are written as

$$\begin{cases} \left[\phi(0) - \lambda\hat{\sigma}_0\right]\hat{\alpha}_0 &= \kappa_0, \\ \left[\phi(i\omega) - \lambda\hat{\sigma}_1\right]\hat{\alpha}_1 e^{i\rho_1} &= \kappa_1. \end{cases} \tag{6.4}$$

We note that $\phi(i\omega)$ is represented by

$$\begin{aligned} \phi(i\omega) &= -i\omega^3 - (b_1+b_2+b_3)\omega^2 \\ &\quad + i(b_1b_2 + b_2b_3 + b_3b_1)\omega + b_1b_2b_3, \end{aligned} \tag{6.5}$$

which means that $\phi_{\mathrm{R},1} = b_1b_2b_3 - (b_1+b_2+b_3)\omega^2$ and $\phi_{\mathrm{I},1} = \omega(b_1b_2 + b_2b_3 + b_3b_1 - \omega^2)$. Hence, the second equation in (6.4) is equivalent to the following two equations:

$$\begin{aligned} &\big[(b_1b_2b_3 - (b_1+b_2+b_3)\omega^2 - \lambda\hat{\sigma}_1)^2 + \\ &\quad \omega^2(b_1b_2 + b_2b_3 + b_3b_1 - \omega^2)^2\big]\,\hat{\alpha}_1^2 \;= \kappa_1^2, \end{aligned} \tag{6.6}$$

$$-\frac{\omega(b_1b_2 + b_2b_3 + b_3b_1 - \omega^2)}{b_1b_2b_3 - (b_1+b_2+b_3)\omega^2 - \lambda\hat{\sigma}_1} = \tan(\rho_1). \tag{6.7}$$

Similarly to networks of generalized Goodwin-type oscillators, two circumstances are investigated in the next two sections.

6.3 Entrainment properties

Note here that the necessary condition for entrainment and Conjecture 5.1 for sufficiency of entrainment in Section 5.4 are also applied here since the third-order Goodwin oscillator networks is a special case of the generalized Goodwin-type oscillator networks. Therefore, we do not present them again for brevity.

6.3.1 Graph Laplacian case

In this situation, the harmonic balance equations in (6.4) become

$$\begin{cases} \phi(0)\hat{\alpha}_0 & = \kappa_0, \\ \phi(i\omega)\hat{\alpha}_1 e^{i\rho_1} & = \kappa_1. \end{cases} \tag{6.8}$$

Similarly to Subsection 5.5.1, we can obtain an estimation of the entrained oscillations in the network and hence we omit here for brevity.

We now present a new result, which shows the monotonic relation between the phase shift ρ_1 and the frequency of the zeitgeber, in particular the Light-Dark signal. Note that the relation between the phase shift and the frequency of the zeitgeber has a significant importance in the study of circadian oscillations [84]. This relation has been observed in biology but its underlying mechanism is still unclear. Recently, Granada et al. present a theoretical study on the relation between the entrainment phase of circadian oscillations and the zeitgebers [84]. Nevertheless, the mathematical models utilized in [84] are different from ours. The interesting point here is that the obtained result agrees with the result in [84] even though our model is different.

Proposition 6.1. *Suppose that the interconnection matrix A is a Laplacian matrix. Then, the phase shift ρ_1 of entrained oscillations in the circadian network (5.7) with $n = 3$ is a monotonically decreasing function of the frequency ω of the zeitgeber, in particular the Light-Dark signal.*

Proof. If $\lambda = 0$ then we obtain from (6.7) that

$$\tan(\rho_1) = -\frac{\omega(b_1b_2 + b_2b_3 + b_3b_1 - \omega^2)}{b_1b_2b_3 - (b_1 + b_2 + b_3)\omega^2} = -\frac{\omega(\beta_2 - \omega^2)}{\beta_3 - \beta_1\omega^2}.$$

Denote $g(\omega) = \dfrac{\omega(\beta_2 - \omega^2)}{\beta_3 - \beta_1\omega^2}$. We have

$$\frac{dg(\omega)}{d\omega} = \frac{\beta_1\omega^4 + (\beta_2\beta_1 - 3\beta_3)\omega^2 + \beta_2\beta_3}{(\beta_3 - \beta_1\omega^2)^2}.$$

Employing Cauchy-Schwarz inequality gives us

$$\begin{aligned} & (b_1b_2 + b_2b_3 + b_3b_1)(b_1 + b_2 + b_3) \geq 9b_1b_2b_3 \\ \Leftrightarrow \quad & \beta_2\beta_1 \geq 9\beta_3. \end{aligned} \tag{6.9}$$

Consequently, we can write

$$\beta_1\omega^4 + (\beta_2\beta_1 - 3\beta_3)\omega^2 + \beta_2\beta_3 = \beta_1(\omega^2 + \omega_1)(\omega^2 + \omega_2),$$

where $\omega_1 + \omega_2 = \dfrac{\beta_2\beta_1 - 3\beta_3}{\beta_1} > 0$ and $\omega_1\omega_2 = \dfrac{\beta_2\beta_3}{\beta_1} > 0$. This leads to a fact that $\omega_1 > 0$ and $\omega_2 > 0$. As a result, $\beta_1\omega^4 + (\beta_2\beta_1 - 3\beta_3)\omega^2 + \beta_2\beta_3 > 0 \; \forall \; \omega$. Thus, $\dfrac{dg(\omega)}{d\omega} > 0 \; \forall \; \omega$, i.e., $g(\omega)$ is a strictly monotonically increasing function of ω. Note that tan is monotonically increasing, and hence we see from (6.9) that ρ_1 is a monotonically decreasing function of ω. □

Remark 6.1. *It should be noted in [84] that the authors consider the entrainment phase ψ, which is equal to the difference between the phase of zeitgebers and the phase of induced circadian oscillations. This quantity in fact is equal to $-\rho_1$ in this paper. We then obtain immediately from Proposition 6.1 that the entrainment phase ψ is a monotonically increasing function of ω. Furthermore, let us denote T and T_z the period of autonomous circadian oscillations and the period of zeitgebers, respectively, then the period mismatch $T_z - T = T_z - \dfrac{2\pi}{\omega}$ is monotonically increasing with respect to ω. Hence, the entrainment phase ψ is a monotically increasing function of the period mismatch $T_z - T$. This result agrees with the observations in [70, 84, 85]. Therefore, our result supports the biological evidences and may be helpful for further investigating the circadian oscillations.*

6.3.2 General case

Likewise in subsection 5.5.2, we assume here that the integral in the describing function $\hat{\sigma}_1$ is a monotonically decreasing function of $\hat{\alpha}_0$ and $\hat{\alpha}_1$. Moreover, we can also show that $\hat{\sigma}_1 < 0$. The following corollaries show the monotonic dependence of the amplitudes and phases of entrained circadian oscillations to the amplitude of the zeitgeber in the 3rd-order Goodwin oscillator networks.

Corollary 6.1. *The amplitude $\hat{\alpha}_1$ of entrained circadian oscillations is a monotonically increasing function of the amplitude κ_1 of the zeitgeber if the following condition holds:*

C2. $[b_1b_2b_3 - (b_1 + b_2 + b_3)\omega^2]\lambda > 0$.

Corollary 6.2. *The phase shift ρ_1 of the 1st harmonic component in the entrained network oscillations is a monotonic function of the amplitude κ_1 of the zeitgeber as indicated in Table 2, where $-$ and $+$ mean negative and positive, respectively; $\uparrow$ and $\downarrow$ mean monotonically increasing and decreasing, respectively.*

Proof. This corollary can be proved similarly to Proposition 5.4 with a note that $\dfrac{b_1b_2b_3}{b_1 + b_2 + b_3} < b_1b_2 + b_2b_3 + b_1b_3$ holds, and hence we can deduce that $\phi_{\mathrm{R}} < 0$ if $\phi_{\mathrm{I}} < 0$ and $\phi_{\mathrm{R}} > 0$ leads to $\phi_{\mathrm{I}} > 0$. Therefore, the cases corresponding to $\phi_{\mathrm{R}} > 0, \phi_{\mathrm{I}} < 0$ cannot occur. □

Table 6.1: Monotonic dependence of the phase shift to the zeitgeber in networks of 3rd-order Goodwin oscillators.

λ	ϕ_{R}	ϕ_{I}	$\hat{\varphi}$
$-$	$-$	$-$	$-\uparrow$
$-$	$-$	$+$	$+\downarrow$
$-$	$+$	$+$	$-\downarrow$
$+$	$-$	$-$	$-\downarrow$
$+$	$-$	$+$	$+\uparrow$
$+$	$+$	$+$	$-\uparrow$

6.4 Numerical Example: *Neurospora crassa* circadian network

Consider a network of 50 circadian oscillators with $h(s)$ given in (6.2) and the original parameters are adopted from [31] for the model of circadian oscillations in *Neurospora crassa* as follows: $k_1 = 1, k_2 = 1, k_3 = 1, k_4 = 0.2, k_5 = 0.2, k_6 = 0.1, K = 1, p = 9$. These parameters corresponds to autonomous circadian oscillations with period 22.3 hours. Hence, we can compute the dimensionless parameters to be $b_1 = 0.2, b_2 = 0.2, b_3 = 0.1$. We assume that the network has the same structure as in Example 1, i.e., the interconnection matrix in the whole network is $A = I_5 \otimes A_1 + L \otimes I_{10}$. Then A_1 is randomly generated such that it admits $\mathbf{1}_{10}$ as one of its eigenvectors and the associated eigenvalue is 15, while L is chosen to be a Laplacian matrix as in Example 1. As a result, the interconnection matrix in the whole network A has one eigenvector $\mathbf{1}_{50}$ and the associated eigenvalue is 15.

To demonstrate the amplitude condition of the external input for entrainment, we first simulate the autonomous oscillations in the network, i.e., without the zeitgeber and then simulate the oscillator network forced by a sinusoidal zeitgeber with period equal to 24 hours $w(t) = \kappa_0 + \kappa_1 \sin(\frac{2\pi}{24}t)$, where κ_0 and κ_1 are subjected to be gradually changed. Then Figure 6.1 shows the simulation results with different values of κ_0 and κ_1. It can be observed that the autonomous oscillations are asynchronous and when κ_0 and κ_1 increase from 0.001 to 0.004, the induced oscillations in the network are not synchronized. Afterward, the induced network oscillations are synchronized as κ_0 and κ_1 are equal to 0.006 and they are synchronized as we continually increase κ_0 and κ_1. Thus, the amplitude of the zeitgeber should be large enough to make the network oscillations entrained as stated in Conjecture 5.1.

Next, we attempt to verify another condition on the frequency of the zeitgeber which should be close enough to the natural frequency of the autonomous network oscillations so that there exist induced oscillations in the network under the effect of the zeitgeber. To do so, we apply a sinusoidal zeitgeber $w(t) = 0.1 + 0.1 \sin(\omega t)$ with oscillating period changes from 3 hours to 28 hours to the oscillator network. The simulation results are displayed in Figure 6.2 in which the first subplot exhibits the asynchronous autonomous network oscillations and the next two subplots with period of the zeitgeber to be 3 hours and 5 hours shows

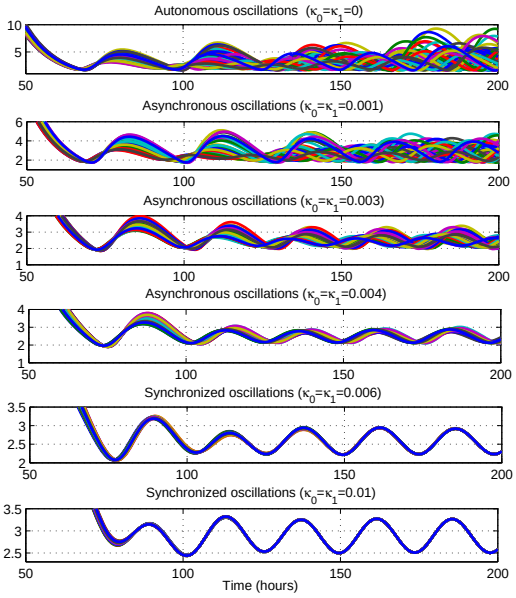

Figure 6.1: Entrainment in the oscillator network as the amplitude of the zeitgeber varies.

that there are no oscillations in the network though the output of oscillators converge to a same value. The sequent subplots reveal that as we increase the period of the zeitgeber, the oscillations occur in the network. In addition, they are synchronized and their frequency changes respectively to the variance on the period of the zeitgeber. More specifically, the period of induced network oscillations is exactly equal to the period of the zeitgeber. This clearly demonstrates Conjecture 5.1.

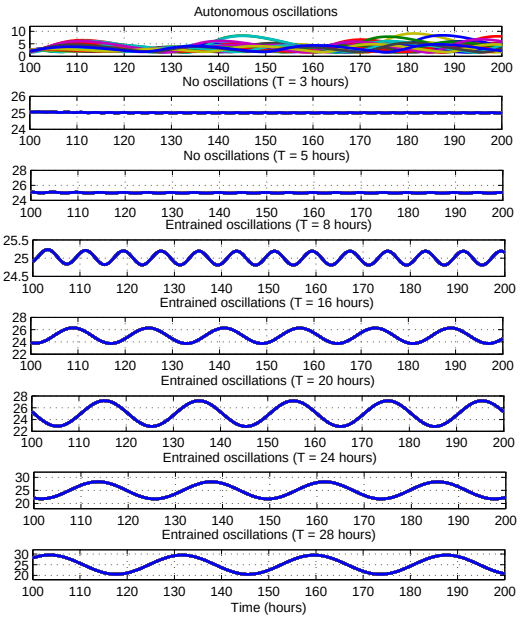

Figure 6.2: Entrainment in the oscillator network as the frequency of the zeitgeber varies.

The monotone dependence of the amplitude $\hat{\alpha}_1$ of circadian oscillations to the amplitude κ_1 of the zeitgeber as the bias κ_0 is kept unchanged is a direct consequence of Proposition 5.3, so we do not introduce the simulation result here.

In the next step, the local interconnection matrix A_1 in each oscillator groups is randomly generated such that it is a Laplacian matrix. Figure 6.3 then shows that the phase shift ρ_1 is monotonically increasing with respect to the period T_z of the zeitgeber, i.e., monotonically decreasing with respect to the frequency ω of the zeitgeber which clearly demonstrates the statement in Proposition 6.1.

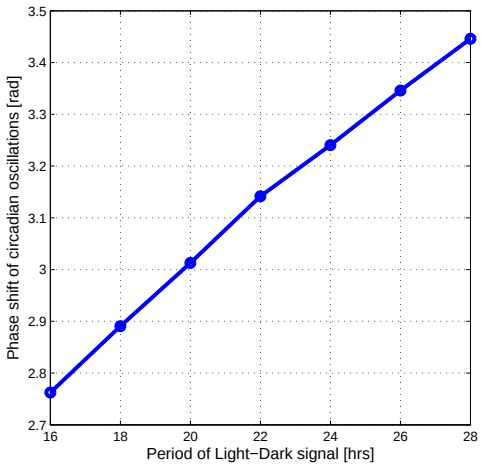

Figure 6.3: Monotonicity of the phase shift of entrained circadian oscillations to the period of the zeitgeber.

Now, we assume that each circadian oscillator is driven by a zeitgeber containing higher-order harmonics represented by

$$w(t) = 1 + \sin(\frac{2\pi}{24}t) + 2\sin(\frac{2\pi}{24}t + \frac{2\pi}{5}) + 3\sin(\frac{2\pi}{24}t + \frac{3\pi}{7}). \tag{6.10}$$

Then the induced circadian oscillations in the network are exhibited in Figure 6.4. We can see that the circadian oscillations still synchronize at the frequency of the zeitgeber and they contain higher order harmonics instead of having only zero and first order harmonics.

6.5 Summary

This chapter presents an analysis framework for studying the entrainment in the networks of 3rd-order Goodwin oscillators excited by an external periodic input. It was proved [50] that the frequency of the induced network oscillations is entrained to the frequency of the external iput. Consequently, a condition is proposed for the synchronization of network oscillations and the relations between the phases and amplitudes of the harmonic components in the induced network oscillations and thoses in the external input are revealed based on the harmonic

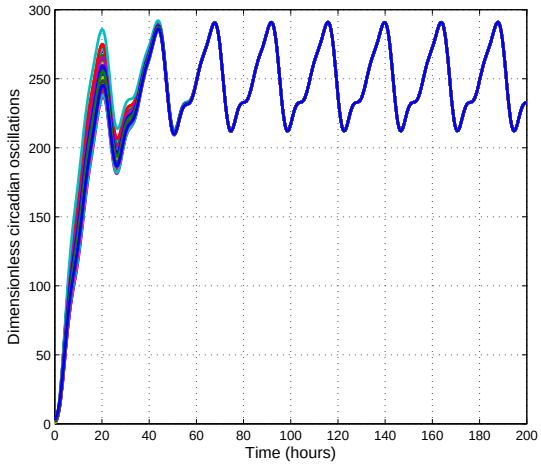

Figure 6.4: Synchrony in a randomly interconnected network of *Neurospora crassa* circadian oscillators by a periodic zeitgeber with higher order harmonics.

balance method. Furthermore, we figure out that in some cases those relations are monotone. Interestingly, the obtained results show some agreements with the observations from biological experiments on circadian oscillations. Therefore, the study of 3rd-order Goodwin oscillators in this chapter may be useful to gain more insights and to further investigate the circadian oscillations.

CHAPTER 7

CONCLUSIONS AND FURTHER RESEARCHES

7.1 Conclusions

This thesis contains three main parts. The first part given in Chapter 2 introduces a review of previous related researches and the formulation of the problems we considered in this thesis and then our proposed approaches to resolve them. The second part is devoted to the design of hierarchical optimal controller for hierarchical linear dynamical systems including Chapter 3 and Chapter 4. The last part studies the entrainment and its properties in the Goodwin-type nonlinear oscillator networks which is presented in Chapter 5 and Chapter 6.

In Chapter 2, we present our formulation of linear multi-agent systems as two-layer hierarchical dynamical systems and nonlinear oscillator networks. The linear multi-agent systems are cast as two-layer hierarchical dynamical systems . Then we introduce the design of hierarchical feedback controllers such that the obtained hierarchical network achieve a prescribed hierarchical structure. The approache to solve that design problem is based on the LQR method. In the next part, we consider the networks of nonlinear oscillators where the oscillators are described by Goodwin-type models representing biochemical processes with negative feedback. Accordingly, we propose an analysis framework based on the harmonic balance method to investigate the entrainment in that oscillator networks as well as the entrainment properties.

Chapter 3 proposes a new and systematic design approach for hierarchical, optimal feedback controllers for linear, hierarchical, homogeneous dynamical networks. Employing the LQR approach with proper choices of weighting matrices, the derived hierarchical controller preserves the prescribed hierarchical structure of the network. Furthermore, by further choosing the weighting matrices, only undesirable eigenvalues of the local interconnection matrices are shifted while the others eigenvalues are not altered. The proposed approach is then summarized into a design procedure showing the steps in the design. In the scenario that only partial states of agents can be measured, we introduce local observers to reduce the output feedback design problem to the state feedback design situation.

Chapter 4 develops a new and systematic design method for hierarchical, optimal feedback controllers for linear, hierarchical, heterogeneous dynamical systems containing subsystems with different numbers of agents and different local interconnection structures. Obviously, the design in this circumstance is different an more difficult than in Chapter 3. Then LQR approach is still employed but the selection of the weighting matrices are more involved due to the different network setting. The method is then summarized into a design proce-

dure to clearly see the design steps. After that, we introduce an application of the proposed method to a practical problem of velocity consensus in vehicle platoons.

Chapter 5 introduces a framework based on the harmonic balance method for studying the entrainment in the network of Goodwin-type oscillators. A necessary condition for entrainment is proposed of which the interconnection matrix in the network must have a one-column eigenvector. Furthermore, a conjecture on certain ranges of frequency and amplitude of the external periodic input should be satisfied such that the entrainment can occur. Next, the monotonic properties of the entrainment are revealed which are confirmed by numerical examples.

Chapter 6 presents the study of third-order Goodwin oscillator networks describing circadian networks. In addition to the results obtained in Chapter 5, some further results for this type of oscillator networks are then proposed which show the interesting agreements with the experiments on circadian oscillations in the literature. Thus, the obtained theoretical results may bring more insights and be helpful for further exploring circadian oscillations.

7.2 Further researches

- Study on discrete-time hierarchical dynamical systems.
- Consideration of uncertainty, time delay, etc, to obtain robust designs.
- Extension for directed communications among subsystems.
- Consensus controllers for hierarchical dynamical systems based on the proposed method.

REFERENCES

[1] Z. Q. H. Zhang, F. L. Lewis. Lyapunov, adaptive, and optimal design techniques for cooperative systems on directed communication graphs. *IEEE Transactions on Industrial Electronics*. 59(7). (2012): 3026–3041.

[2] E. Ravasz and A.-L. Barabasi. Hierarchical organization in complex networks. *Physical Review E*. 67:026112. (2003): 1–7.

[3] M. Girvan and M. E. J. Newman. Community structure in social and biological networks. *PNAS*. 99(12). (2002): 7821-7826.

[4] S. Fortunato. Community detection in graphs. *Physics Reports*. 486. (2010): 75-174.

[5] U. Alon. Network motifs: theory and experimental approaches. *Nature Reviews Genetics*. 8. (2007): 450–461.

[6] V. P. Zhdanov. Hierarchical genetic networks and noncoding rna. *Chaos*. 20:045112. (2010): 1–9.

[7] T. Nakamura, S. Hara, and Y. Hori. Local stability analysis for a class of quorum-sensing networks with cyclic gene regulatory networks. in *SICE Annual Conference*. (2011): 2111–2116.

[8] R. Olfati-Saber, J. A. Fax, and R. M. Murray. Consensus and cooperation in networked multi-agent systems. *Proceeding of the IEEE*. 95(1). (2007): 215–233.

[9] W. Ren, R. W. Beard, and E. M. Atkins. Information consensus in multivehicle cooperative control. *IEEE Control Systems Magazine*. 27(2). (2007): 71–82.

[10] H. Shimizu and S. Hara. Cyclic pursuit behavior for hierarchical multi-agent systems with low-rank interconnection. in *Proc. of SICE Annual Conference*. (2008): 3131–3136.

[11] H. Shimizu and S. Hara. Hierarchical consensus for multi-agent systems with lowrank interconnection. in *Proc. of ICCAS-SICE*. (2009): 1063–1067.

[12] S. Hara, H. Shimizu, and T.-H. Kim. Consensus in hierarchical multi-agent dynamical systems with low-rank interconnections analysis of stability and convergence rates. in *American Control Conference*. (2009): 5192–5197.

[13] S. L. Smith, M. E. Broucke, and B. A. Francis. A hierarchical cyclic pursuit scheme for vehicle networks. *Automatica*. 41. (2005): 1045–1053.

[14] D. Tsubakino and S. Hara. Eigenvector-based intergroup connection of low rank for hierarchical multi-agent dynamical systems. *Systems and Control Letters*. 61. (2012): 354–361.

[15] N. Fujimori, L. Liu, S. Hara, and D. Tsubakino. Hierarchical network synthesis for output consensus by eigenvector-based interlayer connections. in *Proc. of IEEE Conference on Decision and Control and European Control Conference*. (2011): 1449–1454.

[16] B. Bamieh, F. Paganini, and M. A. Dahleh. Distributed control of spatially invariant systems. *IEEE Transactions on Automatic Control*. 47(7). (2002): 1091–1107.

[17] N. Motee, A. Jadbabaie, and B. Bamieh. On decentralized optimal control and information structures. in *Proc. of American Control Conference*. (2008): 4985–4990.

[18] M. Fardad. The operator algebra of almost toeplitz matrices and the optimal control of large-scale systems. in *Proc. of American Control Conference*. (2009): 854–859.

[19] Y. Cao and W. Ren. Optimal linear-consensus algorithms: An lqr perspective. *IEEE Transactions on Systems, Man, and Cybernetics-Part B: Cybernetics*. 40(3). (2010): 819–830.

[20] D. Tsubakino, T. Yoshioka, and S. Hara. An algebraic approach to hierarchical lqr synthesis for large-scale dynamical systems. in *Proc. of Asian Control Conference*.

[21] N. Kawasaki and E. Shimemura. Determining quadratic weighting matrices to locate poles in a specified region. *Automatica*. 19(5). (1983): 557–560.

[22] N. Kawasaki, E. Shimemura, and J.-W. Shin. On the quadratic weights of an lq-problem shifting only the specified poles. *Proceedings of the Society of Instrument and Control Engineers*. 25(11). (1989): 1248–1250.

[23] F. Kraus and V. Kucera. Linear quadratic and pole placement iterative design. in *Proc. of IEEE European Control Conference*.

[24] J. Cigler and V. Kucera. Pole-by-pole shifting via a linear-quadratic regulation. in *Proc. of the 17th International Conference on Process Control*.

[25] J.-C. Leloup, D. Gonze, and A. Goldbeter. Limit cycle models for circadian rhythms based on transcriptional regulation in drosophila and neurospora. *Journal of Biological Rhythms*. 14(6). (1999): 433–448.

[26] P. Ruoff, J. Loros, and J. Dunlap. The relationship between frq-protein stability and temperature compensation in the neurospora circadian clock. *PNAS*. 102(49). (2005): 17681–17686.

[27] A. Liu, W. Lewis, and S. Kay. Mammalian circadian signaling networks and therapeutic targets. *Nature Chemical Biology*. 3(10). (2007): 630–639.

[28] E. Herzog. Neurons and networks in daily rhythms. *Nature Reviews Neuroscience*. 8. (2007): 790–802.

[29] D. Golombek and R. E. Rosenstein. Physiology of circadian entrainment. *Physiological Reviews*. 90. (2010): 1063–1102.

[30] M. J. Rust, S. S. Golden, and E. K. OShea. Light-driven changes in energy metabolism directly entrain the cyanobacterial circadian oscillator. *Science*. 331. (2011): 220–223.

[31] P.Ruoff, M. Vinsjevik, S. Mohsenzadeh, and L. Rensin. The goodwin model: Simulating the effect of cycloheximide and heat shock on the sporulation rhythm of neurospora crassa. *Journal of Theoretical Biology*. 196. (1999): 483–494.

[32] R. Olfati-Saber. Flocking for multi-agent dynamic systems: Algorithms and Theory. *IEEE Transactions on Automatic Control*. 51(3). (2006): 401–420.

[33] R. M. Murray. Recent research in cooperative control of multi-vehicle systems. *Journal of Dynamic Systems, Measurement, and Control*. 129. (2007): 571–583.

[34] C. W. Reynolds. Flocks, herds, and schools: A distributed behavioral model. *Computer Graphics*. 21(4). (1987): 25–34.

[35] T. Vicsek, A. Czirok, E. B. Jacob, I. Cohen, and O. Schochet. Novel type of phase transitions in a system of self-driven particles. *Physical Review Letters*. 21(4). (1995): 1226-1229.

[36] A. Jadbabaie, J. Lin, and A. Morse. Coordination of groups of mobile autonomous agents using nearest. *IEEE Transaction on Automatic Control*. 48(6). (2003): 988-1001.

[37] H. G. Tanner, G. J. Pappas, and V. Kumar. Leader-to-Formation stability. *IEEE Transactions on Automatic Control*. 20(3). (2004): 443–455.

[38] R. Olfati-Saber and R. M. Murray. Consensus problems in networks of agents with switching topology and time-delays. *IEEE Transaction on Automatic Control*. 49(9). (2004): 1520–1533.

[39] J. A. Fax and R. M. Murray. Information flow and cooperative control of vehicle formations. *IEEE Transaction on Automatic Control*. 49(9). (2004): 1465-1476.

[40] S. Hara, T. Hayakawa, and H. Sugata. Lti systems with generalized frequency variables: A unified framework for homogeneous multi-agent dynamical systems. *SICE Journal of Control, Measurement, and System Integration*. 44. (2009): 001–009.

[41] H. Tanaka, S. Hara, and T. Iwasaki. Lmi stability condition for linear systems with generalized frequency variables. in *Proc. of 7th Asian Control Conference*. (2009): 136-141.

[42] S. Hara, T. Hayakawa, and H. Sugata. Stability analysis of linear systems with generalized frequency variables and its applications to formation control. in *Proc. of IEEE Conference on Decision and Control*. (2007): 1459-1466.

[43] Y. Hori and S. Hara. Oscillation pattern analysis for gene regulatory networks with negative cyclic feedback. in *Proc. of IEEE Conference on Decision and Control*. (2010): 5798–5803.

[44] Y. Hori, T.-H. Kim, and S. Hara. Existence criteria of periodic oscillations in cyclic gene regulatory networks. *Automatica*. 47(6). (2011): 1203–1209.

[45] T.-H. Kim, Y. Hori, and S. Hara. Robust stability analysis of gene-protein regulatory networks with cyclic activation repression interconnections. *Systems and Control Letters*. 60(6). (2011): 373–382.

[46] F. Dorfler and F. Bullo. Synchronization and transient stability in power networks and nonuniform kuramoto oscillators. *SIAM Journal on Control and Optimization*. 50(3). (2012): 1616–1642.

[47] F. Dorfler, M. Chertkov, and F. Bullo. Synchronization in complex oscillator networks and smart grids. *Proceedings of the National Academy of Sciences*. 110(6). (2013): 2005–2010.

[48] D. Romeres, F. Drfler, and F. Bullo. Novel results on slow coherency in consensus and power networks. in *Proc. of European Control Conference*.

[49] R. Carareto, M. S. Baptista, and C. Grebogi. Natural synchronization in power-grids with anti-correlated units. *Communications in Nonlinear Science and Numerical Simulations*. 18. (2013): 1035-1046.

[50] A. Pikovsky, M. Rosenblum, and J. Kurths. *Synchronization: A universal concept in nonlinear sciences*. New York: Cambridge University Press. 2001.

[51] S. H. Strogatz. From kuramoto to crawford: exploring the onset of synchronization in populations of coupled oscillators. *Physica D*. 143. (2000): 1–20.

[52] J. D. Murray. *Mathematical biology: An introduction*. Berlin: Springer-Verlag. 2002.

[53] L. Glass. Synchronization and rhythmic processes in physiology. *Nature*. 418. (2001): 277–284.

[54] S. M. Reppert and D. R. Weaver. Coordination of circadian timing in mammals. *Nature*. 418. (2002): 935–941.

[55] S. Yamaguchi, H. Isejima, T. Matsuo, R. Okura, K.Yagita, M. Kobayashi, and H. Okamura. Synchronization of cellular clocks in the suprachiasmatic nucleus. *Science*. 302. (2003): 1408–1412.

[56] A. T. Winfree. *The Geometry of Biological Time*. Springer, New York. 1980.

[57] E. Izhikevich. *Dynamical Systems in Neuroscience: The Geometry of Excitability and Bursting*. The MIT Press. 2007.

[58] Y. Kuramoto. *Chemical Oscillations, Waves, and Turbulence*. Springer-Verlag, Berlin. 1984.

[59] H. Daido. Why circadian rhythms are circadian–competitive population dynamics of biological oscillators. *Physical Review Letters*. 87(4). (2001): 048101:1–4.

[60] B. C. Goodwin. An entrainment model for timed enzyme syntheses in bacteria. *Nature*. 209. (1966): 479–481.

[61] J. S. Griffith. Mathematics of cellular control processes i. negative feedback to one gene. *Journal of Theoretical Biology*. 20(2). (1968): 202–208.

[62] A. Williams, S. Glavaski, and T. Samad. Formations of formations: Hierarchy and stability. in *Proc. of American Control Conference*. (2004): 2992–2997.

[63] S. C. Hamilton and M. E. Broucke. Patterned linear systems: Rings, chains, and trees. in *Proc. of IEEE Conference on Decision and Control*. (2010): 1397–1402.

[64] J. A. Marshall, M. E. Broucke, and B. A. Francis. Formations of vehicles in cyclic pursuit. *IEEE Transaction on Automatic Control*. 49(11). (2004): 1963–1974.

[65] N. Fujimori, L. Liu, S. Hara, and D. Tsubakino. Hierarchical network synthesis for output consensus by eigenvector-based interlayer connections. tech. rep.. Technical Report METR2011-29, The University of Tokyo. 2011. [Online] Available at http://www.keisu.t.u-tokyo.ac.jp/research/techrep/.

[66] T. Yoshioka. Distributed hierarchical optimal control based on the algebraic approach. Master's thesis. The University of Tokyo. 2012.

[67] A. A. Alam, A. Gattami, and K. H. Johansson. Suboptimal decentralized controller design for chain structures: Applications to vehicle formations. in *Proc. of IEEE Conference on Decision and Control and European Control Conference*. (2011): 6894–6900.

[68] F. Borrelli and T. Keviczky. Distributed lqr design for identical dynamically decoupled systems. *IEEE Transactions on Automatic Control*. 53(8). (2008): 1901–1912.

[69] P. Massioni and M. Verhaegen. Distributed control for identical dynamically coupled systems: A decomposition approach. *IEEE Transactions on Automatic Control*. 54(1). (2009): 124–135.

[70] J. Aschoff and H. Pohl. Phase relations between a circadian rhythm and its zeitgeber within the range of entrainment. *Naturwissenschaften*. 65. (1978): 80–84.

[71] U. Abraham, A. E. Granada, P. O. Westermark, M. Heine, A. Kramer, and H. Herzel. Coupling governs entrainment range of circadian clocks. *Molecular Systems Biology*. 6(438). (2010): 1–13.

[72] C. Saini, J. Morf, M. Stratmann, P. Gos, and U. Schibler. Simulated body temperature rhythms reveal the phase-shifting behavior and plasticity of mammalian circadian oscillators. *Genes and Development*. 26. (2012): 567–580.

[73] D. Gonze, S. Bernard, C. Waltermann, A. Kramer, and H. Herzel. Spontaneous synchronization of coupled circadian oscillators. *Biophysical Journal*. 89. (2005): 120–129.

[74] Y. Wang and F. J. D. III. On influences of global and local cues on the rate of synchronization of oscillator networks. *Automatica*. 47. (2011): 1236–1242.

[75] B. D. O. Anderson and J. B. Moore. *Optimal Control: Linear Quadratic Methods*. Englewood Cliffs, NJ: Prentice Hall. 1990.

[76] H. S. Khalil. *Nonlinear systems*. New Jersey: Prentice Hall. 2002.

[77] W. Smith. Hypothalamic regulation of pituitary secretion of luteinizing hormone-ii. feedback control of gonadotropin secretion. *Bulletin of Mathematical Biology*. 42. (1980): 57–78.

[78] G. Enciso and E. Sontag. On the stability of a model of testosterone dynamics. *Journal of Mathematical Biology*. 49. (2004): 627–634.

[79] W. Khaisongkram and S. Hara. Performance analysis of decentralized cooperative driving under non-symmetric bidirectional information architecture. in *Proc. of IEEE Multi-Conference on Systems and Control*. (2010): 2035–2040.

[80] R. Y. Moore. Circadian rhythms: Basic neurobiology and clinical applications. *Annual Review of Medicine*. 48. (1997): 253–266.

[81] P. M. P. C. Zee. The brains master circadian clock: Implications and opportunities for therapy of sleep disorders. *Sleep Medicine Reviews*. 11. (2007): 59–70.

[82] P. C. Z. A. Barion. A clinical approach to circadian rhythm sleep disorders. *Sleep Medicine*. 8. (2007): 566–577.

[83] Y. Wang, Y. Hori, S. Hara, and F. J. D. III. The collective oscillation period of inter-coupled goodwin oscillators. in *Proc. of IEEE Conf. on Decision and Control*. (2012): 1627–1632.

[84] A. E. Granada, G. Bordyugov, A. Kramer, and H. Herzel. Human chronotypes from a theoretical perspective. *PLoS ONE*. 8(3): e59464. (2013): 1–10.

[85] C. Pittendrigh. Circadian systems: entrainment. *Handbook of behavioral neurobiology*. 4. (1981): 95–124.